A study on material design for selective cement activation 3D printing

by

Geert Schouten

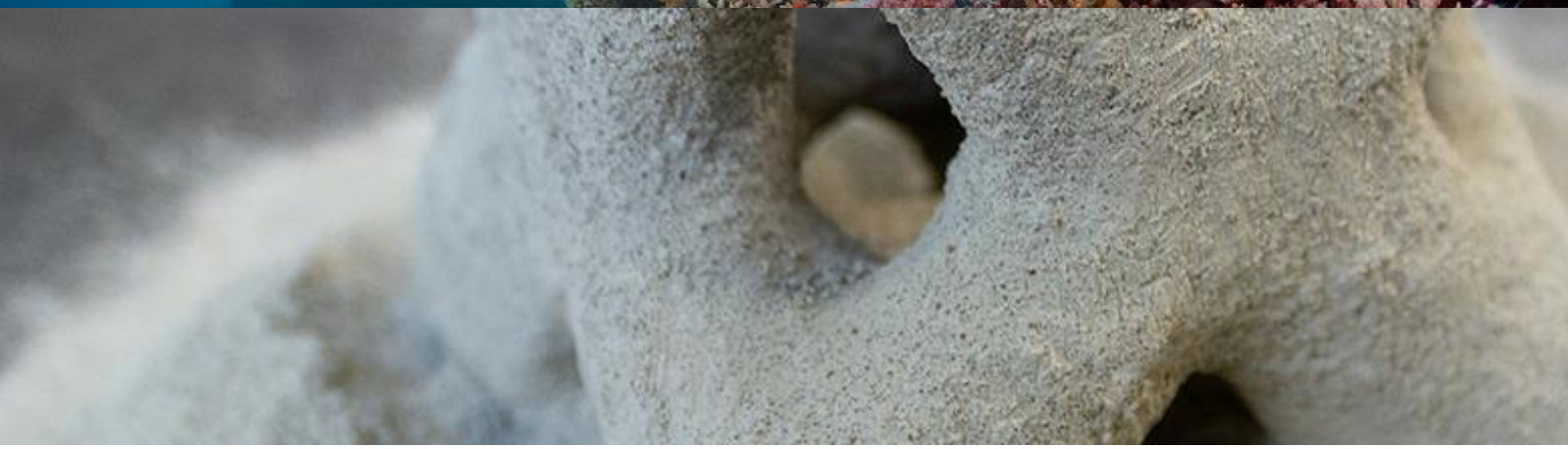

TU Delft

Coastruction

A study on material design for selective cement activation 3D printing

Developing a strong and sustainable concrete mix suitable for additive manufacturing and underwater application

by

Geert Schouten

Student number: 4476395

University: Delft University of Technology

Faculty: Civil Engineering and Geosciences

Master track: Structural Engineering

Specialization: Concrete Structures

In partial fulfilment of the requirements for the degree of:

Master of Science

in Civil Engineering

at the Delft University of Technology,

to be defended publicly on Thursday January 22, 2026 at 10:00 AM.

Thesis committee: Dr. Branko Šavija (Chairman)

Dr. Sandra Barbosa Nunes (Supervisor)

Ir. Andries Koopmans (company supervisor)

I. Preface

Before you lies my master thesis "*A study on material design for selective cement activation 3D printing*". It has been written as a fulfilment of the Master of Science degree in Civil Engineering, with a specialty in Concrete Structures at the TU Delft University of Technology. This thesis has been carried out in collaboration with Coastruction. The topic of concrete printing has always been of great interest to me, and this work provided a valuable opportunity to deepen my understanding of the field.

I would like to thank my graduation committee for their support and patience during this thesis. Firstly, I want to thank Andries Koopmans for his enthusiasm and the incredibly helpful daily discussions we had, especially in the early stages of this thesis. Secondly, I would like to thank Dr. Sandra Nunes for the thorough feedback she provided on the report after every meeting. And lastly, I want to thank Dr. Branko Šavija for help keep me pointed in the right direction and helping me get started through the in-depth meetings we had during the first few months of this thesis.

I would also like to thank everyone at Coastruction. At Coastruction, I was given great freedom to pursue the topics I was most interested in and how I would go about this research. The supervisors and their colleagues at the company provided excellent support throughout, including finding the right materials or tools, sharing topics of interest, and engaging in fruitful discussions. I would like to give special thanks to Nadia Fani, for giving me this great opportunity. I would also like to give special thanks to Sam van den Oever and Rutger Semp for their interest in my research and for their support.

And last but not least, I am grateful for the support and encouragements of my family, friends and my girlfriend who certainly helped successfully finalizing this thesis. I am grateful for the opportunity to have carried out this work within this collaboration and with this amazing group of people, and I hope that reading this thesis sparks interests and curiosity on this topic.

Geert Schouten

Delft, January 2026

II. Abstract

The increasing urgency of global warming and resource depletion demands more sustainable construction methods capable of reducing material use. Additive manufacturing (AM), in particular selective cement activation (SCA), offers such potential; however, its adoption remains limited due to challenges in mechanical performance and shape accuracy. Current SCA systems, including the custom-built printer used in this study, often exhibit low strength and require high water dosages to compensate, resulting in excessive penetration depth and thereby a loss of detail in the product.

This research aims to develop a concrete mix suitable for printing reef-like structures using SCA by optimising both strength and shape accuracy. Eighteen mix designs were investigated through small-scale mechanical testing, including compression and bending. Additionally, four different curing regimes were tested. Shape accuracy was evaluated using a visual grading method applied to complex printed geometries. Key mix parameters—particle-size distribution, cement-to-aggregate (C/A) ratio, binder composition, and additives—were systematically studied to identify their influence on water penetration behaviour and resultant print quality.

The results show that increasing the C/A ratio and adjusting the PSD significantly improve mechanical performance, while cellulose ether considerably enhances shape accuracy when applied within a narrow dosage range. A ternary binder of 90% ordinary Portland cement (OPC), 5% calcium sulphate (CS), and 5% calcium aluminate cement (CAC), combined with a C/A ratio of 0.4 and 0.25% cellulose ether, produced the most favourable balance between strength and geometric accuracy. This final mix design increased bending strength from 0.37 MPa to 1.62 MPa and compressive strength from 0.38 MPa to 1.15 MPa without sacrificing shape accuracy.

Overall, the study advances the understanding of material design for SCA-based 3D concrete printing and highlights sustainable binders and improved layer compaction methods as key directions for continued development. At the same time, it underscores that the recommended mix design is not universal but must be tailored to the specific requirements of the intended application.

III. List of abbreviations

3DCP	Three-dimensional concrete printing
AAB	Alkali-activated binder
AM	Additive manufacturing
BFS	Blast furnace slag
C/A ratio	Cement to aggregate ratio
CAC	Calcium Aluminate Cement
CDF	Cumulative distribution function
CE	Cellulose Ethers (e.g. Tylose)
CS	Calcium Sulphate
E-modulus	Elastic modulus (Young's Modulus)
EMMA	Elkem Materials Mixture Analyzer
FA	Fly Ash
GC	Geopolymer concrete
HEMC	Hydroxyethyl Methyl Cellulose
MAA	Modified Andreasen and Andersen model
MIP	Mercury Intrusion Porosimetry
OPC	Ordinary Portland Cement
PDF	Probability distribution function
SCA	Selective Cement Activation
SSC	Seawater and sea-sand concrete
w/c ratio	Water-to-cement (or water-to-binder) ratio
wt%	Percentage of weight

Contents

1. Introduction

Concrete is the second most used material in the world after water (Scrivener et al., 2018). Concrete contributes to between 4 and 8% of the global CO2 emissions, and contributes to the consumption of a significant amount of natural resources (de Brito & Kurda, 2021). With the threat of global warming, it is imperative to find ways to reduce global CO2 emissions and to transition to more sustainable ways of using natural resources. Additionally, with the effects of global warming becoming increasingly apparent, it is of huge importance to protect and preserve vulnerable ecosystems all over the world before the damage done becomes irreversible. Coastal habitats like coral reefs are facing ever higher threats due to human activity (Narayan et al., 2016). In addition to providing important ecosystem services, coral reefs also provide vital coastal protection against flooding and erosion (Narayan et al., 2016). Therefore, there is great interest in protecting and conserving these natural habitats. Currently there are already numerous solutions for breakwater structures. However they usually involve large casted concrete structures, the production of which emits a large amount of CO2, exacerbating global warming. On top of that, the surfaces of these breakwaters are often smooth, making it difficult for marine life to attach to the structures. Furthermore, they lack features like holes and crevices, which can act as hiding places for smaller marine animals. A way to reduce the amount of material required, as well as implement rough surfaces and organic designs, is with the use of additive manufacturing (AM). Additive manufacturing, also known as 3D printing, is a method of fabricating complex geometrical elements directly from a three- dimensional computer model (Mohan et al., 2021). Due to several advantages of AM, like increased geometric freedom, reduced labour cost and time, and reduced material use, the technology has gained the interest of many industries, including in the concrete construction industry (Mohan et al., 2021). The variant of AM using concrete, commonly referred to as 3D concrete printing (3DCP) may reduce material usage by up to 70% (Lowke et al., 2020) and thereby reduce CO2 emissions and natural resource usage by a similar amount, assuming a similar mix design is used as with conventional concrete casting.

Additive manufacturing can be divided into three main 3D printing techniques: Material extrusion, material jetting and particle- bed binding (Lowke et al., 2020), of which only material extrusion and particle bed binding are used in large- scale construction (Chen et al., 2017). Material extrusion 3D printing is the most popular 3D concrete printing technique to date, and involves a nozzle depositing the cementitious material layer upon layer, see Figure 1 (Mohan et al., 2021).

Figure 1: An extrusion based 3DCP technique (Project Milestone)

Notable structures created by 3D concrete printing may include a house in Eindhoven, the Netherlands, under the name 'Project Milestone' (Figure 2), or a bridge in Nijmegen, the Netherlands (Figure 3).

Figure 2: 3DCP house in Eindhoven (Project Milestone)

Figure 3: 3DCP bridge in Nijmegen (TU/e, 2021)

Particle- bed binding is a 3D printing technique where a fluid is selectively deposited onto a particle bed using a print head or nozzle in order to bind the particles, after which another layer of particles is deposited and the process is repeated (Lowke et al., 2018). When the printing process is finished, the de-powdering process can begin, where unreacted particles are removed so that only the 3D printed structure remains. According to Lowke et al. (2018), there are three main strategies of particle bed 3D printing (see Figure 4):

1. Selective binder/cement activation (SCA) is a technique where the particle bed consists of an aggregate and a binder. During printing, the cement (or other binder) in the powder is activated by selectively spraying water (or another liquid activator) on the particle bed.
2. Selective paste intrusion is a similar technique where the particle bed only consists of aggregate and the cement, along with water and admixtures, is then sprayed onto the particle bed.

3. Binder jetting does not deposit the activator (water) but instead sprays the binder onto a particle bed containing the aggregate and the activator. The binder usually is a resin with a hardener being the activator in the particle bed.

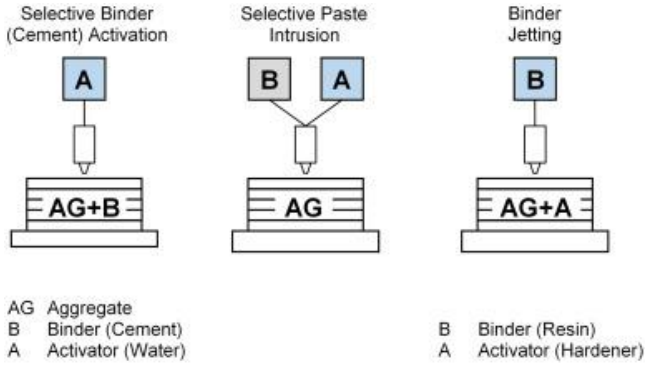

Figure 4: The three different particle bed 3D printing techniques (Lowke et al., 2018)

The main advantage of the particle bed 3D printing technique over other 3D printing techniques is that there are almost no design restrictions in terms of shape. The unreacted particles will act as a temporary support for the printed structure, making it possible to print overhangs, arches and cantilevers. A big limitation however is that the size of the 3D printed structure is limited by the size of the printer. Real world examples of particle bed 3D printed structures are few and rare but can very well illustrate the possibilities of this technique (see Figures 5, 6 and 7).

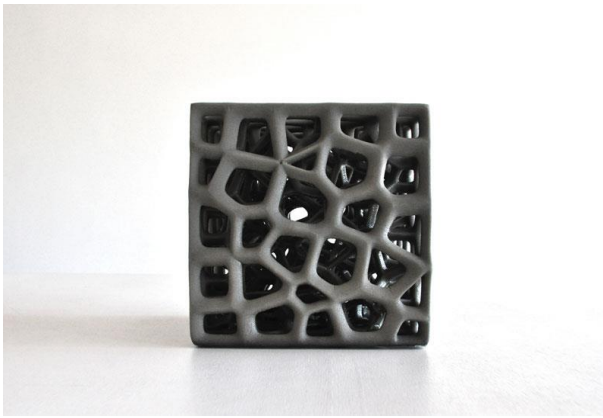

Figure 5: A 3D printed concrete structure made by the company Emerging Objects

Figure 6: A 3D printed structure from D-shape made using a magnesium- based binder (Edwards, 2010)

Figure 7: A footbridge in Milan printed using selective cement activation (de la Fuente et al., 2022)

1.1 The company

Coastruction is a small startup company situated in Rotterdam, the Netherlands. Their goal is to design, produce and install 3D printed artificial reefs to help restoration of damaged reef systems and protect vulnerable coastlines. The company currently tests and produces small artificial reef structures (see Figure 9) using small SCA type printers (see Figure 8) and are currently developing a larger printer to be able to print bigger structures.

The short- term goal of the company right now is to print and cure the artificial reefs in- house and ship them to their destination, while in the long term, they would like to lease the printer to wherever it is needed and use local materials to print on- site. The company wants to use as little as PC as feasible, in order to make the 3D printed concrete as environmentally friendly as possible.

The printer

The printer used in this work is a prototype particle bed 3D printer made by Coastruction that uses the Selective Cement Activation (SCA) technique, see Figure 8. Current printable dimensions are either a box by 150x150x150 mm or 250x250x150 mm and 3 possible layer heights of 2.5/3.0/3.5 mm, but for this research, the height is fixed at 2.5mm. The printer uses a hopper to place the particle bed and then uses a nozzle to deposit droplets of water onto the particle bed. The powder is placed on top of a stainless-steel plate using a hopper and then a nozzle sprays a fine mist on the powder bed to locally hydrate the cement. Then, the plate is lowered by 2.5 mm into a stainless-steel box after which a new layer can be deposited.

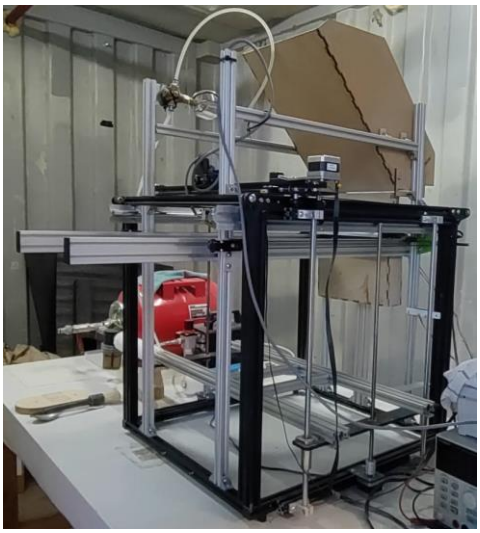

Figure 8: The printer used in this study

The amount of water that is deposited can be controlled by changing the speed at which the nozzle moves. The powder mix can also be changed from layer to layer since the hopper can be emptied and refilled with another mix. A modified slicer software is used to translate a 3D design into coordinates where the nozzle should move to, and when the nozzle should open and close. A compressor is used to keep the water pressure constant so that the amount of water that flows through the nozzle is at a known constant rate.

The product

The printer itself is highly adaptive and can in theory be used for all kinds of applications that require complex 3D designs, like art installations, furniture, vases, or façade elements. However, the company is currently focused on designing, producing and installing 3D printed artificial reefs to help restoration of damaged reef systems and protect vulnerable coastlines, see Figure 9 (Coastruction, 2023). Therefore, this work will primarily focus on this specific type of application.

Figure 9: Some of the complex shapes that have already been produced

The type of application mentioned in the introduction has some specific requirements. The product needs to withstand salt water, the product needs to be heavy in order to stay on the ocean or seafloor, and the product needs to have some porosity and surface roughness for the marine life to be able to attach or grasp onto the structures. The 3D printed artificial reefs have an organic design containing holes, arches, and cantilevers. Therefore, the reefs also need to have sufficient bending strength to avoid collapsing under their own self-weight. And after curing, the product needs to have sufficient bending strength to be able to be lifted from its arches and to withstand the impact of waves. Additionally, the product also has a lot of requirements that are not application-specific. The artificial reefs need to have sufficient early strength in order to be properly de-powdered, they need to have enough strength after 7 days of curing to be able to be packaged and shipped, they need to be sustainable and durable, the mix design needs to be printable, the mix design needs to (primarily) contain readily available raw materials, and it preferably needs to be cheap.

1.2 Research objectives

All in all, there are a lot of requirements in order to make the concrete suitable for this type of application. The high number of requirements, together with the novelty of the technology make finding the right mix design very challenging. Currently, the company is already able to print structures, however the structures lack sufficient early strength, making it hard to de- powder them. The reefs also sometimes break during transport and so a higher early age strength is required. The research question therefore is as follows:

How to design a strong and sustainable concrete mix for use in 3D concrete printing artificial reefs?

The main objective of this research is to design a concrete mix suitable for 3D concrete printing using selective cement activation to be used to print concrete reef- like structures. The most important objectives are to achieve sufficient early age strength to allow easy de-powdering of the structures and to prevent failure during handling and transport, while still enabling the printing of well-defined and detailed shapes. Making the concrete as sustainable as possible is a secondary goal. Other considerations like product availability, ease of use, durability and cost might also briefly be discussed but are subordinate to the previously mentioned requirements and will not play a significant role in the design process.

1.3 Scope and description of the end product

The final product will be a report consisting of a literature study as well as numerous experiments. This research will try to find a suitable mix design for this specific printer and application. This research does so by investigating the effects of most of the basic material properties, like w/c ratio and particle size distribution, on the strength of the final product. This study also evaluates some additives that may positively affect the properties of the product, e.g. microfibres and accelerators. Additionally, the literature study will also cover some variables unique to 3D printing, like water penetration, layer height and printing speed. The final product will also cover some variables that are unique to 3D printing, like water penetration, layer height and printing speed. The final product will however not go too deep into the working of the printer itself, as the author is only limited to using this specific printer, and therefore cannot study the characteristics of the printer that cannot easily be changed. So, the final product will not contain experiments on the layer depth, type and number of nozzles, material choices not compatible with the machine, and software limitations of the printer. Since this work will contain specific examples using this printer, the report will briefly go into the workings of the printer and its specifications in order to make the reader aware of the possibilities and limitations, and to be able to better justify some of the design decisions made by the author. Stating specific strength requirements are beyond the scope of this report, but the product will be tested and compared with the strength of ordinary mortar. Additionally, the final product will be tested against the initial product to find whether the mix design has improved.

The main objective, improving the early age strength, will be explored by adjusting the w/c ratio, optimizing the particle size distribution, exploring different types of cements and binders, studying certain additives, as well as looking at the printing process and curing stage.

The secondary objective is to improve the printing accuracy and the ease of de-powdering of the printed product.

A third, subordinate objective, making the concrete more sustainable, will be studied by exploring different types of cements and binders and studying the effect of reducing the amount of binder in the particle bed.

1.4 Requirements and restrictions

There are some requirements that the mix design must meet in addition to the mechanical and sustainable requirements stated above. It must be considered that the raw materials and additives need to be able to be handled without very expensive equipment or too much protective clothing, that they have to be widely available, and that they will not affect the local water quality. The powder mix also needs to be able to produce sufficiently accurate shapes and needs to be able to be de-powdered as easily as possible using conventional, simple tools.

The concrete or mortar mix design made in this report will be focusing on production in- house in the Netherlands. Some materials used might not readily be available elsewhere, but the availability and feasibility of certain raw materials and additives will briefly be discussed.

Only basic equipment was available at the printing facility, but the researcher had the option to use more sophisticated testing equipment provided by the Delft University of Technology. This, however, was not always practical due to the printing site not being located near the university.

1.5 Research methodology

The research started with identifying the research question and main objectives of the study, which can be found at the end of the introduction. This was done by talking to the people in the company, reading about the technology, and experiencing the strengths and challenges of this technology first hand. The next step was to do a literature study on the current problems facing this way of 3D printing and finding possible solutions. Afterwards, methods of finding those solutions had to be found. A lot of small experiments have been conducted, some of which can be found in chapter **3.** , and most of them were not very effective. However, after some experimenting, the current approach was found (which is also explained in chapter 3.).

The research is split into three iterations of testing, in order to be able to learn from and improve upon the results found in previous rounds of testing. Every round will consist of the same steps:

1. Identifying current issues with the mix design
2. Literature study and discussions on how to adjust the mix design to mitigate the identified issues
3. Testing preparations, which includes:
    a. Making a timetable
    b. Acquiring the raw materials and testing equipment
    c. Preparing the 3D printer and designing the 3D models
4. Printing the test specimens, and carrying out the strength testing
5. Processing the results
6. Discussing the results and drawing conclusions
7. Repeat

The objective of the first round of testing is to understand the effects of the more basic parameters in the mix design, mainly being the particle size distribution (PSD), the water cement ratio, and the cement content. The second round of testing comprised experiments on accelerators, different types of cement, viscosity modifiers, fibres, and combinations of CAC, gypsum and OPC. The advantage of first splitting the basic material properties and the additives/ materials is that it allows for a better isolation of their effects.

The third round of testing combined the first two rounds. Different basic parameters and additives/ materials were tested simultaneously to try and reach the desired combination of properties. This round aims to learn more about the effects of combining properties and/ or materials on the concrete, so that in this round, a final product can be formulated, which will then be tested and will ideally be an improvement over the current mix design.

2. Literature study

2.1 Mix design

One of the primary objectives of this research is to improve the bending and compressive strength of the concrete, especially the early age strength. In general, there are two ways to improve the strength. The first one is adding, removing or changing the proportions of the 'ingredients' in the powder bed and activator, like adding more water or adding fly ash. The second option is to change the process by for example curing the printed product in a misting chamber after printing or by compacting the concrete. Figure 10 illustrates these different methods of improving the strength. Some methods of adjusting the powder bed, activator or process are discussed below the figure.

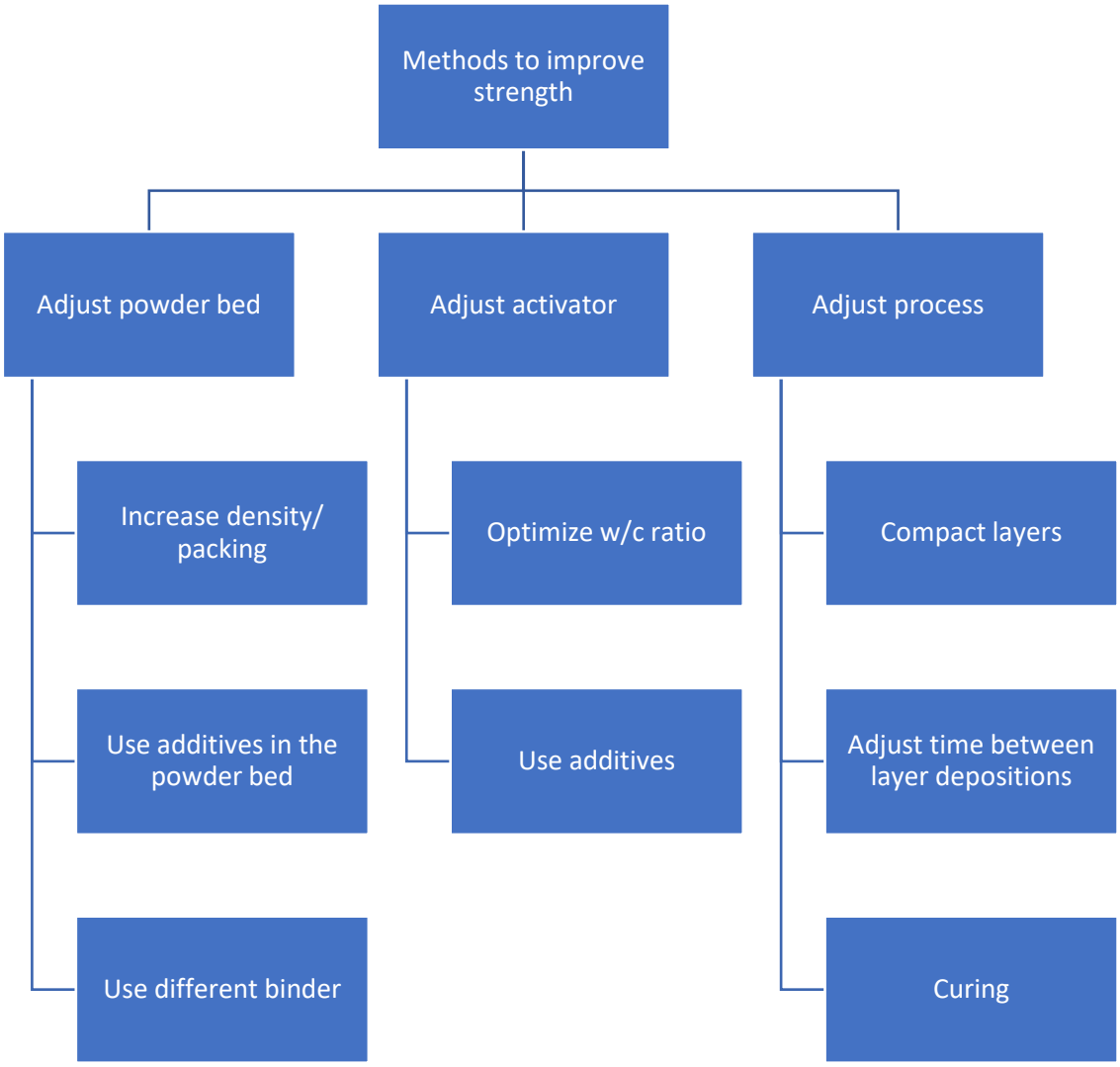

Figure 10: Methods to improve early age strength

Increase density or packing in order to decrease porosity

A lower porosity generally corresponds to a higher strength (Dushimimana et al., 2021).

Use additives in the powder bed

Razzaghian Ghadikolaee et al. (2023) studied the effect of nanomaterials like nano-silica, nano-clay and nanotubes and found them to be promising additives for making high- performance 3D concrete. Such additives might not be cheap and readily available, but they might be worth it when exceptional strength is required. Another example of a powder bed additive is methylcellulose. Lowke et al. (2022a) studied the effect of adding methylcellulose like hydroxyethyl methyl cellulose HEMC to the mixture of a powder bed 3D printer. According to the study, HEMC is a thickener that can affect the penetration depth and speed of the water into the powder bed. This can be useful because it can prevent the water from penetrating into the lower layers with higher w/c ratios, while the high water content can effectively hydrate the current layer.

Use different binder

A secondary goal in this research is to make the concrete more environmentally friendly. Using as little OPC as possible will help accomplish that goal. It is therefore important to look at alternatives that offer as much strength or more as OPC, while also being more environmentally friendly. One promising alternative to OPC that is currently being studied extensively are alkali activated binders (AAB), also known as geopolymer concrete (GC). This alternative will be discussed more extensively further in this report. Other types of binders like CEM II and CEM III still use OPC, but some amount is replaced by industrial waste products. Different binders also exhibit different rates of strength development.

Optimize the w/c ratio

Increasing the w/c ratio usually means lower strength for conventional concrete where the binder and activator are mixed prior to pouring. However, with SCA systems, the activator is poured on top of the particle bed. This results in a relative abundance of activator on top of the layer, but lower amounts in the bottom part of the layer. Increasing the w/c ratio ensures that the lower part of the layer is also sufficiently activated. The water penetration depth ideally needs to be equal to the layer height to reach optimal maximum strength and mechanical bonding with the underlying layer, whilst retaining good shape accuracy (Lowke et al., 2022a; Mai et al., 2022a).

The w/c ratio has a large effect on the strength (Xia et al., 2019a) and the right w/c ratio is not easy to determine for SCA printers. Therefore, this topic will extensively be discussed in this thesis.

Use additives in the water

Additives in the water can serve different purposes. They can increase early age strength by accelerating the hydration, they can modify the viscosity of the water, or they can serve as a plasticizer. Potential additives might be alkali like waterglass or NaOH, especially in combination with GC.

Compacting the layers

Lowke et al. (2022a) studied the effect of compacting the layers and came to the conclusion that compacting the layers could increase the density of the layer by about 30%. It is difficult to adjust the compacting of the layers using the printer used in this study, but the amount of compacting might be studied to make recommendations for future hardware design.

Adjust time between layer depositions

Adjusting the time between layer depositions might affect the water distribution in the layers. Depositing the layer quickly might lead to the water migrating up from the layer below. Depositing too late can expose the layer to the air too long and cause it to dry out (Chen et al., 2022).

Curing

(Lowke et al., 2022a) showed that after- printing treatment leads to a significant increase in strength. Curing can be done by for example submersion in water, but this is only practical for small scale operations. Curing in a misting chamber or by frequently wetting and covering the object are more practical methods for larger structures.

Now that some possible solutions to increasing the strength have been identified, some of these will be discussed in a literature study to better understand what the best options are for optimizing the strength of the concrete. The most promising solutions will then be tested using the available 3D printer. Furthermore, secondary design requirements will also be briefly discussed at the end of this section.

Before these potential solutions are examined, the fundamental mechanics of 3D printing are introduced, beginning with water penetration depth. Studying how the water migrates through the cement- sand mixture is crucial for understanding why parameters like the water cement ratio and the compacting of the layers, or certain additives can have such a huge effect on the strength and printing accuracy of the object that is to be printed.

2.1.1 Adjust activator

Adjusting the activator can involve optimizing the w/c ratio to ensure sufficient hydration and adequate strength development without introducing excess water. The activator may also be modified by incorporating additional liquids or by dissolving supplementary components into the water.

2.1.1.1 Optimize w/c ratio (water penetration depth)

Water penetration depth is an important factor in SCA 3D printing. Too little penetration and the layers will not bond, too much penetration and the lower layers will become oversaturated and start to slump (Lowke et al., 2022a; Zuo et al., 2022). The penetration depth is the measure of how far the water will propagate downwards in a certain timeframe. The penetration depth is dependent on a lot of factors, including the PSD, the reactiveness of the powder (Lowke et al., 2022a), the viscosity of the penetrating liquid and the use of additives. Because increasing the w/c ratio increases the strength in SCA (Lowke et al., 2020; Xia et al., 2019a), using as much water as possible without sacrificing too much printing accuracy is crucial. Consequently, evaluating the activator penetration depth is essential for selecting the optimal water dosage for spraying the powder bed and ensuring sufficient strength

According to Lowke et al. (2022b) the penetration depth is both dependent on the fineness of the particle bed and the reactiveness of the powder. They filled tubes with reactive or unreacted particles and applied fluid from either the bottom or the top. The penetration length was then measured over time, see Figure 11. The figure shows that fine particle beds have substantially lower penetration depths than coarse powder beds, and that the reactive powder (cement) penetrates far less than the unreactive powder (limestone powder).

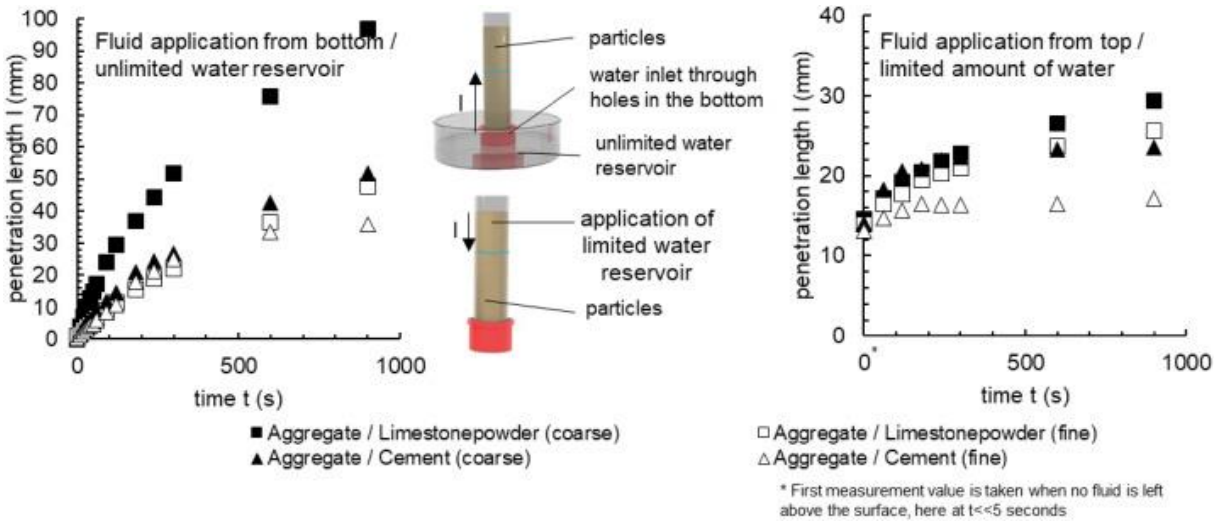

Figure 11: Penetration depth for different powder beds (Lowke et al., 2022b)

Zuo et al. (2022) found in their research that the onset of hydration of the cement does not influence the water penetration depth. The results of their study can be found in Figure 12. In this experiment, three different reactive powder beds were hydrated from the top with a similar setup to the one found in Figure 11. The water penetration through these pure powder beds, which contained no aggregates, was monitored. The onset of hydration for that specific powder bed is denoted with a star. The authors point out that the onset of hydration does not seem to affect the speed at which the water penetrates through the powder bed. However, they say, that around the time of the hydration peaks of the cement and plasters, the water front vanishes preventing further measurement. This disappearance of the water might indicate that if the onset of hydration is accelerated, the water front might disappear faster, and the total penetration depth might be decreased.

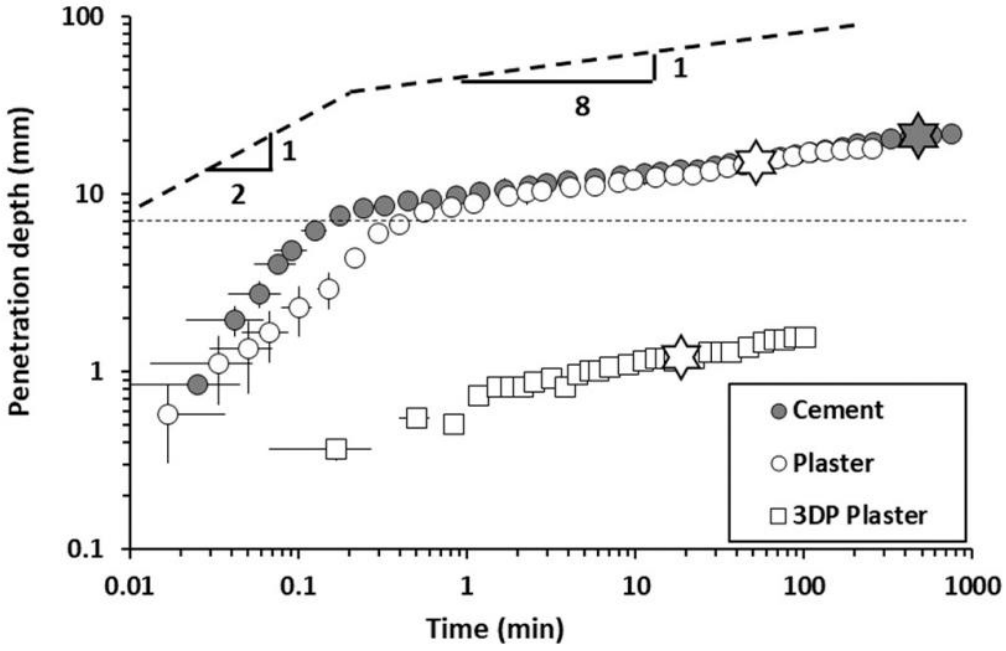

Figure 12: The penetration depth in three different reactive powder beds. The star represents the onset of hydration (Zuo et al., 2022)

An analytical approach to the water penetration depth problem for a very similar SCA printer has also been formulated by (Mai et al., 2022b). The model is based on Darcy's law and the Washburn equation:

$$\text{Darcy's law:} \quad dV = \frac{KA\Delta p}{\eta l} dt \tag{1}$$

With V being the volume, K being the permeability, A being the area of the sample, p is the pressure, η is the fluid viscosity and l being the wetted height.

$$\text{Washburn equation:} \quad \Delta p = \Delta p_{hyd} + \Delta p_{cap} = \rho g l + \frac{2\gamma cos\vartheta}{r_p} \tag{2}$$

Where p_{hyd} and p_{cap} are hydrostatic and capillary pressure respectively, ρ being the fluid density, g being the gravitational acceleration, γ is the fluid surface tension, ϑ is the contact angle between the liquid and solid and r_p is the capillary radius. In particle beds, the capillary radius can be simplified to be a function of the particle radius: $0.2r_{particle} \leq r_p \leq r_{particle}$ (Mai et al., 2022b). Mai et al chose the pore radius to be equal to $0.2r_{particle}$ and found this to be a valid assumption in their case.

Mai et al. state that the water penetration consists of 2 phases: the spontaneous capillary intrusion phase and the capillary- induced intrusion phase. These two phases can also be clearly seen in Figure 18, Figure 11, and Figure 12, where there seems to be a very fast initial penetration phase and a second slower penetration phase. The spontaneous capillary intrusion is the first phase and is driven by laminar flow. Zuo et al. (2022) describe the first phase as being the fast penetration regime, which ends when the water on top of the sample has fully penetrated and the pores in the powder bed have been fully saturated. The spontaneous capillary intrusion length of a droplet in a tube with area *A* can be described using the following equation:

$$l_s = \frac{V_0}{p\varepsilon A} \tag{3}$$

Where l_s is the spontaneous capillary intrusion length, V_0 is the volume of the penetrating droplet, ε is the porosity and p is the pore filling degree. Mai et al. found the pore filling degree to be approximately 0.62 but mentioned that this value may change slightly with the particle size distribution. However, in their investigated range, the pore filling degree varied by less than 10%. The spontaneous capillary intrusion phase stops when there is no more water on top of the particle bed and only takes a couple of seconds.

The capillary induced intrusion phase starts when the first phase ends and is governed by capillary suction (Mai et al., 2022a). The saturated pores will now start to desaturate as water penetration goes on (Zuo et al., 2022). The speed at which the water penetrates the powder is significantly slower than in the first phase, and gradually slows down as a decrease in saturation of the pores leads to a decrease in relative permeability (Zuo et al., 2022). Mai et al. found that in their investigated range, the capillary intrusion length was independent of the amount of applied fluid. In the paper the fluid is considered to flow through a cylindrical tube filled with particles:

$$dV = \varepsilon A \, dl \tag{4}$$

Where V is the fluid volume, ε is the porosity and A is the area of the tube. According to Zuo et al. (2022), this water penetration stops when the pore saturation reaches a critical saturation level where the liquid network in the porosity will disconnect.

This slowly desaturating of the pores might be an issue if the onset of hydration is slow, since the saturation level might reach a level below which proper cement hydration can occur (Zuo et al., 2022). Zuo et al. (2022) then state that this can be solved by using a correct sizing of the aggregates to decrease the porosity of the powder bed. This will increase the time for the spontaneous capillary intrusion to take place and will also slow down the capillary- induced intrusion phase.

When substituting Darcy's law (*1*) and the Washburn equation (*2*) into (*4*), the equation for the capillary fluid intrusion time can be obtained:

$$t_c = \tau \left[\frac{l_c}{H_{eq}} - ln\left(1 + \frac{l_c}{H_{eq}}\right) \right] \quad (5)$$

Where $\tau = \frac{\varepsilon \eta H_{eq}}{\rho g K}$ and $H_{eq} = \frac{2\gamma \cos(\vartheta)}{r_p \rho g}$ are introduced to simplify the equation. To apply this equation to the 3D printing process, the authors introduced two experimentally obtained functions; the pore saturation function $S(t)$ and the hydration function $H(t)$. The pore saturation is introduced because only a fraction of pores is actually transport relevant, as is evident by the previously mentioned pore filling degree being only 0.62. However, this fraction of transport relevant pores decreases as the fluid is distributed over a larger volume and some of the fluid will remain on the surface of already wetted particles. Mai et al. determined the saturation function by measuring pore saturation in non- reactive particle beds and using linear regression to fit the function to the measurements. The pore saturation function $S(t)$ was found to be as follows:

$$S(t) = 0.637 - 0.0072\sqrt{t} \quad (6)$$

Where the start value is equal to the initial pore filling degree p mentioned earlier.

The hydration function $H(t)$ was found by fitting the modelled values to the measured capillary intrusion lengths of a number of reactive particle beds used in the study and with varying cement/ aggregate ratios, see Figure 14. The hydration function was then found to be:

$$H(t) = \begin{cases} 0.196 - 0.003\sqrt{t}\,; & for\ reactive\ mixes \\ 1\,; & for\ non-reactive\ mixes \end{cases} \quad (7)$$

The functions can then be added to the model by adjusting τ:

$$\tau = \frac{\varepsilon \eta H_{eq}}{S(t)H(t)pgK} \quad (8)$$

In order to apply this model to a multilayer SCA 3D printer, the authors point out that a number of constants need to be given. Firstly, the point in time when the final intrusion depth is reached, i.e. the setting time ($t_{setting}$) needs to be estimated. Next, the layer height (l_{lay}) needs to be given as well as the layer application time (t_{lay}). With these constants, the final printed height of the printed specimen can be estimated (Mai et al., 2022b):

$$l_{print,calc} = n_{tot} l_{lay} + l\left(t_{setting}\right) - l_{lay} + \begin{cases} 0\ ; & if\ l_{lay} \geq l_s \\ \left(l_s - l_{lay}\right)\frac{t_{lay}}{t_{setting}}\ ; & if\ l_{lay} < l_s \end{cases} \quad (9)$$

With $l\left(t_{setting}\right)$ being the total intrusion length ($l_{tot} = l_s + l_c$) when no further fluid intrusion takes place.

According to Mai et al., there are a large number of variables that influence the penetration depth/ intrusion length: pore size r_p, porosity ε, permeability K, contact angle ϑ, the amount, fineness and type of cement and aggregates, fluid viscosity η and the applied amount of water V_o.

2.1.2 Adjust powder bed

Modification of the powder bed can entail several types of adjustments. First, optimizing the particle packing can increase the density and consequently reduce the porosity. In addition, various additives may be introduced to achieve different effects, such as accelerating hydration, providing mechanical reinforcement, or regulating water penetration. Finally, the selection and dosage of binders can be varied to further control the mechanical and microstructural characteristics of the powder bed

2.1.2.1 Particle size

Correct aggregate particle size distribution is a crucial step in the design process of particle bed 3D printing. The sizes of the particles determine the porosity of the particle bed. The porosity of the particle bed in turn affects the strength and the required w/c ratio. Additionally, the particle sizes govern the penetration depth and speed of the liquid into the particle bed (Lowke et al., 2020). Therefore, adjusting the aggregates and their size distribution is a complex process that affects the properties and printing process (Lowke et al., 2022a).

A method to determine the particle size distribution is to use the Modified Andreasen and Andersen model (MAA), see equation (*10)* (Yu et al., 2015). The distribution modulus q is firstly taken as 0.23 based on previous studies that used it for fine particle sizes (Indhumathi et al., 2022).

$$CPFT = 100\left[\frac{d-d_{min}}{d_{max}-d_{min}}\right]^{q} \qquad (10)$$

Where,

d is the size of the particle, d_{min} is the minimum particle size, d_{max} is the maximum particle size
q is the distribution exponent
$CPFT$ is the Cumulative Percent Finer Than the particle size d.

This MAA model can be combined with the known PSD of the raw materials that are available for use to reach the optimal overall PSD.

Elkem Materials Mixture Analyzer (EMMA) is a free software program that can be used to predict this optimum blend of raw materials. The user inputs the particle size distribution of the raw materials, and then by adjusting the material percentages, the program can find the optimal material quantities to best fit the MAA curve. Figure 13 shows a PSD used in this study (blue line) that follows the MAA PSD (red line) as closely as possible, given the available aggregate sizes. The table on the right, created in EMMA, shows the PSD in terms of percentage of volume of this optimized PSD.

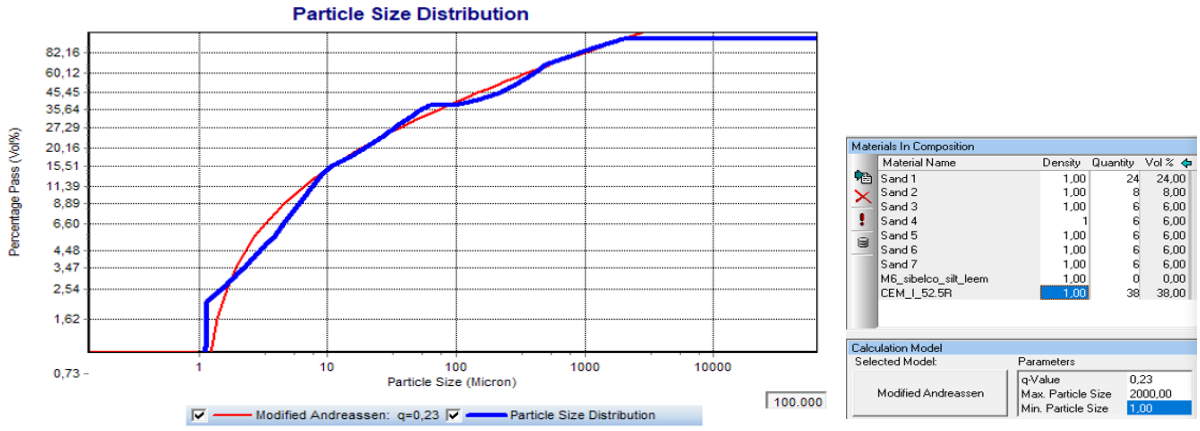

Figure 13: The optimal particle size distribution, according to EMMA software, using the available grain sizes. The red line represents the optimal PSD according to MAA, and the blue line represents the PSD that is being used in this study.

Lowke et al. (2020) reported that an increase in aggregate size, from 140 µm to 450 µm, was accompanied by an increase in strength, from 6 MPa to 16 MPa. They reasoned that this was due to the increase in pore size when using larger particles, which made the water penetrate deeper into the layer. It must be noted that this means the increase in strength is more attributed to the water penetration depth than to the particle packing itself. Additionally, the larger aggregate sizes meant that the aggregates were larger than the layer height used in their study. This particle interlocking between the layers allows for the transfer of shear forces between the layers (Lowke et al., 2020).

Aggregate sizing influences the porosity and therefore also the water penetration depth, as was found in the analytical approach of Mai et al. (2022b) and the experimental approach by (Lowke et al., 2022a) found in Figure 11 (see section 2.1.1.1).

2.1.2.2 Binder content

The cement content should preferably be kept as low as possible to reduce costs and make the concrete more sustainable. However, binder content can also be used to control the water penetration depth. First, the cement/ aggregate ratio can play an important role in obtaining the desired particle size distribution. Cement has a very small particle size, much smaller than sand, and is therefore useful in optimizing the PSD, by for example using the MAA method. Secondly, cement is reactive and influences the penetration depth, as is illustrated by equation (*7)*. Lowke et al. (2022a) showed that reactive particle beds behave differently than unreactive ones. Furthermore, Mai et al. (2022b) measured the water penetration depth in particle beds with different cement contents and found that a higher cement content corresponds to a lower penetration depth, as shown in Figure 14.

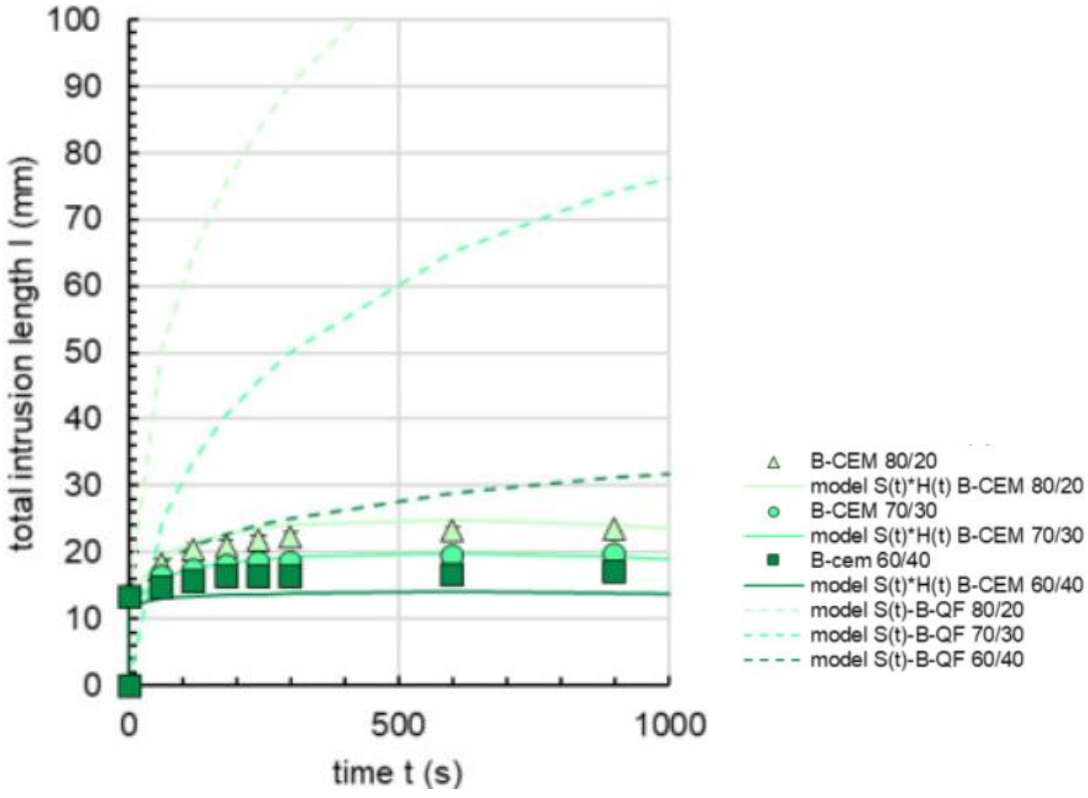

Figure 14: Intrusion lengths for different cement/ aggregate ratios (Mai et al., 2022b). The numbers followed by CEM is the ratio of aggregate to cement. This figure, amongst others, was used in their study to find equation (7)

2.1.2.3 Alternative binders

In section 2.1.1.1, it was found that the setting time influences the penetration depth. A longer setting time corresponds to a larger penetration depth. This can be intuitively explained by the fact that the water has more time to permeate through the particle bed. Therefore, an accelerated cement hydration can be beneficial when a decrease in water penetration depth is needed.

Another reason to experiment with alternative binders is to increase early strength. Alternative binders may have faster initial strength development, compared to OPC. An example of such an alternative binder is Calcium Aluminate Cement (CAC). CAC is generally made from limestone and a source of aluminium like bauxite (Scrivener, 2003). CAC by itself has a similar setting time to OPC, but when adding varying amounts of CAC to OPC, the setting time can dramatically be reduced, and in some ratios, can even result in flash setting of the mortar (Dorn, 2022)(Scrivener, 2003). CAC can be used by itself, or can be mixed with other binders like OPC, limestone or gypsum to combine properties and create a broad range of specialist mortars (Scrivener, 2003). Dorn et al. (2022) categorized these mortars using the ternary diagram found in Figure 15. According to the researchers, there are six distinct types of mortars to be found when combining CAC, OPC and CS in various proportions. In this case CS stands for calcium sulphate, like gypsum or bassanite. Blended systems outside these zones are rarely used as these show various shortcomings, like excessive expansion (Das et al., 2022). Zone 1 contains binary compositions of OPC and CAC where CAC content is under 10 wt%. In this zone, setting time decreases with increasing relative amounts of CAC due to increased initial ettringite formation (Dorn et al., 2022). The main silicate reaction of the OPC is not delayed, and may even be accelerated (Dorn et al., 2022). However, with higher ratios of CAC in zone 3 (<30 wt%), the silicate reaction is significantly delayed and flash setting occurs due to fast ettringite precipitation (Dorn et al., 2022). Correct mix designs in zones 1 and 3 can have setting times of around 2 hours and can achieve strengths of up to 20 MPa after 6 hours, but will have poor long-term strength development (Scrivener, 2003). Additionally, binary systems can be prone to shrinkage issues (Das et al., 2022). The heat generation of CAC's is very high, and therefore the concrete needs to be kept wet to prevent drying and dehydration (Scrivener, 2003). Scrivener (2003) recommends the formwork needs to be removed in 6 hours to spray the surface for larger sections. Similarly, shrinkage also happens faster in CAC compared to OPC due to the much faster hydration according to Scrivener (2003). They therefore recommend prolonged moist curing, minimizing paste volume, and the use of polymeric fibres to prevent excessive cracking due to shrinkage.

Zone 2 includes compositions where CS is added to prevent this retardation of the main silicate reaction (Dorn et al., 2022). Initial and final settings times in this zone can be under 20 minutes, which can be controlled with mix composition (Dorn et al., 2022). Blended systems in this zone also show fast strength development but do not suffer from shrinkage problems and have better long term strength development (Das et al., 2022).

Zones 5 and 6 are compositions containing mostly CAC and CS, with small additions of OPC only acting as a source for calcium in systems with lower calcium/ aluminate ratios in the CAC (Das et al., 2022). These zones show fast ettringite and AH_3 formation (Dorn et al., 2022). Ratios in these zones can be adjusted to be fluid for a few hours and then harden rapidly (Scrivener, 2003). The main difference with the compositions of these zones compared to the zones 1 and 3 is their rapid drying, which is why they are most commonly used for floor-levelling (Scrivener, 2003). Similarly to zones 1 and 2, these zones show rapid early strength development mostly attributed to ettringite formation (Scrivener, 2003). Moreover, mixes in zones 5 and 6 are shown to improve dimensional stability in extrusion 3D printing applications (Das et al., 2022).

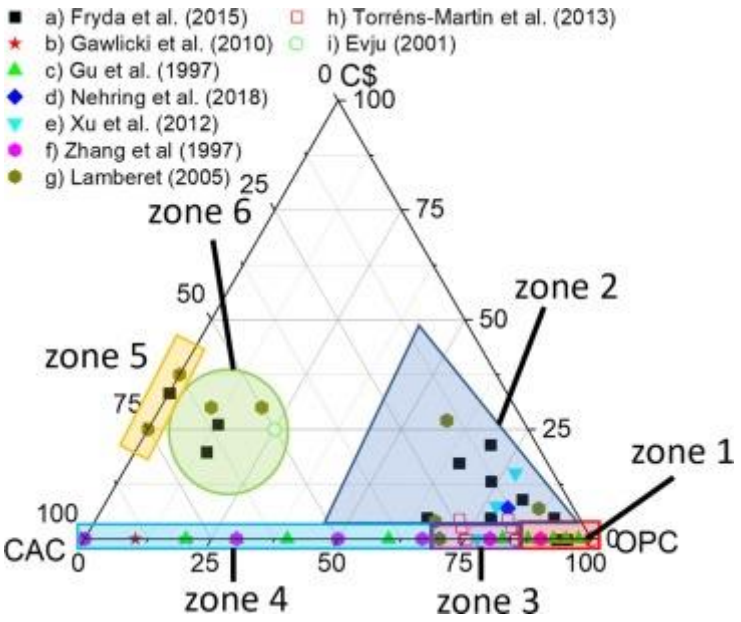

Figure 15: The ternary diagram of CAC-OPC-CS (Dorn et al., 2022)

Blended systems of CAC-CS-OPC can be very useful for powder bed 3D printing, due to their early strength development and fast setting. Additionally, most zones show fast ettringite formation, which can bind a lot of water very rapidly, impacting the rheology within minutes (Das et al., 2022). This may be used to decrease water penetration depth and may therefore achieve higher dimensional accuracy of the printed products.

The production of OPC is paired with a high amount of CO2 emissions (de Brito & Kurda, 2021). It is therefore preferred to use as little OPC as possible. An option to decrease the OPC usage is by choosing to use CEM III. CEM III/B is a more sustainable choice since it replaces 66 – 80% of the OPC with blast furnace slag (BFS) (EN 197-1).

Another benefit of cement with BFS over OPC is that it improves durability, for instance when used in seawater (Jau & Tsay, 1998; Qu et al., 2021)).

The compressive strength of OPC decreases when exposed to salt water, while the strength of OPC in combination with BFS increases over time (Jau & Tsay, 1998; Qu et al., 2021)). An explanation for this phenomenon is that the BFS in the cement mix produces C-S-H gels that fill the pores, increasing the strength over time, even when immersed in seawater (Jau & Tsay, 1998).

Another way to limit the amount of OPC in the powder bed is to instead use an Alkali Activated Binder (AAB), also known as Geopolymer concrete (GC). Geopolymer concrete consists of a binder like, BFS Fly-ash or metakaolin, and an activator, like sodium hydroxide (NaOH) or waterglass (Na2O / SiO2) (Verma et al., 2022). Besides being more sustainable, GC has other benefits over OPC, like improved early age strength and better properties against seawater (Verma et al., 2022). However, there are some significant practical downsides. First of all, GC needs an alkali activator, which are often corrosive. This means that some of the components of the 3D printer need to be alkali-resistant. A second downside is curing. After printing the GC needs to be cured in order to reach proper strength. During curing, the GC needs to be wetted using an alkali solution, and in some cases even needs to be cured under elevated temperatures (Verma et al., 2022; Xia et al., 2019b). Possibly even bigger downsides are the required safety precautions and the ease of use. The alkali activator that is used can cause skin burns and therefore requires the operator of the printer to wear protective equipment like gloves and safety goggles. Furthermore, respirators and mechanic ventilation might also be required because some geopolymers like metakaolin and silica fume are very fine and therefore become airborne very easily. Working with these materials in a closed facility indoors might exceed the permissible dust exposure limits regulations set by the EU (Keramost, 2008).

2.1.2.4 Cellulose Ethers

Additives can be used to decrease the penetration depth, to be able to add more water without oversaturating the lower layers. One possible method to test the ideal penetration depth and w/c ratio is to use tubes as described by Lowke et al. (2022a) and Mai et al. (2022a). The researchers filled glass tubes with cement and sand and added varying amounts (up to wt 5%) of Hydroxyethyl Methyl Cellulose (HEMC) to the cement (see Figure 16). Then a finite amount of water was added to the top of the tube, to simulate the conditions in a 3D printer. The penetration depth over time for different amounts of HEMC can be found in Figure 17 and 18. It can be seen that even a small amount of HEMC can drastically reduce the penetration depth. It has to be noted however that HEMC is lighter than cement and that 3 wt% of HEMC amounts to 8 vol% in the powder mix used in the research of Lowke et al. (2022a). The researchers even found that HEMC increased the compressive strength of the mix in low dosages. In their study, the compressive strength increased from 14 MPa (0 wt% HEMC) to 20.5 MPa (1 wt% HEMC).

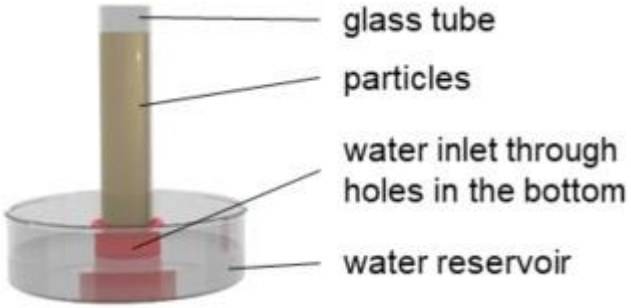

Figure 16: The test setup used in both experiments by Lowke et al. (2022a) and Mai et al. (2022a). Photo taken from Mai et al. (2022a). In this picture the water inlet is at the bottom, but in some experiments the bottom reservoir was left empty and only the top part was filled.

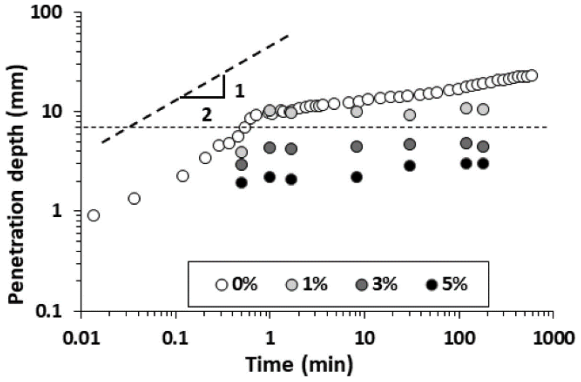

Figure 17: The effect of HEMC on the water penetration depth (mass ratio) (Lowke et al., 2022a).

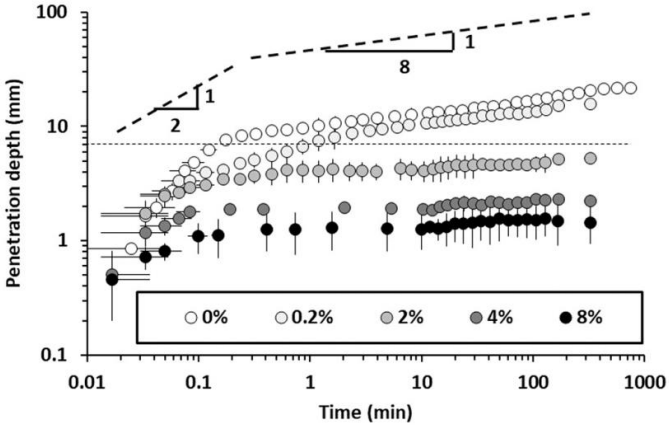

Figure 18: The effect of HEMC on penetration depth (mass ratios) (Zuo et al., 2022)

The researchers attributed this increase in strength to the absorption and subsequent release of the water by the methylcellulose, which may increase the degree of hydration around the methylcellulose. At higher dosages, the HEMC will provide an adverse effect on the strength, which the author had several possible explanations for. Firstly, the HEMC will decrease the density and porosity of the particle bed (Zuo et al., 2022). Secondly, the high dosage of HEMC reduced the penetration depth excessively, leading to insufficient hydration in the lower part of the layer and, consequently, poor bonding to the previous layer. And lastly, the cellulose can cause a delay in cement hydration, resulting in a delayed setting and hardening time (Li et al., 2025).

2.1.2.4 Fibres

The main reasons for adding fibres in the matrix are to improve flexural strength properties and prevent cracking (Dushimimana et al., 2021). Different types of fibres improve upon different material properties, and so combining fibres can be helpful to improve the overall mix design (Dushimimana et al., 2021). Steel fibres for example can increase the tensile strength significantly, while synthetic fibres can improve compressive strength in regular concrete (Dushimimana et al., 2021).

de la Fuente et al. (2022) use a very similar type of 3DCP as used in this study and tested steel, polymeric and PVA fibres in their study. They recommend a volumetric fibre content of 1 to 1.8%, depending on the type of fibre. Steel fibres significantly outperformed other types of fibres in their study, as seen in Figure 19. However, steel fibres are susceptible to corrosion when used in seawater applications. Furthermore, both synthetic and steel fibres are not sustainable options.

The type of fibre needs to be carefully chosen in applications where sea life comes into close contact with the objects to prevent accidental ingestion.

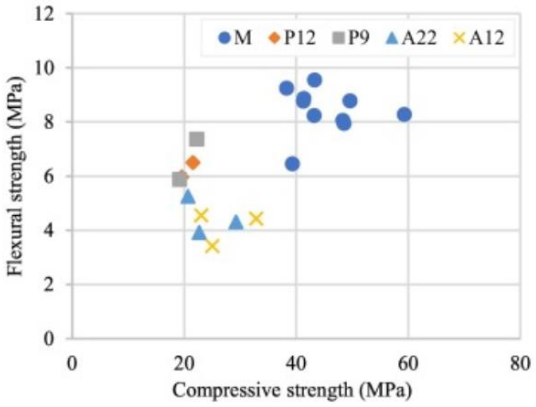

Figure 19: Flexural strength for different types of fibres (de la Fuente et al., 2022). 'M' is metallic, 'P' is polymeric and 'A' is PVA.

Cellulose fibres are a sustainable alternative to other, more conventional types of fibres like steel or synthetic fibres. Cellulose fibres are derived from wood, bark, leaves or other plant- based materials like bacteria (Li et al., 2025). Because of this, cellulose fibres are biodegradable (Santos et al., 2021) and are therefore safer to introduce in structures for underwater use without posing harm to the environment or underwater life. Cellulosic fibres are available in different sizes, but sizes under 1 cm, often referred to as pulp, are often used in 3D concrete extrusion printing for their workability (Li et al., 2025). However, these shorter fibres are often not as effective at bridging cracks and are relatively weak (Li et al., 2025).

Cellulose fibres influence the strength of the cementitious material in multiple ways. Natural fibres like cellulosic fibres have been shown to be able to reinforce concrete, increasing the mechanical strength, durability and ductility (Pacheco-Torgal & Jalali, 2011). Moreover, cellulosic fibres can act as fillers, improving the PSD, and can also act as nucleation sites and promote hydration (Li et al., 2025). Li et al. (2025), state that the improved hydration is due to the fibres adhering to the cement particles. During hydration, a layer of hydration products surrounds the cement particle, inhibiting further hydration. However, the cellulose fibres create a pathway for the water to reach the cement particles, improving hydration, and therefore, strength (Li et al., 2025).

In recent years, wastewater treatment facilities have begun experimenting with extracting cellulose fibres from the wastewater, further improving the circularity of these fibres (Li et al., 2025).

2.1.3 Adjust process

The material properties of a 3DCP object are not only dependent on the aggregate, binder, additives and activator, but also on the printing and curing regimes. The printing and curing procedures play a crucial role in determining the properties of the final product.

2.1.3.1 Compacting

Compacting is a key step in the printing process. Similar to vibrating fresh concrete, compacting will reduce the amount of voids in the material, increasing its density. This decrease in porosity comes with an increase in particles directly contacting each other, improving load transfers (Lowke et al., 2022a). Studies have shown that even a slight increase of 1 percent in void space can decrease the compressive strength of concrete by 4 to 6 percent (Gao et al., 2015).

However, because compacting means decreasing the porosity, it will also decrease both the spontaneous and capillary intrusion lengths (Mai et al., 2022b). A decreased penetration depth can be disadvantageous, as the water should at a minimum penetrate through the entire layer and reach the layer below it to have a good bond between the layers. However, in most cases a lower penetration depth is desirable, since excessive penetration can compromise printing accuracy. Decreasing the porosity will also slow down the capillary induced intrusion phase, as discussed in section 2.1.1.1. In short, a reduced capillary intrusion rate can be beneficial because it limits water migration before cement hydration occurs. This helps maintain the pore saturation level above the threshold required for proper hydration.

Compacting can be done in multiple different ways. de la Fuente et al. (2022), used a weight that was manually placed on the layer, but this is only useful in small scale test setups. For their larger scale tests, they would switch to a roller that applied a constant force.

Lowke et al. (2022a) also used a forward rotating roller to compact the layers. In both studies, the degree of compacting was controlled by increasing or decreasing the amount of deposited material. So, if the height of the initially deposited material would be 1.5mm, and the final height of the layer would measure 1.0mm, then the compacting height would be 0.5mm. Both studies showed a significant increase in strength with higher degrees of compaction. de la Fuente et al. (2022) even managed to increase their compressive strength from 15.9 to 20.0 MPa just by adjusting their level of compression and layer height. The results from Lowke et al. (2022a) can be found in Figure 20. The increase in strength found in this figure is even more pronounced, going from about 16 MPa to 26 MPa. However, the compaction height cannot be increased infinitely. Since compaction needs to take place after every deposited layer, the layers below will also undergo some compression. This can become problematic once the printing process takes long enough for the lower layers to start setting. Once the lower layers get stiffer, they might crack due to the tensile strength induced by the compressive force applied on the top layer (Lowke et al., 2022a).

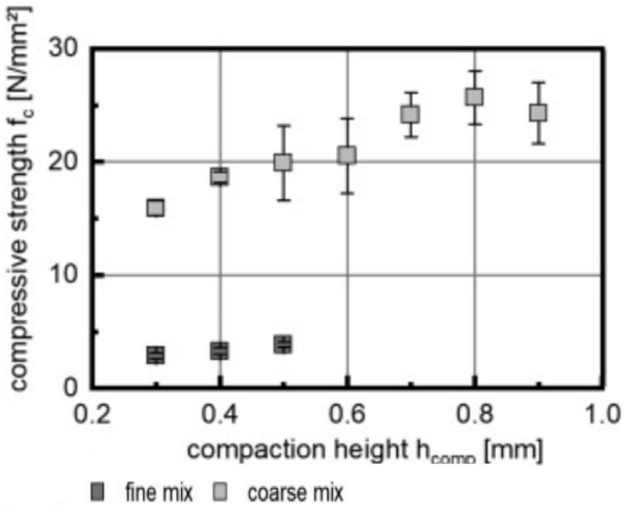

Figure 20: Compaction height versus compressive strength. The final layer height is 1.0 mm (Lowke et al., 2022a).

Another method of compaction is the use of an inclined blade, which is likely popular due to its simplicity. However, an inclined blade delivers less force on the underlying layer than a roller would (Wang et al., 2021). Furthermore, a blade might degrade the layer surface by dragging larger particles across its surface (Talke et al., 2023).

2.1.3.2 Curing

Curing is the process of controlling the temperature and promoting the hydration of the mortar or concrete after casting, or printing. The aim of curing is to allow for hydration of the cementitious material, increasing the strength. Promoting this hydration is done by introducing moisture. Sufficient moisture is critical, as without at least 80% relative humidity in the pores, hydration stops (Pawar & Kate, 2020). Moreover, without proper hydration, the surface may dry and shrink, causing microcracking (Pawar & Kate, 2020). There are multiple ways to introduce this moisture and prevent drying. Some of these are: spraying the surface with water, submerging the object and covering the object with plastic or another impermeable material to prevent evaporation. There are also more advanced curing methods such as steam curing. Curing is often maintained for at least 7 days for achieving maximum strength (Al-gburi et al., 2025).

Not all curing methods perform the same. Pawar and Kate (2020) compared submerged curing and wet gunny bag curing, which involves covering the concrete with a wet sack made of canvas to prevent it from drying out. After 28 days, the respective compressive strengths were 26.8 MPa and 25.5 MPa.

2.2 Tertiary design requirements

2.2.1 Toxicology

The concrete structures are intended to come into close contact with fish and other marine animals. It is therefore important that the concrete does not leak harmful substances into the environment. Berthomier et al. (2021) researched the leaching of crushed CEM I and III in water and found that only small percentages of the heavy metals found in the pastes leached into the water, as can be seen in Figure 21. It needs to be noted that this experiment was done using crushed cement, and that thus the amount of harmful elements leaked into the environment for intact structures is likely lower.

Leaching coefficient	Ca	Si	Al	Mg	Total
CEM III paste leached by DW	32.4	9.2	1.4	2.2	45.2
CEM III paste leached by MW	29.1	8.6	1.1	1.5	40.3
Slag leached by DW	14.9	8.1	0.9	2.8	26.7
CEM I paste leached by DW	49.2	11.8	1.0	0.6	62.6
CEM III paste leached by DW estimated by Eq. (1) with y = 31	25.6	9.3	0.9	2.1	37.9

Figure 21: Coefficients of leached for different elements (Berthomier et al., 2021). Leaching coefficient is defined as the amount leached over the amount originally found in the paste.

Furthermore, the contents of some (harmful) compounds in cement are regulated by NEN- EN 197. It is very difficult to estimate the amount of harmful substances that the fish will come into contact with, as this would depend on the leaching of the concrete, the dispersion of the elements in the water, and the behaviour of the marine animals. To find a definitive answer, more research needs to be done on this topic, but due to the amount of work this would require, this falls beyond the scope of this research.

2.2.2 Sustainability

Water and aggregates (e.g. sand) are the first and second most exploited natural resources in the world (UNEP, 2022). Environments where sand bodies are subject to erosional and deposition processes, like rivers and estuaries, require careful management (UNEP, 2022). Since both fresh water and river sand are increasingly scarce, it is more sustainable to use seawater and sea- sand for printing. Using seawater and/ or sea- sand in the mix design also has the added benefit of potentially reducing transport lengths and thus reducing transport- related CO2 emissions, making the concrete more sustainable.

Sea-sand is already widely used in coastal countries like Japan, the Netherlands and Hong Kong, but the sea- sand is usually desalted (e.g., washed with freshwater) to avoid steel corrosion (Xiao et al., 2017). The printed product used in this study is not reinforced with any steel reinforcement, however, the printer itself does contain steel parts susceptible to corrosion.

A literature review by Xiao et al. (2017) describes the effects of using sea- sand and/ or seawater in the production of concrete. Firstly, most researchers have agreed that the early age compressive strength of sea- sand concrete using OPC is equal to or slightly higher than that of ordinary concrete. Sea- sand concrete was even found to have better flexural strength than ordinary concrete. Additionally, many studies found that the seashell content in the sand had little to no effect on the compressive strength (Xiao et al., 2017).

Secondly, most research found that seawater concrete had a higher early age strength, similar to sea-sand concrete. Additionally, the strength of seawater concrete seems to have a lower 28- day strength while the long- term strength was found to again be a little higher than that of ordinary concrete.

When using both sea-sand and seawater in concrete (SSC), existing studies found that SSC has a significantly higher 7- day compressive strength, followed by a slower compressive strength development than ordinary concrete (Xiao et al., 2017).

3. Materials and methods

In the literature study some variables have been found that (likely) influence the strength and shape accuracy of the 3D printed concrete produced with SCA. To determine the most suitable powder mix, it is necessary to understand how each parameter affects the final product. This requires experiments in which the influence of individual parameters is isolated, allowing their optimal values to be established. For example, the water cement ratio can be varied to see at what value the strength is optimal and at what value the shape accuracy is still acceptable. To achieve this parameter isolation, multiple mix designs were prepared and tested under identical conditions to identify differences between them. A basic mix design currently being used in this printer was chosen as the standard design to compare every other mix to (see section 3.3). Every mix design only has one parameter that differs from this 'standard' mix in order to isolate the effect of said parameter. Since most of the tested changes to the mix design alter the water requirement, the w/c ratio was varied for every mix design. This approach allows the determination of the optimal w/c ratio for the specific parameter under investigation. For example, the PSD influences the void ratio in the cement and therefore the water requirement might change to get good strength and shape accuracy. Therefore, for every change in PSD that was tested, the w/c ratio would be changed 3-4 times to find the optimal w/c ratio where both the strength and shape accuracy were found to be the best.

The experiments will test both the early age strength and the shape accuracy to find the optimum where the strength is highest and the shape accuracy is still acceptable. Different shapes and methods have been tried to help determine the shape accuracy of a certain powder mix, and eventually a starfish shape was chosen that was to be graded using a 1 to 10 grading system.

There are three phases in the lifespan of a 3DCP product where different forces are acting upon the object: The de-powdering phase, the transportation phase, and the in-use phase. During the de-powdering phase, the object is removed from the supportive powder. The main force acting upon it is the self-weight. However, the object is around one day old in this phase and therefore the strength of the product is still low. The product has undergone some curing when transportation occurs, meaning that some more strength development likely has occurred. The assumption that curing increases the strength will also be tested in this research. Forces acting upon the object in this phase are harder to predict, but could also be critical, especially when lifting the object or when stacking multiple objects on top of each other. During the in-use phase, the concrete is subjected to wave impact forces and possible collisions with boats and recreational vessels, amongst other forces. The strength of the object in this phase is likely even higher than in the transport phase, as even more time has passed in which strength development can occur. However, in this phase durability issues can affect the strength. It was chosen to focus on the strength after the de-powdering phase in this study, since this was the phase where most strength issues arose in previous testing.

One of the biggest benefits of particle bed printing over other types of printing or casting is that it features the possibility of creating unsupported overhangs and arches. This however means that after de-powdering, these arches will have to, at the very least, support their own weight and in some cases also some external forces. Therefore, it is important for the concrete to have some resistance to bending, in addition to having a good compressive strength. Because of this, the decision was made to test the concretes in both bending and compression.

The 3D concrete printer used in this study can print up to 25*25*15 cm, so standard sizes for compressive and bending test specimens were not achievable. Since printing duration scales with the printing dimensions, of which mainly the height increases printing time, it was important to stack as many objects as possible next to each other in the horizontal plane. Moreover, decreasing the height also decreases the material usage. Ultimately, the layout as seen in Figure 22 was chosen with six beams, six compression cubes and one starfish.

After printing, the specimens are placed in the climate chamber where the temperature does not fall below 20 degrees Celsius. After 24 hours ± half an hour, the test specimens are cleaned and immediately tested.

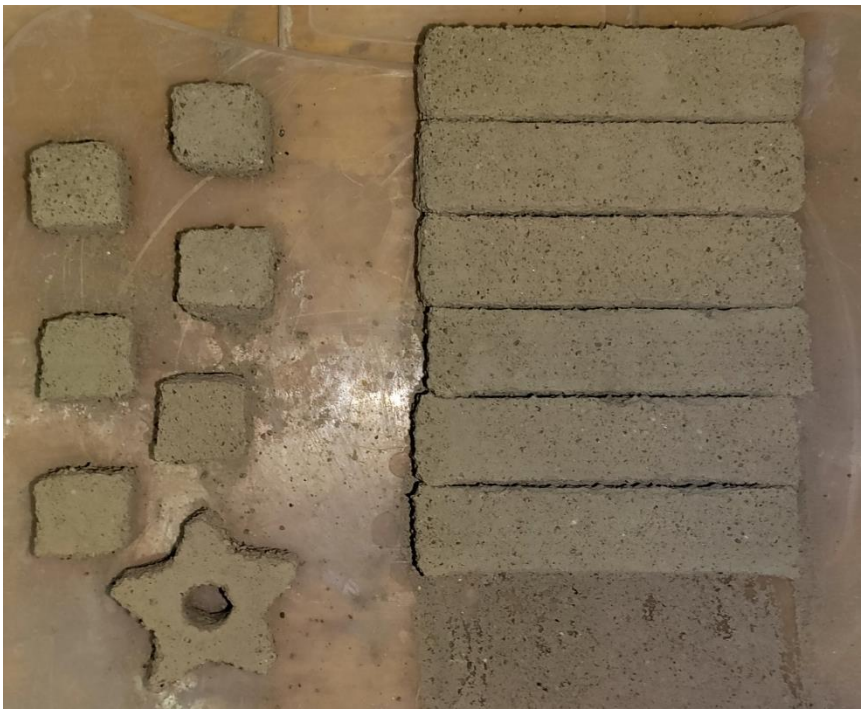

Figure 22: Six beams and cubes can be fitted in the dimensions of the printbox

3.1 Bending and compression tests

Compression and 4- point bending tests were carried out to determine the strength of the concrete mix. Both bending and compression tests were done using a Mecmesin advanced force gauge mounted on a Chatillon TCM 201-M displacement control test stand. The test cubes had dimensions of 30*30*30 mm and were compressed until failure, after which the highest force was noted, see Figure 23. ASTM standard C78 was followed as closely as possible for the bending test setup. According to ASTM C78, the depth and width of the beam need to be 1/3 of the span, but this was not practical since this would mean that only 10 beams could be printed at once. Instead, it was opted to use beams with dimensions of 30*30*130 mm, so that there is room for 18 beams (3 times the layout found in Figure 22). Figure 26 and Figure 27 show that the dimensions of the printed specimens may differ from one another, influencing the strength test results. Larger test objects have more area over which to spread the compressive force, and a larger second moment of area to resist bending. The increase in size is caused by partially hydrated mortar adhering to the intended printed area. Because this material is only partially hydrated and thus the strength is likely far lower than that of the fully hydrated mortar, it was hypothesised that this added size would only play a minor role in the stress distribution within the block.

As a result, the added size is assumed to only marginally affect the strength. For this reason, the modelled dimensions were used to calculate the strength of both the cubes and beams. Furthermore, before testing the blocks were cleaned to such a degree that the size between all the blocks would be reasonably consistent.

The beams were placed on simple supports (see Figure 23) and were then subjected to a force on 1/3 and 2/3 of the span length so that there is a constant moment applied in the middle third of the beam. A piece of rubber was placed at every contact point to allow the test piece to shear. Both the cubes and the beams were loaded in the z- direction, perpendicular to the layers. To begin the test, beams or cubes are placed in the manner shown in Figure 23. The top plate, which is connected to the force gauge, is then lowered at a constant rate. The experiment is stopped when one of two things occurs:

1. The test piece visibly cracks.
2. The force indicated on the force gauge does not increase for a couple of seconds.

Almost all test specimens failed due to visibly cracking. The latter criterion for stopping the experiment only occurred with test specimens that were highly undersaturated, or that contained a high number of fibres.

Figure 23: Test setup for bending (l) and compression (r)

When the test is stopped, the maximum force recorded by the force gauge is used to calculate the strength of the test piece. For cubes, the following formula is used to calculate the cube compressive strength:

$$\sigma_{cube} = \frac{F}{A} \tag{11}$$

With F being the maximum applied force and A being the loaded area.

The flexural strength of the beams can be found using basic statics. The moment line of the 4 point bending test can be found in Figure 24. The maximum moment can be found using moment equilibrium:

$$M = \frac{1}{6}FL \tag{12}$$

The tension in the outer fibre of the square cross-section when the maximum moment is applied can be expressed as:

$$\sigma_{flexural} = \frac{Mz}{I} \tag{13}$$

Where z is the distance from the neutral axis to the outer fibre and I is the second moment of area of the cross section.

$$I = \frac{1}{12}bd^3 \qquad z = \frac{1}{2}d \tag{14},(15)$$

Substituting (*12*),(*14*) and (*15*) into the equation for the flexural strength (*13*) gives:

$$\sigma_{flexural} = \frac{Fl}{bd^2} \tag{16}$$

Equation (*16*) can now be used to calculate the flexural bending strength.

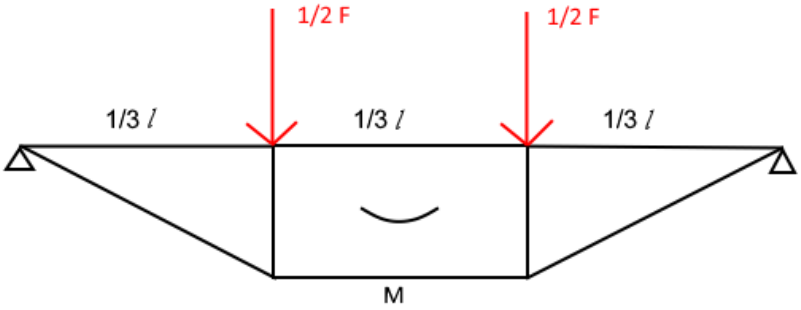

Figure 24: Moment line of the 4-point bending test

3.2 Printing accuracy

To isolate the effects of individual parameters of the concrete mix on the early age strength and post-curing strength, it is important to keep all other variables equal. Keeping all variables constant is hard, since most variables influence each other. For example, increasing the density of the particle bed decreases the porosity, which affects the amount of water that can be used before the layer becomes saturated. Or, increasing the w/c ratio likely increases strength, but also likely decreases shape accuracy, especially in the lower layers. Therefore, different test specimens will have to have similar shape accuracy and dimensions. There are multiple ways in which the shape accuracy could be assessed, for example by defining a certain range wherein the length, width and height of the test specimens must fall. Or, by printing a test piece with different sizes of holes and determining which hole size is still visible after de-powdering or printing squares and measuring the angles of its edges and corners. In the early phases of the research the choice was made to do a combination of measuring dimensions and printing different sizes of holes, see Figure 25.

Figure 25: Test specimens with different w/c ratios to test dimensional accuracy. W/C ratio from left to right: 20,30,40,60 %

While this test shows clear differences in the accuracy of both the small details as well as the overall dimensions, the experiment also found some flaws in this approach of measuring accuracy. Firstly, measuring these shapes proved to be challenging. Measurements of for example the height were found not to be uniform over the depth and width of the structure. The left side of the structure could be millimetres taller than the right side, or vice versa. Taking multiple measurements and averaging the results can solve this problem, but is a time- consuming solution. Another, harder problem to overcome was that the dimensions of the test specimens are reliant on the de-powdering process. The de-powdering is performed manually using tools like brushes, prongs and small scoops. Since the person cleaning the shapes also designed them, the researcher may consciously or unconsciously clean the shapes in such a way that the details become more apparent. The printing technique, the materials used, and the low early-age strength make it difficult to distinguish between fully hardened concrete and partially activated powder outside the printed boundaries. Consequently, it is up to the cleaner to decide when to stop cleaning, or to continue cleaning and possibly damage the structure. This introduces a degree of subjectivity, making the cleaner partially responsible for the final dimensions of the shape. All in all, this experiment made the researchers re-evaluate the method used to quantify the dimensional accuracy of the specimens.

Due to the large amount of human influence on the shape during the de-powdering process, it was decided to use a grading system to determine how well the powder mix performs in terms of printing accuracy and ease of cleaning. A complex shape was printed, see Figure 26, for the researcher to grade the powder mix on a scale of one to ten.

Figure 26: Starfish shapes used to pass or fail the printing accuracy of the powder mix and the ease of cleaning

By cleaning these starfish- like shapes, the researcher could determine if the powder mix could produce a sufficiently accurate shape and how difficult it was to differentiate between partially activated powder and the hydrated concrete. What shape is considered sufficiently accurate is very subjective, but by comparing shapes to one another it becomes apparent which ones perform better or worse. Ultimately, it will be up to the user of the printer to decide between choosing a certain stronger powder mix with less details, or a weaker mix with better shape accuracy.

The initial mix was graded with a 6. The best mix was graded with a 10 and the mixes that were unable to produce a test piece were graded a 1. For the assessment, the researcher took into account the actual dimensions after measuring, the general look of the test specimens, the amount of partially reacted powder adhered to the test piece after light cleaning with a brush, the ease of cleaning, and how consistent the powder was in producing well-defined shapes. In practice, the two most common reasons to lower the grade of a test piece were either undersaturation, usually resulting in a concave shape similar to the one found in Figure 27, or oversaturation which produced an oversized shape and with partially hardened powder on the sides of the beam.

Figure 27: Undersaturation and oversaturation of the pore space in bending test specimens

When cleaning, the two key questions the researchers used to assess the shape accuracy grade were whether the powder could be easily cleaned and how much partially hydrated cement surrounded the elements. These questions are particularly important as a simple cleaning process reduces labour, and less partially hydrated cement not only simplifies cleaning but also allows for more of the powder to be reused, since partially hydrated cement cannot be reused as a binder but only as an aggregate.

3.3 Types of powder mixes

Different types of powder mixes were tested:

1. 'Standard' powder mix, a mortar mix that was already being used for production. The PSD used in this mix was recommended by the aggregate supplier and contains 20% CEM I 52.5 R (see Table 1).
2. Modified Andreasen and Andersen (MAA) mix, using the MAA distribution as discussed in the literature part of this thesis (see section 2.1.2.1). The exact distribution can be found in Table 1.
3. Linear distribution mix. This is a mix using 20% CEM I 52.5 R and equal parts of each available aggregate size, see Table 1. Specifically, 10% of every aggregate size provided by the supplier was incorporated into the mix.

Sieve sizes [mm]	'Standard' PSD [%]	MAA PSD [%]	Linear PSD [%]
Ground quartz meal [0.06]	18%	0%	10%
0.1-0.5	18%	24%	10%
0.2-0.63	9%	8%	10%
0.4-0.8	9%	6%	10%
0.63-1.0	9%	6%	10%
0.8-1.25	9%	6%	10%
1.0-1.6	9%	6%	10%
1.4-2.0	9%	6%	10%
CEM I 52.5 R	20%	38%	20%

Table 1: The different mix designs made with the available aggregate sizes

4. Mixes with increased cement ratio. These mixes all employ the same aggregate sizing as the standard powder mix, but differ in their cement contents, which were set at 30%, 40%, 60% and 100% (the latter containing no aggregate).
5. Methylcellulose (MC) mixes. These mixes have an amount of MC added to the standard mix design. The exact product used is Tylose MH 300 P2 which is hydroxyethyl methylcellulose (HEMC). This is the same powder and supplier used by (Lowke et al., 2022a). The MC was used in the following weight percentages: 0.25%, 0.5%, 1% and 2%. MC was chosen to be tested for its ability to increase the viscosity of the water, possibly decreasing the penetration depth (see section 2.1.1). The chosen weight ratios were deduced from literature and by recommendations from the supplier.
6. Cellulose fibre mixes. Different types and weight percentages of cellulose fibres supplied by Arbocel were added to the standard mix. The specific grades of fibres used were B00, BWW 40 and BE 600-30 PU, all differing in dimensions (see Table 2). This product was chosen for its water- retaining properties, and to reduce cracking. These specific variants were recommended to us by the supplier. The supplier also recommended to not use much more than 2% fibres, so the weight ratios of 0.5%, 1% and 2% were chosen to be tested. First only B00 was tested to see what ratios would yield positive results. B00 was chosen to be the first one tested since it had the average fibre length of the three. The other fibres were tested using the weight ratio that was found to perform the best for B00 type, limiting the size of the experimental campaign.

Name	Fibre length [µm]
B 00	120
BWW 40	200
BE 600- 30 PU	40

Table 2: Different types of fibres used in this study, provided by JRS

7. CEM III. Compared to OPC, this type of cement is a more sustainable option, as a part of the OPC is replaced by blast furnace slag. The tested mix has a cement/ aggregate ratio of 0.20 and contains CEM III/B 42.5 N LH/SR as a binder. The PSD of the aggregate is the same as the 'standard' PSD in Table 1. Near the end of the experimental campaign, the company switched supplier and chose this CEM III as their new standard mix design. This resulted in a limited supply of CEM I available for testing. Consequently, the curing tests and the tests incorporating glass fibres were conducted using this CEM III mix and were compared against it, rather than previously used CEM I mix.
8. Calcium aluminate cement (CAC) mixes. Different mix ratios were made for testing, of which some included calcium sulphate (CS). The tested ratios were:

    a. 15% CAC and 85% CEM I 52.5 R
    b. 5% CAC, 5% CS and 90% CEM I 52.5 R
    c. 15% CAC, 15% CS, 70% CEM I 52.5 R

    All three mixes had a c/a ratio of 0.2, identical to that of the 'standard' mix described above.

9. Glass fibres. One type of glass fibre was tested, the 'Crackstop F 6mm' supplied by Convez. The supplier recommended to use a dosage of 900g / m^3 (about 0.05wt%). Additionally, a much higher dose of 1wt% was also tested. This higher dose selected based on testing the cellulose fibres, and because trials with the recommended dose demonstrated that the fibre content was insufficient to achieve a desired outcome. The glass fibres testing was conducted with CEM III and compared against it.

Table 3 summarizes the properties of the mix designs discussed above.

The w/c ratio was adjusted for each powder mix to investigate the relationship between strength, shape accuracy and water content. The w/c ratios that were tested were typically 20%, 30%, 40% and 60%; however, for some mixes 20%, 60% or both were omitted when previous tests indicated that these ratios would produce unusable test specimens due to insufficient strength or poor shape accuracy. In certain cases, even higher or lower w/c ratios were added to explore the upper or lower bounds of acceptable performance.

To accurately measure the mean strength of a mix design, multiple tests were performed. The 'standard' and CEM III mixes served as baseline tests for comparison with all other mix designs and were therefore especially important to measure accurately. Six beams and cubes were tested for every w/c ratio in these baseline tests. In other words, each point on the graph (for example, the line corresponding to CEM I in Figure 28) represents the mean of six measurements. For instance, the mean cube compressive strength of the 'standard' CEM I mix was evaluated using four different w/c ratios, requiring 24 total measurements, 6 for every w/c ratio. The mean strengths of the other mix designs are based on two mechanical tests per w/c ratio due to size limitations—only six beams and six cubes could fit in the printer. Consequently, when three different w/c ratios were tested, two cubes and beams corresponded to every w/c ratio. Appendix C shows the test volume per mix design.

Name	Binder(s)	C/A ratio(s)	Additive(s)	wt% of additives added	w/c ratios	PSD used
Standard/ CEM I	CEM I	0.2	None	-	0.2/0.3/0.4/ 0.6	Standard
MAA	CEM I	0.38	None	-	0.1/0.2/0.3/ 0.4/0.6	MAA
Linear	CEM I	0.2	None	-	0.2/0.3/0.4	Linear
Increased C/A ratio	CEM I	0.2/0.3/0.4/ 1.0	None	-	0.2/0.3/0.4	Standard
Methyl-cellulose	CEM I	0.2	HEMC	0.25/0.5 /1/2	0.2/0.3/0.4/ 0.6/0.8	Standard
Cellulose fibres	CEM I	0.2	3 different CE microfibres	0.5/1/2	0.3/0.4/0.6	Standard
CEM III	CEM III	0.2	None	-	0.3/0.4/0.6	Standard
CAC mix a	85% CEM I, 15%CAC	0.2	None	-	0.3/0.4/0.6	Standard
CAC mix b	90% CEM I, 5% CAC, 5%CS	0.2	None	-	0.3/0.4/0.6	Standard
CAC mix c	70% CEM I, 15% CAC, 15% CS	0.2	None	-	0.3/0.4/0.6	Standard
Glass fibres	CEM III	0.2	6 mm glass fibres	0.05%, 1%	0.3/0.4/0.6	Standard

Table 3: A summary of all different mix designs used in this research

3.4 Curing

To study the influence of curing on the strength of the design, multiple scenarios were investigated:

1. Delaying the de-powdering process: Instead of removing the powder after 24 hours, the test specimens were de-powdered after 72 hours to investigate whether this would increase strength.
2. Submerged curing of specimens: Test specimens were submerged in a large container filled with tap water for 7 days and were kept at room temperature.
3. Curing using misting: Test specimens were moistened using a spray bottle and were stored in plastic bags or sheets. Thereafter, the test specimens were moistened in a similar manner every 24 hours for a total of 7 days, ensuring that the surface of the concrete was always wet. This type of curing is both very similar to the method of curing the company employs for the larger structures that are printed and to the wet gunny bag method discussed in section 2.1.3.2.
4. No curing/ dry curing: Some test specimens were dry cured to serve as a baseline for comparison to both the submerged and misting curing. After de-powdering, the test specimens were stored in a dry environment at room temperature for 7 days.

The CEM III mix design is used to produce all curing test specimens, as discussed in section 3.3. The w/c ratios used in all curing scenarios are 0.3, 0.4 and 0.6. Varying the w/c ratio is intended to allow for better understanding what strength gain can be attributed to the curing process, and what strength gain is due to the concrete strength development over time.

4. Results

As discussed in the methods section, mechanical and curing tests are carried out in this research to find changes in the mix design or curing regime that improve the strength and/ or sustainability. These alterations to the mix design are chosen based on literature and discussed in section 3.3. The results of the mechanical tests performed on these powder mixes are presented in this chapter. At the end of this chapter, two final mix designs will be formulated and their mechanical test results presented. This chapter is divided into nine subsections, each one dedicated to a change in mix design or curing regime. This chapter presents the results of the altered powder mixes in the same sequence in which the mixes are introduced in section 3.3.

4.1 Particle size distribution

In Figure 28 the relationship between cube compressive strength and particle size distribution is found for different w/c ratios. For the same w/c ratio, the test specimens made with the MAA method seem to significantly outperform the other distributions. It must be noted that the MAA distribution contains 38% cement instead of the 20% in the other specimens. This will be further highlighted in the results section for cement ratio.

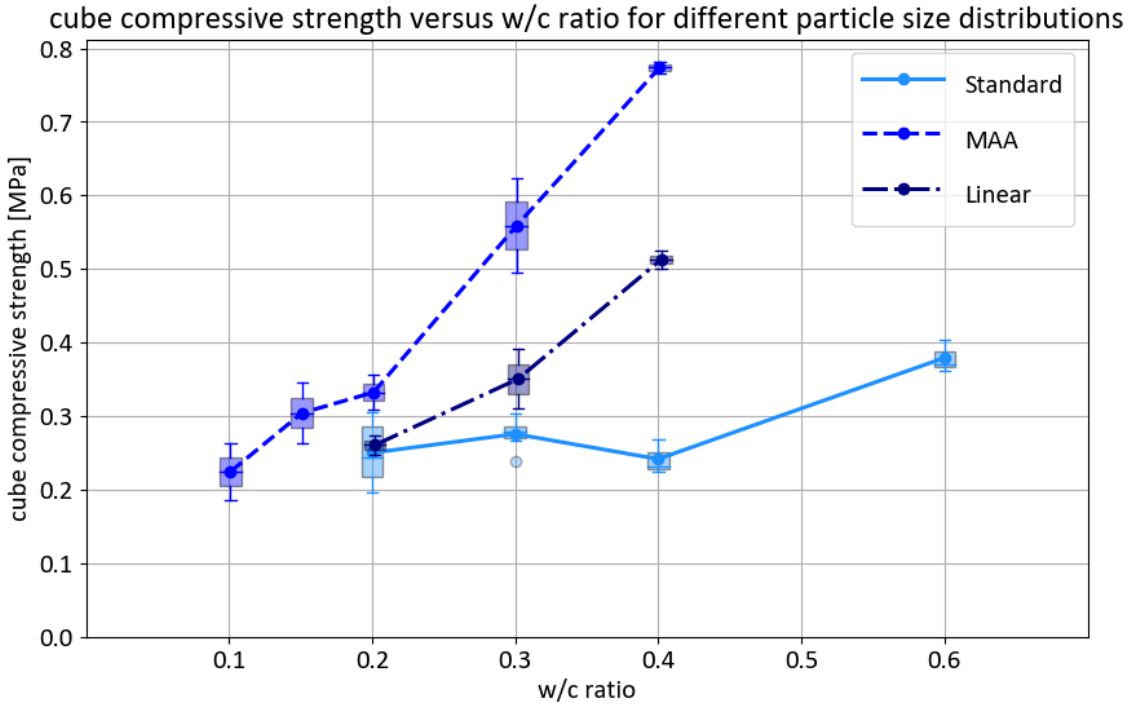

Figure 28: The strength vs water cement ratio for different particle size distributions

The linear distribution seems to also perform better than the standard mix. This linear distribution, which does not follow an optimized particle size distribution, likely has a lower density and was therefore hypothesized to perform worse than the standard distribution. In Figure 29, the relationship between shape accuracy grade and the compressive strength can be found for the different PSD's. Here, the MAA also performs best, while the strength of the linear distribution appears similar to that of the standard PSD. Interestingly, the linear distribution performs slightly better than the standard PSD because its higher strength compensates its lower shape accuracy grade. The grade of the linear distribution is always 1 point lower than that of the standard PSD for the same w/c ratio. For example, with a w/c ratio of 0.4 the linear distribution gets scored a 4, while the standard PSD scores a 5 (w/c ratios not shown here, see Appendix D for grading).

The results for bending strength (not shown here, see Appendix B) show very similar relationships.

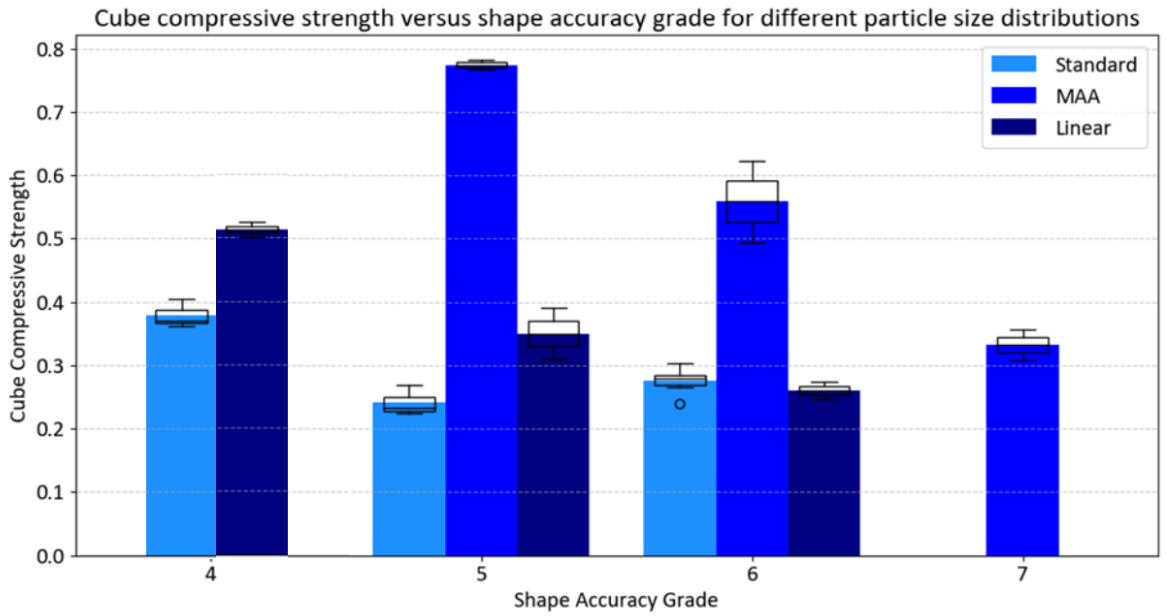

Figure 29: Cube compressive strength versus shape accuracy grade for different particle size distributions. Appendix A presents a connected scatter plot of the same data

4.2 Cement/ aggregate ratio

For a constant w/c ratio, the strength appears to increase with higher cement content (see Figure 30). The three powder mixes with higher cement/ aggregate ratios all have very similar strength, while the powder mix containing only 20% cement is significantly weaker. Also notice how the slope of the lines seems to increase with higher cement contents, indicating that the strength increases when increasing the w/c ratio is more pronounced for test specimens containing more cement. It needs to be noted that, if the w/c ratio is kept constant in specimens with different cement contents, the total volume of water used is not. The steeper slope of the lines can therefore also be a result of this increase in total volume of water that is sprayed onto each layer. Another interesting observation is that the relationship between the strength and w/c ratio appears to be approximately linear, as indicated by the nearly straight lines. This linearity can also be found in the other strength vs w/c ratio graphs in this chapter.

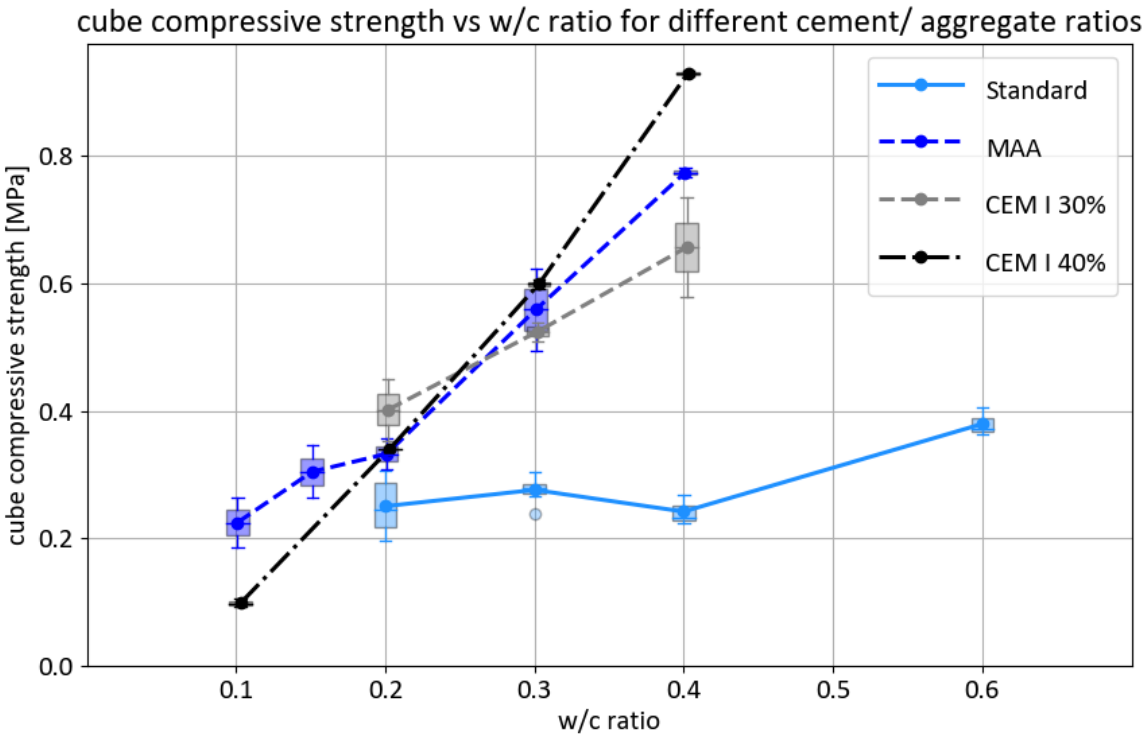

Figure 30: Strength vs w/c ratio for different cement/aggregate ratios

Figure 31 shows that the higher cement ratios appear to have good shape accuracy whilst also having excellent early age strength. Similar to the linear PSD, the reason why higher cement ratios exhibit high strength without compromising shape accuracy is their inherent strength. Because of this, these mixes can be printed with lower w/c ratios whilst still achieving sufficient shape accuracy. This is advantageous as the general trend is that an increase in w/c ratio results in a reduction in shape accuracy.

The cube compressive strength for a cement to aggregate ratio of 40% and a w/c ratio of 0.6 was also tested, however after 24 hours the test cubes were so strong that they exceeded the strength limit of the testing equipment. Therefore, they could not be tested and are not shown in the figure. The shape accuracy of these test specimens was graded with a 2 however, as they proved to be challenging to properly remove from the powder bed and did not retain their designed shape very well. Test specimens with 100% cement also showed excellent strength but were too difficult to clean and exhibited irregular shapes. This was likely due to their brittleness, with some specimens even delaminating, likely due to an insufficient water penetration depth. This phenomenon was visible during printing, with the water poorly penetrating and forming puddles on the printing surface.

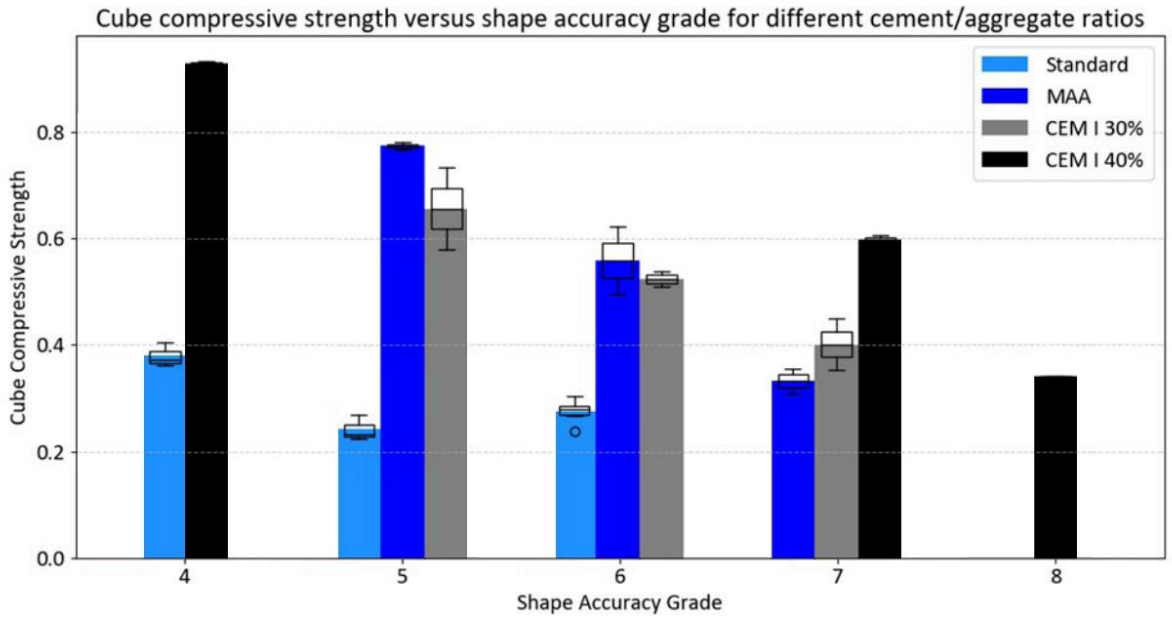

Figure 31: Cube compressive strength vs shape accuracy grade for different cement/ aggregate ratios. Appendix A presents a connected scatter plot of the same data

4.3 Cellulose powder

When comparing the CE mixes to the standard mix at a given w/c ratio, the CE mixes exhibit lower strengths in both bending and compression. As shown in Figure 32, increasing the amount of CE in the mix drastically reduces the compressive strength at the same w/c ratio, and most mixes with CE exhibit poor bending strength, or almost no bending strength at all. The sudden decrease in strength from a dosage of 0.25% to 0.5% seen in Figure 32 illustrates that after only slightly changing the dosage, strength drastically drops. A weight percentage of 0.25 shows comparable strength to that of the mix without any HEMC, while a 0.5wt% dosage is more comparable to the higher dosages of 1 and 2 wt%, offering very little strength.

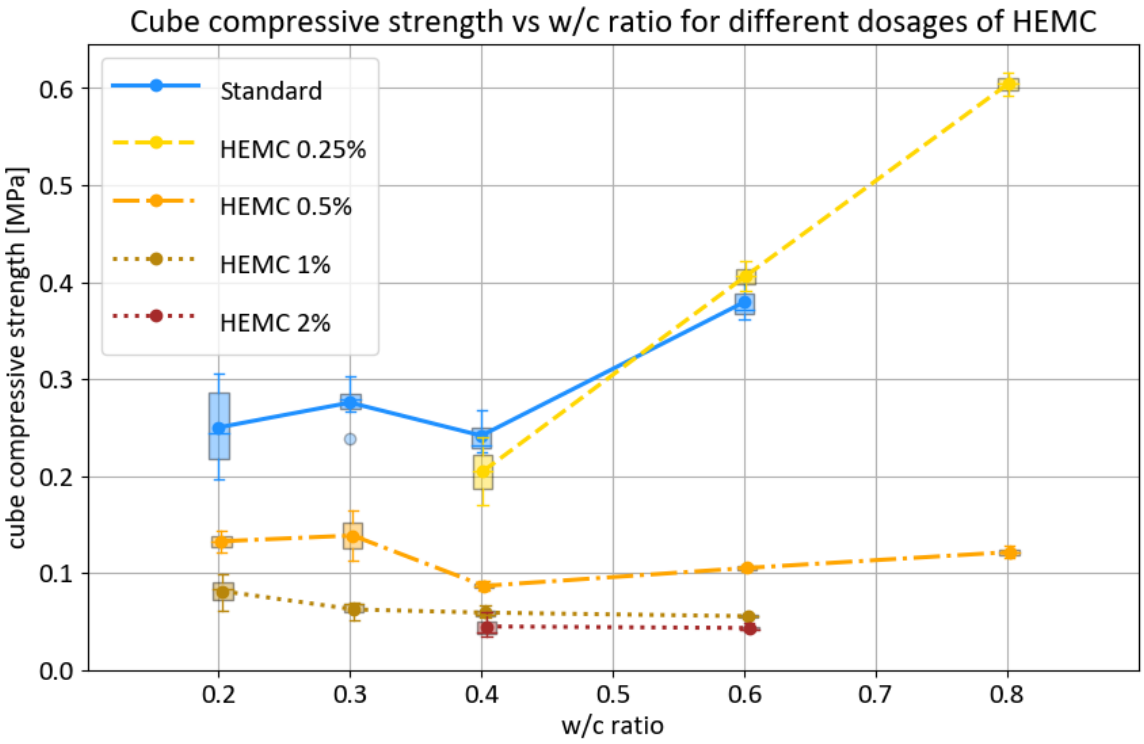

Figure 32: Cube compressive strength vs w/c ratio for different dosages of HEMC

The influence of CE on the hydration can clearly be seen after failure of the bending beams (see Figures 33 and 34). In these cross-sections, a clear distinction between a darker material and lighter material can be seen. There are exactly 12 dark layers to be seen in Figure 33, matching the 12 printing layers. The layers seem to rarely touch each other. When looking closely, it can be seen that the dark layers are not very consistent in height, it varies over the width of the beam. The top part of the dark lines seem to be relatively straight compared to the bottom. The lines also seem to be less pronounced in the beams containing less HEMC and with a lower w/c ratio, seen in Figure 34. There is a clear difference between these beams, and those shown in Figure 35.

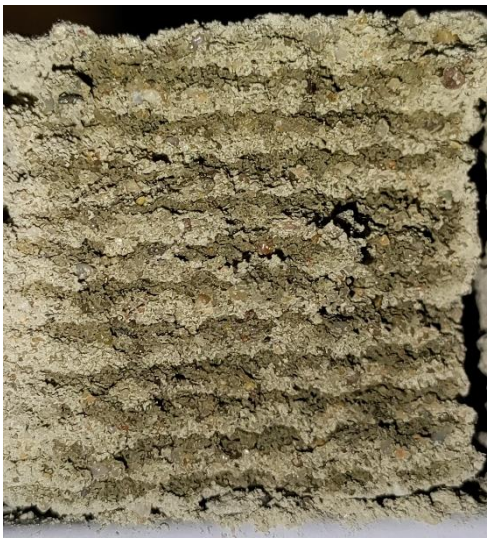

Figure 33: Photo of cross- section of a concrete bending test piece with 1% Tylose taken directly after bending failure

Figure 34: Photo of cross section of multiple bending test specimens taken directly after a bending test. Top row is 0.25% Tylose, bottom row contains 0.5% Tylose. The w/c ratio is increased from left to right

The beams in Figure 35 seem to have a lot less pronounced lines. These figures further confirm that dosages over 0.5 percent are too high because they limit the water penetration depth too much. Arguably, even 0.5 percent is already too large of a dosage.

Figure 35: Cross sections of bending beams captured directly after failure. The beams are made using the 'linear' mix with water cement ratios of 0.2, 0.3 and 0.4 from left to right.

The purpose of these cellulose products is to limit the water penetration depth and retaining the water in the pores that are intended to be filled. Section 2.1.2.4 discussed that CE absorb water. Therefore, it is possible that the water requirements for these mixes are higher, and that the strength curves are simply shifted to the right compared to the standard powder. When looking at the slopes of the lines in Figure 32, the HEMC seem to behave somewhat similar to the standard powder in lower dosages, only shifted down and to the right. This shifting indicates that the amount of water required to reach a similar strength to that of the reference test specimens has risen. Therefore, comparing the mixes by keeping the w/c ratio constant is not fair comparison. A more interesting comparison is looking at the shape accuracy grade and the strength (Figure 36).

The first thing that stands out when looking at this figure is that all the test specimens containing HEMC show excellent shape accuracy. The shape accuracy only starts to diminish at a very high w/c ratio of 0.8 (w/c ratio not shown in figure, see Appendix D). As seen in the figure, this is very beneficial to the strength that can be achieved without compromising on shape accuracy. One thing that however was compromised is speed of printing. Since the amount of deposited water is determined by the speed at which the nozzle moves, extremely high w/c ratios take a long time to print. This issue can be solved by using another nozzle with a higher flow rate. Another downside of using HEMC is that the required dosages are very low. As seen in the figures, even a small increase in HEMC of 0.25% has a very large influence on the strength. This makes working with this material very prone to errors like spillage, not using accurate scales and poor mixing. The biggest issue with this material is that it is hard to reuse. One of the big benefits of this technology is that the material that has not been wetted can be reused. However, defining what material has been wetted is not so straightforward. It could well be that some of the HEMC that surrounds the material is partially wetted and so if this material would be reused, the dosage of dry HEMC is now unknown. While printing with cement has the same problem, products with only cement are a lot less susceptible to small changes in cement contents as seen in Figure 30.

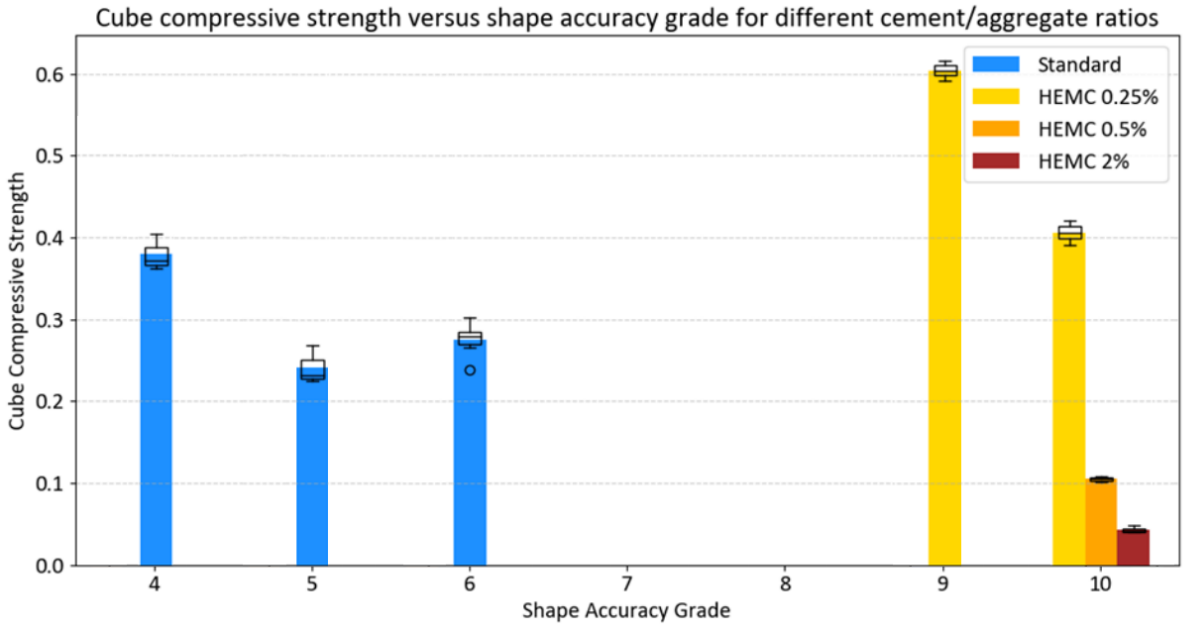

Figure 36: Shape accuracy grade versus cube compressive strength for different dosages of HEMC. Appendix A presents a connected scatter plot of the same data

4.4 Cellulose fibres

Cellulose microfibres were hypothesised to have two benefits:

1. They could increase the bending strength of the material.
2. They could reduce the water penetration depth, allowing for more accurate prints.

The benefit of allowing more accurate prints consequently means that higher w/c ratios can be used, increasing strength. These fibres are made from cellulose and retain some water, however, the water retention is a lot less potent when compared to the HEMC powder.

The bending strength vs the w/c ratio can be found in Figure 37. This however is not a fair comparison because, similarly to HEMC, the water requirement of the material to undergo proper hydration has increased, due to the water retention of the fibres. The slope of the lines in the figure is similar to that of the CEM I line, however they are again shifted slightly down and to the right. Regardless of the higher water requirement, the dosage of one percent seems to outperform the CEM I for a given w/c ratio.

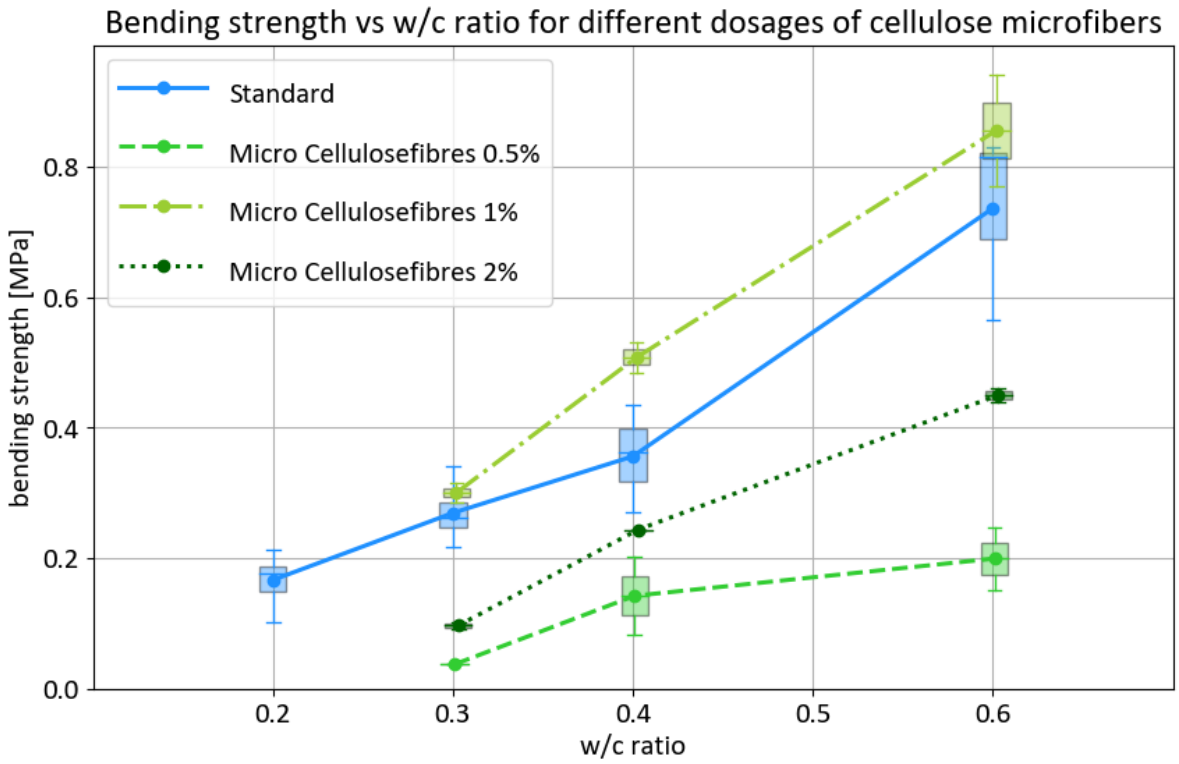

Figure 37: Bending strength vs w/c ratio for different dosages of cellulose microfibres

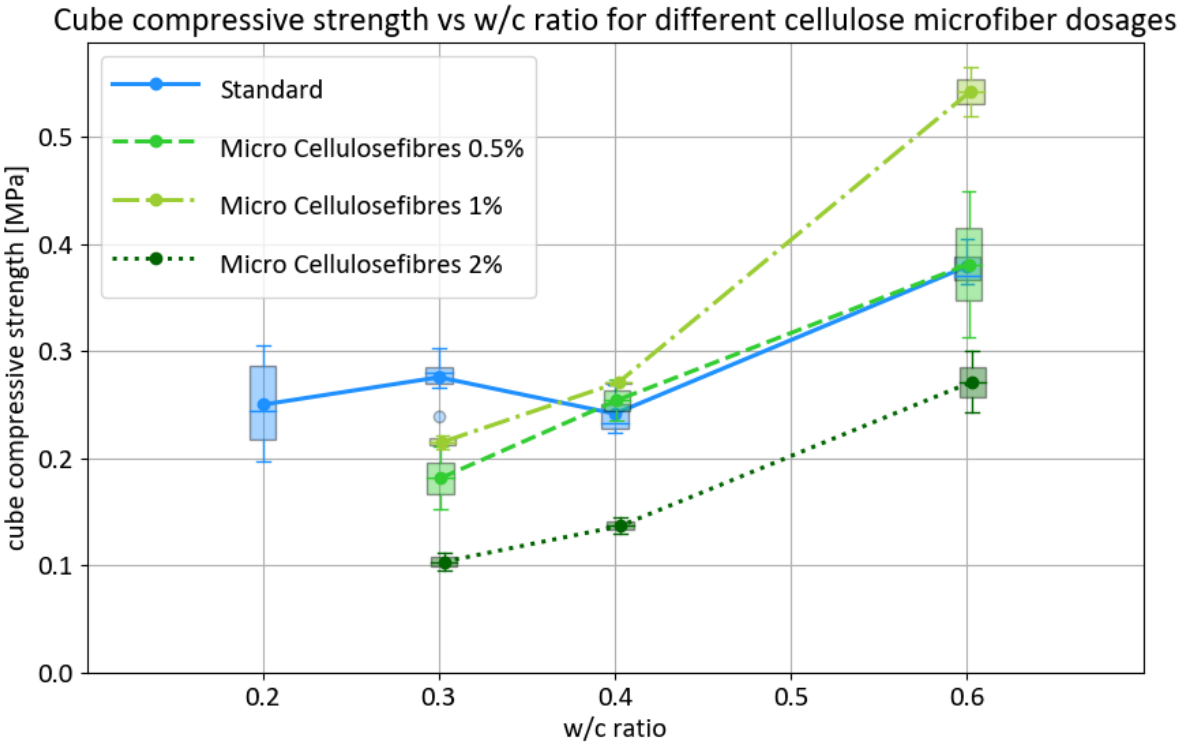

Figure 38: Cube compressive strength vs w/c ratio for different cellulose microfibre dosages

The fibres seem to positively affect the bending strength, especially when factoring in the extra water requirement. However, there is a downside to incorporating them. Because the fibres have a very low density compared to the sand and cement, they occupy a relatively larger volume within the material. When an excessive amount of fibres are added, the particle size distribution is disturbed, resulting in an increase in porosity and, as a result, lowering the compressive strength of the material. This effect can serve as an explanation for what can be seen in Figure 38: the compressive strength of the samples containing 2% fibres is lower than that of the reference test. This however would not explain why the samples with one percent fibres perform a bit better than the reference test. One of the benefits of using cellulose fibres, is that the fibres improve moisture distribution through the powder mix, and act as nucleation sites, increasing the degree of hydration (Li et al., 2025). This improved hydration consequently improves mechanical properties, including compressive strength. The fibres containing 0.5% of fibres were expected to also show an increase in mechanical properties over the CEM I due to the same aforementioned reasons, however this does not seem to be the case.

Figure 39 shows a similar trend as Figure 38. The bending strength of beams containing 1% fibres is slightly higher than that of specimens containing no fibres. Both higher or lower concentrations of fibres reduce bending strength, suggesting that the optimum dosage is near this one percent. Fibres increase bending strength for the same reasons they improve compressive strength, with the added benefit that cellulose fibres can act as a reinforcement, increasing the flexural strength (Li et al., 2025).

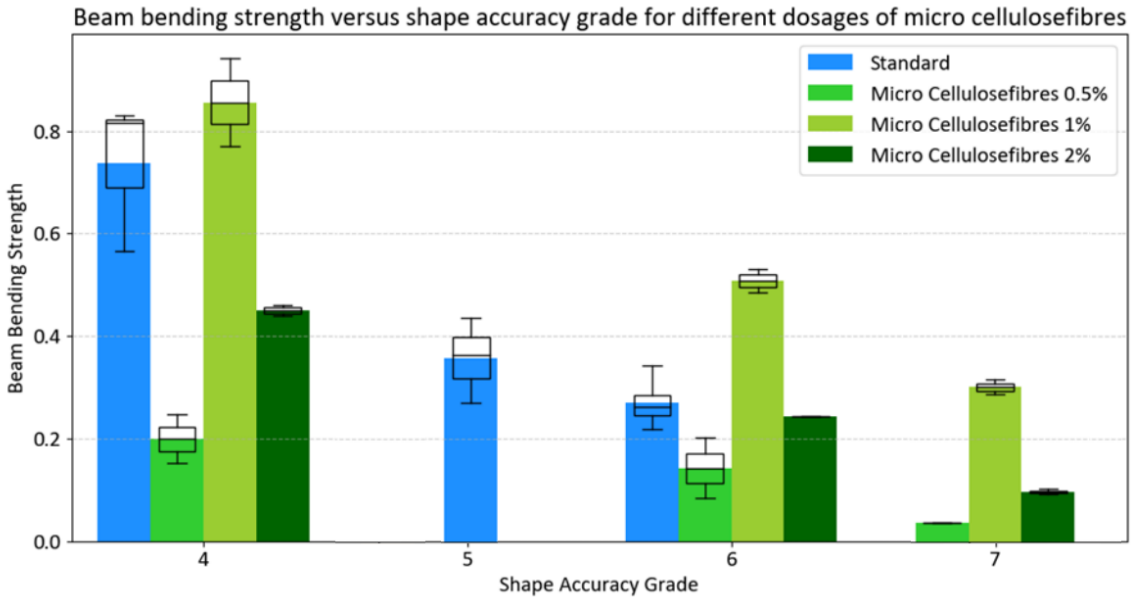

Figure 39: Shape accuracy versus bending strength for different cellulose microfibre dosages. Appendix A presents a connected scatter plot of the same data

From Figure 39, it can be concluded that the shape accuracy of the samples containing fibres is slightly better than that of the reference test. The percentage of fibres does not affect the shape accuracy grade, as all three samples have the same grades. This is worth noting, as cellulose fibres are water retaining and were therefore expected to improve shape accuracy. Again, the beams with one percent fibres exhibit slightly higher strength. Overall, however, the fibres do not perform significantly better than plain powder mixes.

4.5 CEM III

CEM III can be used as an alternative to CEM I. Several variants exist, but the type used in this study is CEM III/B 42.5 N LH/SR. According to EN 197-1, the amount of blast furnace slag (BFS) in this 'B' variant ranges between 66 and 80 percent. Figure 40 compares the compressive strength of this CEM III/B with that of CEM I 52.5 R, used in the 'standard' mix design. The CEM I powder mix exhibits higher strength after 24- hours than the CEM III. This result can be explained by the difference in classification of the cement mixes: the CEM III/B used in this study is of strength class 42.5 while the CEM I is classified as 52.5. In addition, the early strength class of this CEM III is denoted by an 'N' for 'normal', while the early strength class of the CEM I is 'Rapid'. According to Table 3 in section 7.1.2 of EN 197-1, the denotation of 52.5 R should have a strength of ≥30 MPa, while the strength of 42.5 N is ≥10 MPa after 2 days. Furthermore, the speed of hydration of CEM I is faster than that of CEM III, resulting in a higher early age strength (Tracz et al., 2025). While the differences in strength found in Figure 40 are large, the strength of CEM I is not threefold greater than CEM III.

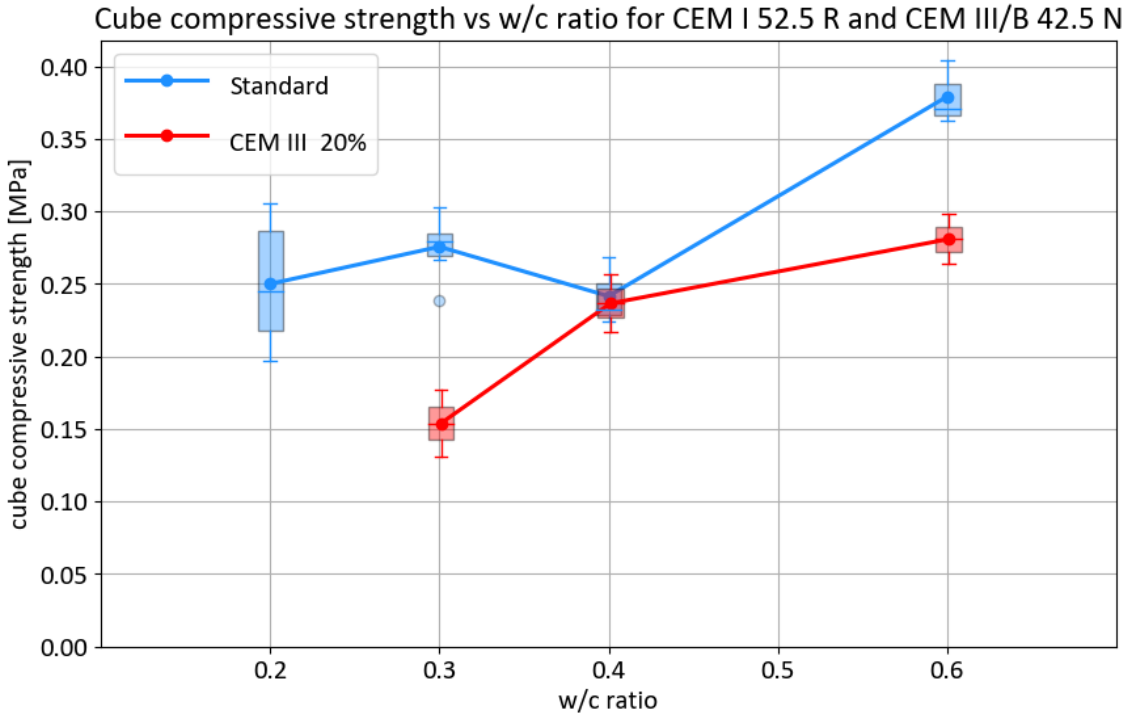

Figure 40: Cube compressive strength vs w/c ratio for CEM I and CEM III

4.6 Calcium aluminate cement mixes

In this study, three different powder mixes with varying OPC, CAC, and CS ratios were tested. Two of these fall in zone 2, and one is located in zone 3 (see Figure 15). Powder mixes containing calcium aluminate hardened significantly faster than ones containing only OPC. Binary or ternary mixes mostly exhibit very fast early age strength development, however when looking at Figure 41, the powder mixes with CAC hardly outperform regular OPC. Due to the fast setting time of mixes with CAC, the water penetration depth decreases, as discussed in 2.1.1.1. This decrease can result in lower strength when the water penetration depth is insufficient. A lower water penetration depth is beneficial for the shape accuracy grade, as it mitigates the migration of water outside of the printing boundaries.

The shape accuracy grade versus the cube compressive strength can be found in Figure 42. The shape accuracy grade of the mixes containing CAC is indeed higher than that of OPC. 15 percent CAC and CS produced significantly undersaturated samples with poor shape definition. 15 percent CAC with 85 percent OPC performed well, but a blend of 5% CAC and 5% CS seems optimal.

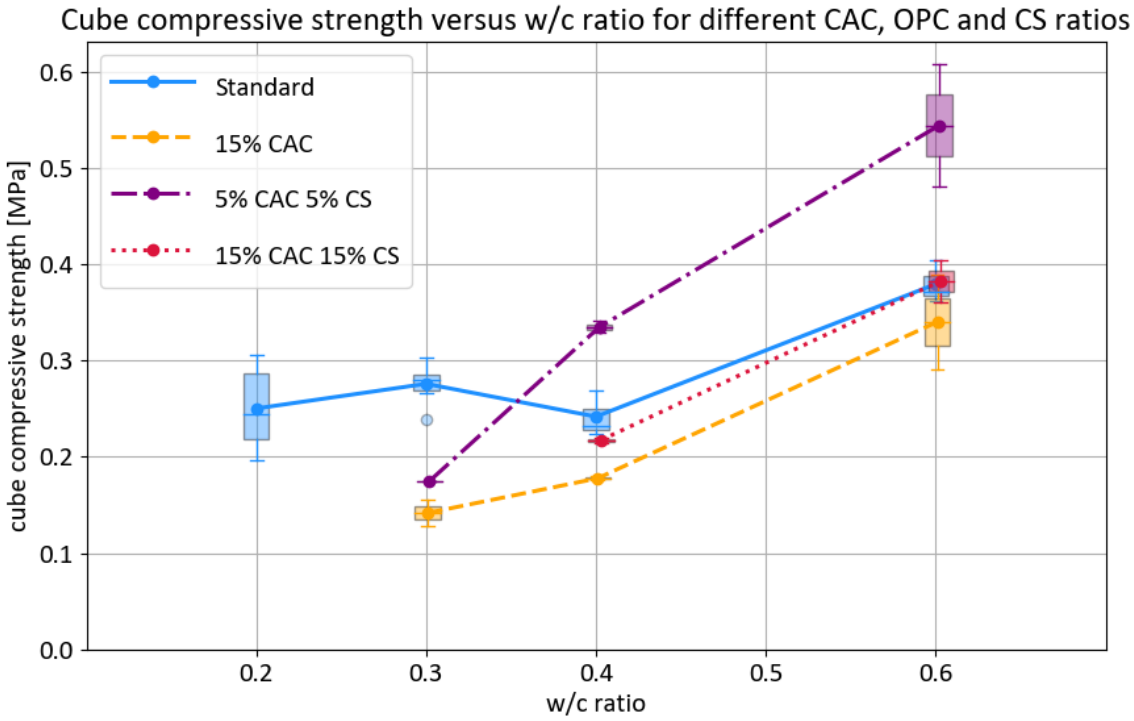

Figure 41: Cube compressive strength versus w/c ratio for different CAC, OPC and CS ratios

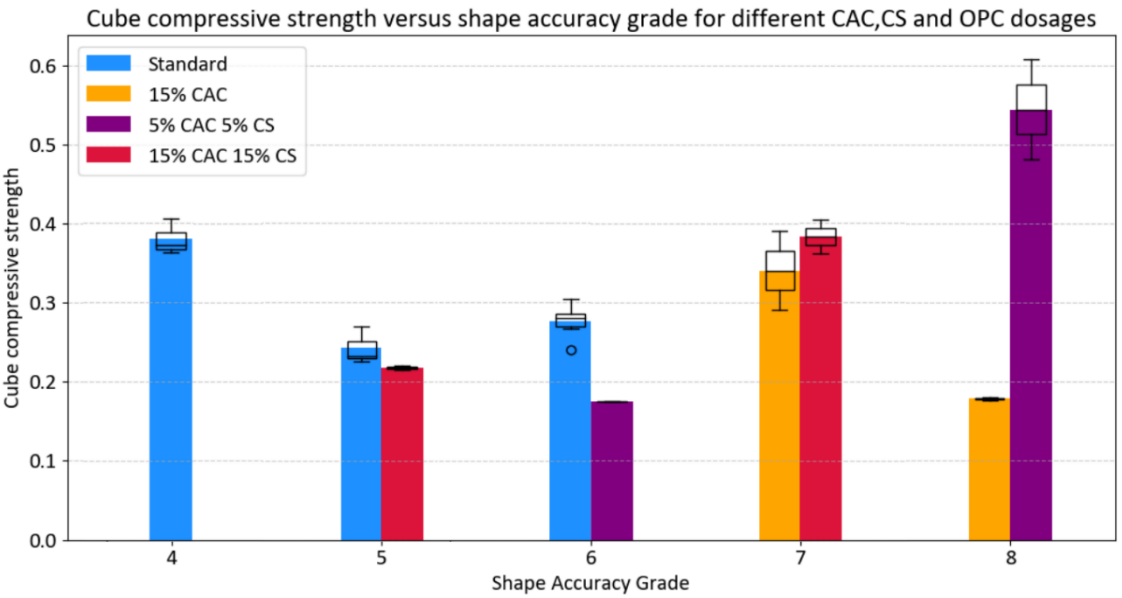

Figure 42: Shape accuracy grade versus cube compressive strength of different ratios of CAC,OPC and CS. Appendix A presents a connected scatter plot of the same data

4.7 Glass fibres

Glass fibres were hypothesized to influence the bending strength, and to decrease cracks. It seems that the glass fibres do not increase the bending strength, regardless of dosage, see Figure 43.

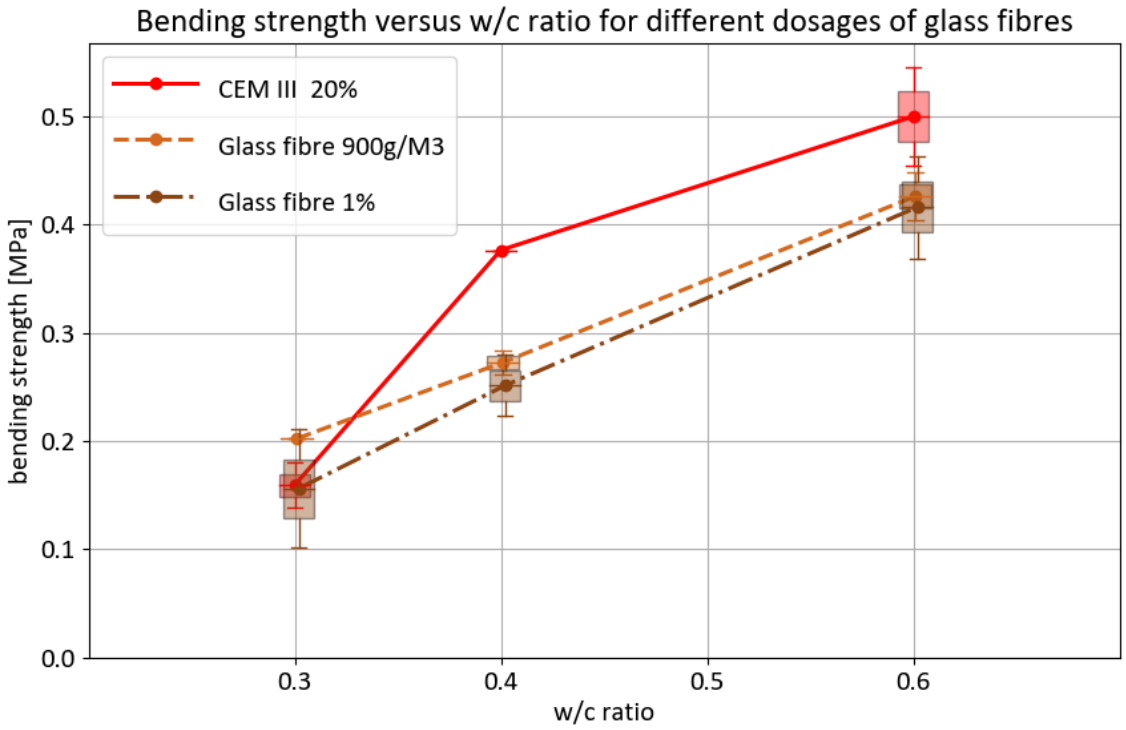

Figure 43: Bending strength versus w/c ratio for different dosages of glass fibres. Please note that CEM III is used in all three of these powder mixes. Therefore, CEM III (without fibres) is added in this figure for comparison, instead of the usual 'standard' mix design.

Since glass fibres do not influence the water penetration depth, the shape accuracy grade of the lower dosage is the same as that of the reference test. However, when a weight percentage of 1% is incorporated, the samples become challenging to de-powder and are not graded higher than a 4, regardless of water cement ratio. These samples also proved to be problematic to print, as the fibres clogged up the hopper, making it difficult to properly deposit the layers. Another issue with using fibres is that sometimes the nozzle hits a fibre that protrudes from the surface of the layer, shielding some of the cement under the fibre from wetting, see Figure 44.

Figure 44: The uneven printing surface that occurs when printing with fibres

Another downside of fibres that came up when cleaning these samples is that the fibres protrude outside of the layer and bind the partially activated cement around the samples very well, making it difficult to identify the printing dimensions. This can be seen in Figure 45.

Figure 45: How the samples of 1% glass fibres looked

One huge benefit of using fibres, is the increased ductility. When a crack occurs, the printed object now is still able to be repaired. This ductility can be seen in the bending test illustrated in Figure 46. The beam shown in the figure is still held together by fibres connecting both sides of the specimen.

Figure 46: A beam containing fibres after a 4-point bending test

4.8 Final design

When all the other results in this chapter were analysed, it was found that 3 strategies stood out in particular: an increased cement content, partially replacing OPC with CAC and CS, and incorporating cellulose ether. Increasing the cement content has shown to result in a substantial increase in strength after 24-hours. Adding small amounts of CAC and CS also resulted in an increase in strength, whilst also improving shape accuracy. Cellulose ether proved to be very effective in improving the shape accuracy, at the cost of strength.

Since the results showed that using cellulose ether can have downsides, it was decided to make two final designs, one with and one without the HEMC. Both mix designs can be found in Table 4.

Name	C/A ratio	Binder	Additives
Final v1	0.4	90% OPC, 5% CAC, 5% CS	None
Final v2	0.4	90% OPC, 5% CAC, 5% CS	0.25% HEMC (cellulose ether)

Table 4: Mix designs for the two final products

In Figure 47 the compressive strength after 24 hours can be found for the two final mix designs, compared to the 'standard' design. Both final products show a clear improvement over the standard, and seem to perform very similar to one another. Interestingly, the final design containing a slight amount of CE shows slightly better results than the final design without additives.

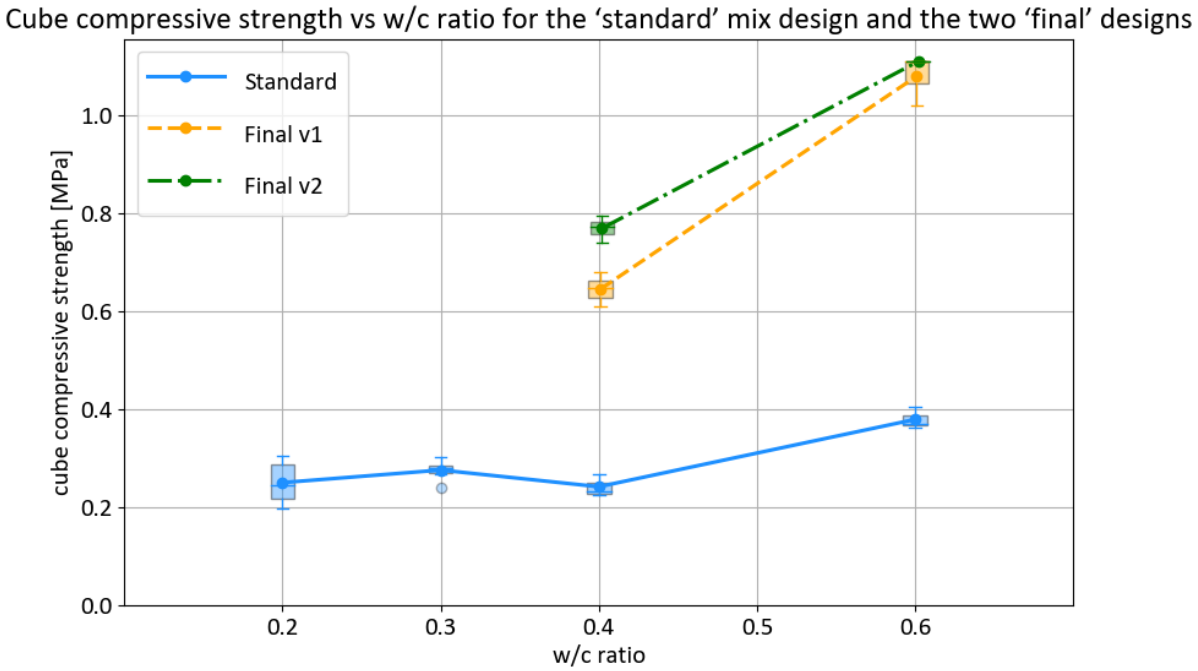

Figure 47: Cube compressive strength vs w/c ratio for the 'standard' mix design and the two 'final' designs

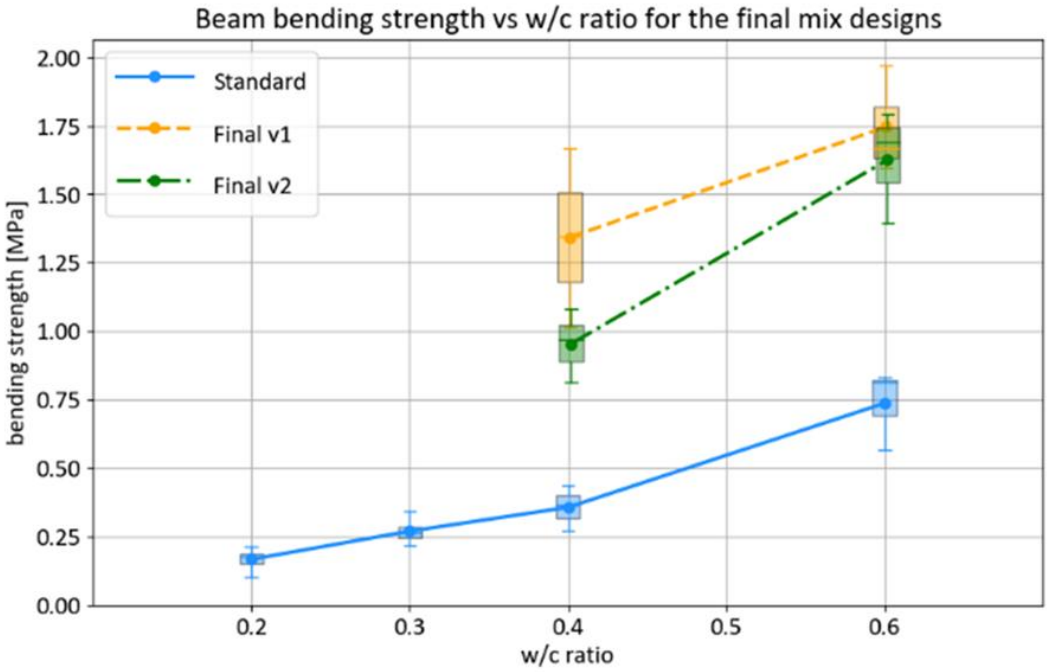

Figure 48: Beam bending strength vs w/c ratio for the final mix designs compared to the 'standard' design

An important note regarding Figure 47 is that the cubes of both mix designs reached the upper strength limit of the testing equipment, so the true strength of the cubes made with a w/c ratio of 0.6 is unknown. All three cubes of the second final design reached the upper limit. For the first final design, the upper limit was reached 2 out of 3 times, with the last cube failing slightly under the upper limit. While this data is not usable in the figures, it does indicate that the strength is somewhere close to the upper limit for that mix design. For the second design, there is no such indicator, and so the true upper limit remains unknown. For this reason, the beam bending strength, shown in Figure 48 is a more complete comparison between all three mix designs.

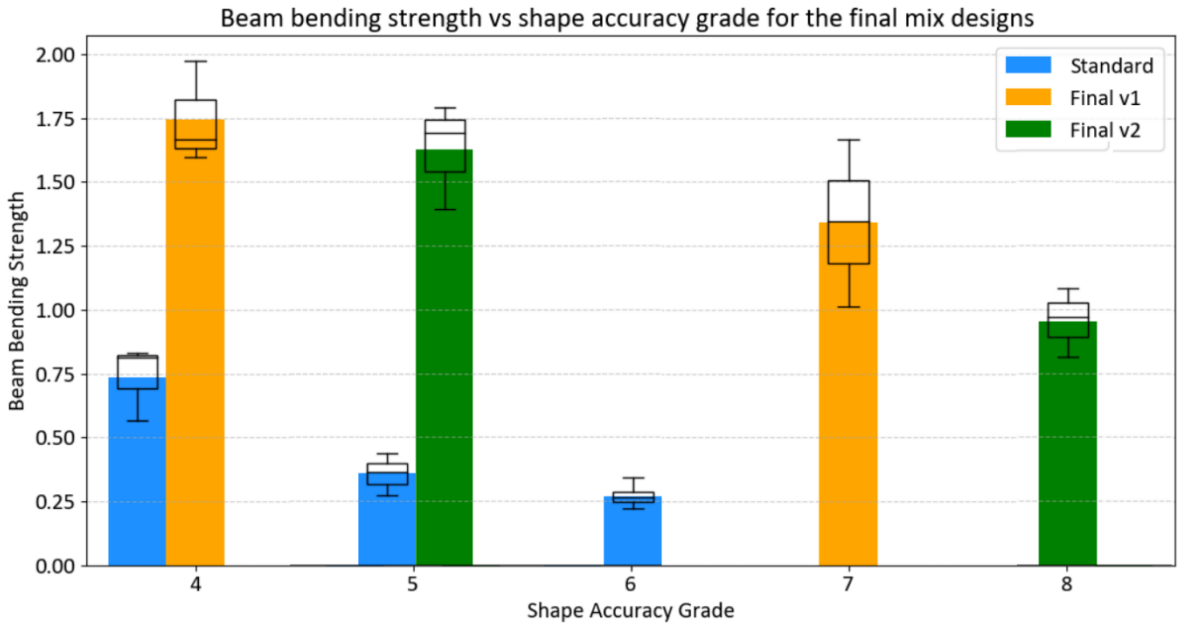

Figure 49: Beam bending strength vs shape accuracy grade for the final mix designs compared to the 'standard 'mix design. Appendix A presents a connected scatter plot of the same data

Interestingly, when comparing Figure 48 to Figure 47, the final design without cellulose ether has a slightly higher strength than the one with cellulose ether. This result is more in line with what was found in section 4.3, where an increase in CE generally resulted in lower strength.

The beam bending strength vs shape accuracy grade of the final mix designs are compared to the 'standard' mix design in Figure 49. The results are as expected, adding CAC and CS improves shape accuracy and adding CE is a further improvement. Both 'final v1' and 'final v2' show good shape accuracy results and both only differ slightly. Despite using CAC,CS and CE however, both designs still score insufficient shape accuracy grades when using a w/c ratio of 0.6.

The effect of an increase of cement content on the strength after 24 hours is found in Figure 50. The bending strength of the two final mix designs is very similar to the other mix designs with 40 percent cement content (or rather, MAA has a cement content of 38%, but this small difference likely will not have a great effect on the strength). However, the results found in Figure 51 show that there is a difference between the final mix designs and the 'CEM I 40%' and 'MAA' designs. While the strength is comparable, both final mix designs have significantly better shape accuracy grades.

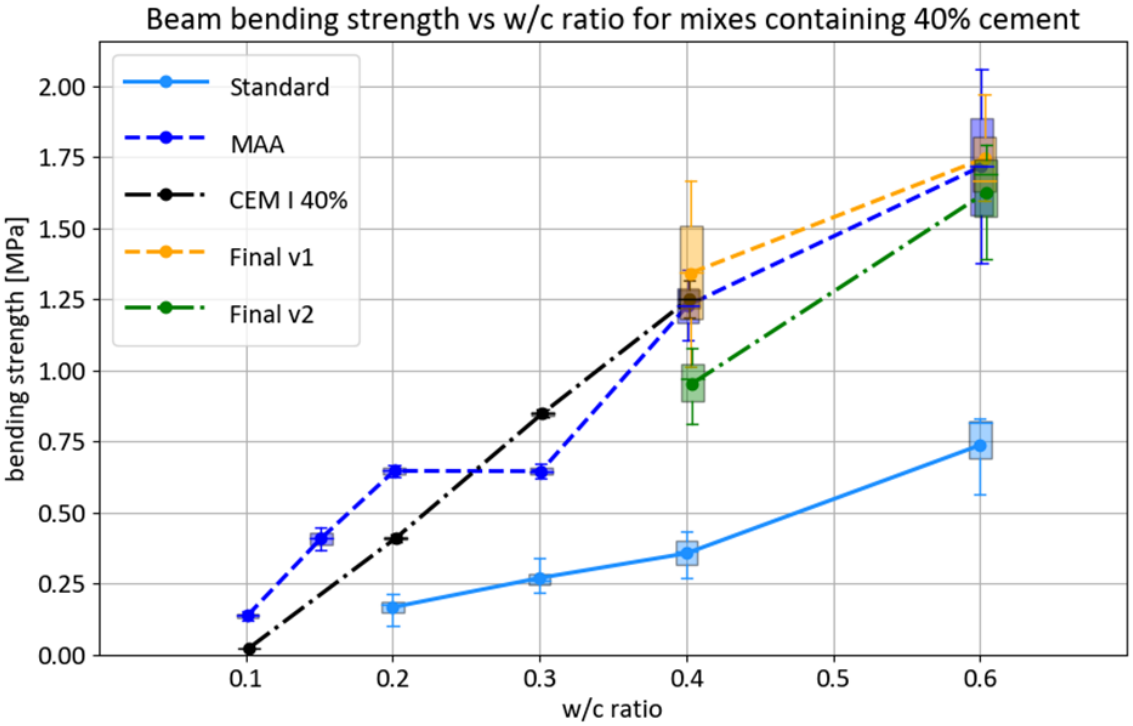

Figure 50: Beam bending strength vs w/c ratio for mixes containing 40% cement, compared to the 'standard' mix design

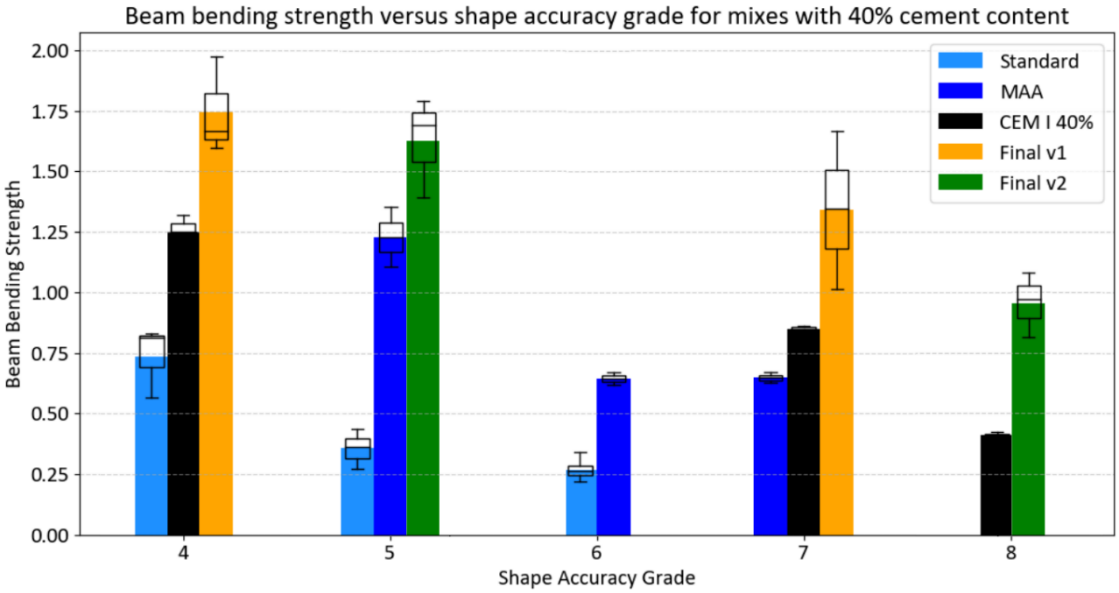

Figure 51: Shape accuracy grade vs beam bending strength for mixes with 40% cement content, compared to the 'standard' mix design. Appendix A presents a connected scatter plot of the same data

4.9 Curing

Curing the specimens might be especially important with C3DP, as it is likely that there is not enough free water to fully hydrate all the cement in the powder bed. Curing the specimens by wetting them introduces more water that might activate the remaining unhydrated cement particles. In Figure 52, the effectiveness of wetting the specimens is clear. Both submerged and 'misting' curing are shown to significantly improve the cube compressive strength after seven days, when comparing their results to that of dry curing. Furthermore, submerging the cubes is shown to yield better results than spraying the cubes every 24 hours, referred to as 'misting' in this research. Submerging the cubes produced such high strength values that the cubes with a w/c ratio of 0.6 did not fail under the maximum load of the force gauge. Consequently, this data point has been omitted.

A notable comparison is one between the seven- day dry curing experiment and the delayed de-powdering experiment. After only three days, the cubes that were left to cure in the powder are already comparable to, or even slightly stronger than the cubes that were stored in an open and dry place for seven days.

Lastly, the figure shows delaying the de-powdering process increases the strength. While perhaps not a surprising result, it does illustrate that when a higher strength is needed, for example when de-powdering a delicate object, delaying the de-powdering process can be up for consideration.

Figure 53, which shows the bending strength obtained by different curing methods, largely follows the same results found in Figure 52. There is however one big difference; the 'misting' method now yields stronger results than when submerging the beams. The reason for this is unclear; it could be a statistical outlier, or it may indicate that this method is better suited for measuring bending strength than compressive strength for some unknown reason. The cubes and the beams of the 'misting' experiment were cured at the same time in the same container, so large fluctuations in temperature or water quality can be ruled out.

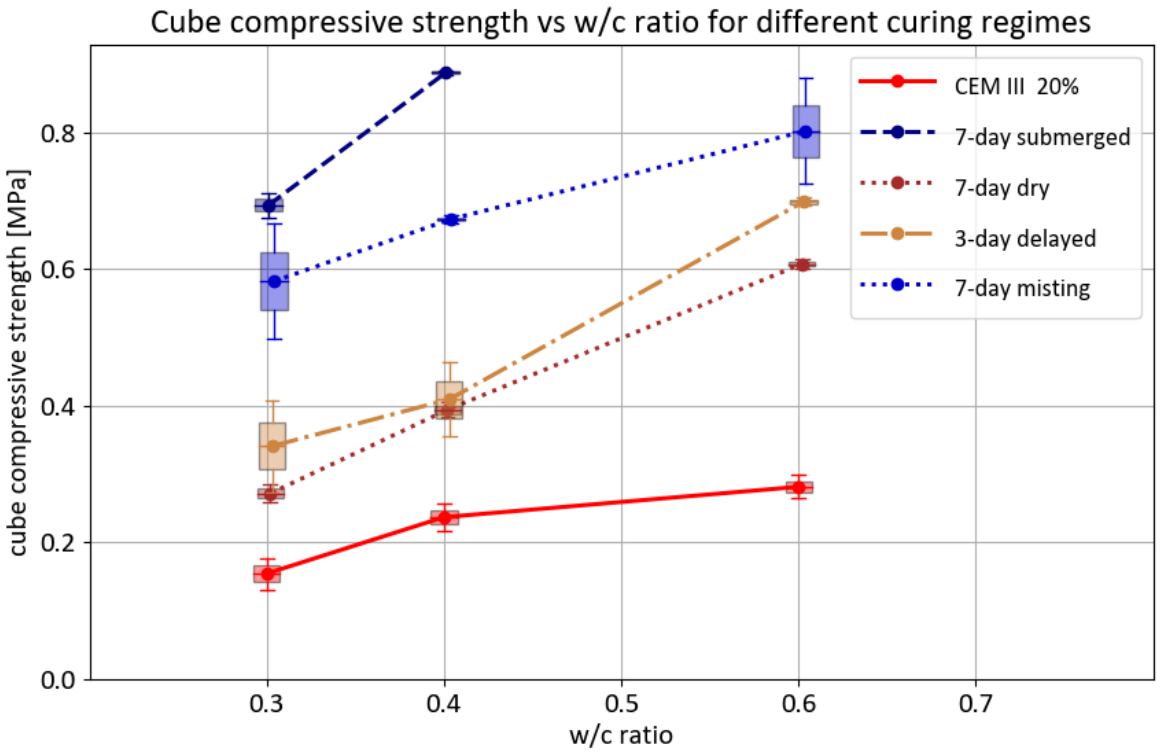

Figure 52: The influence of curing on the cube compressive strength. The cube compressive strength is plotted against the w/c ratio

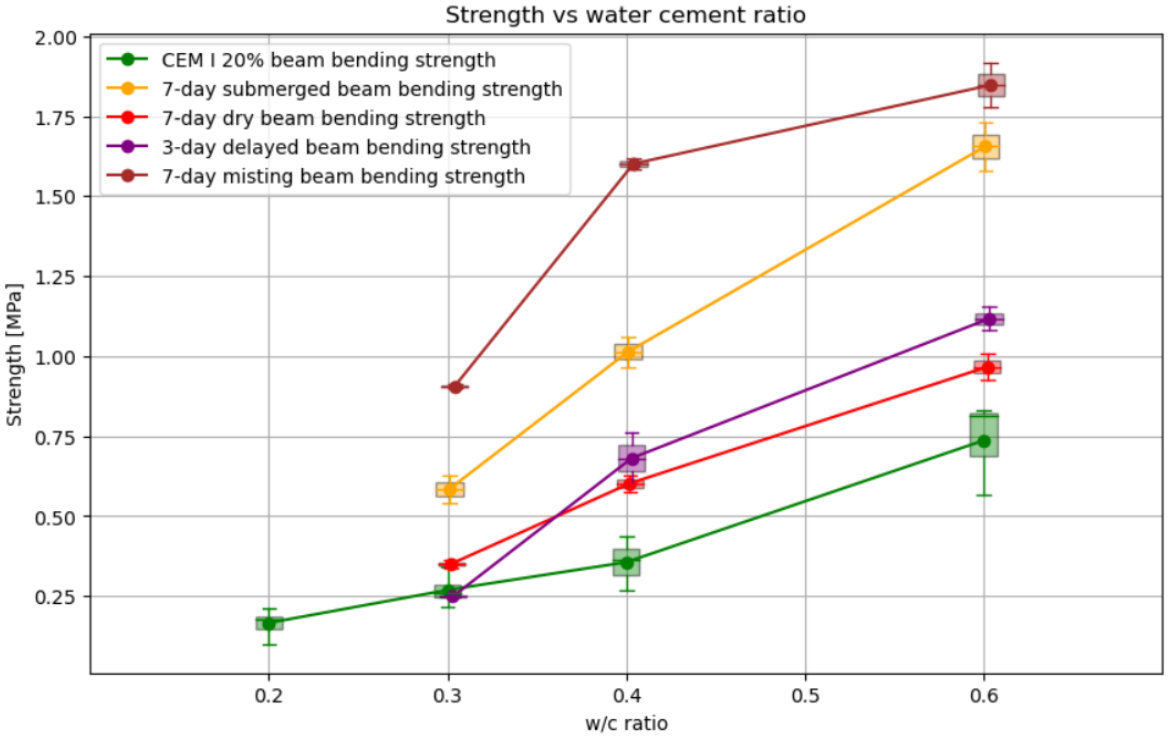

Figure 53: Beam bending strength versus w/c ratio for different curing methods

5. Discussion

This research aimed to identify adjustments in the activator, powder bed, or process that could improve the strength, sustainability or shape accuracy of 3DCP objects. Several potential modifications were selected from literature and subsequently evaluated through mechanical testing. The results of these tests were presented in the previous chapter. This lists the key findings, interprets the observed trends found in the results section, and provides possible explanations for these trends based on observations and literature. Furthermore, this discussion compares the mix designs to formulate the optimal mix design. Reasons for deviating from this optimal design will also be given, as it might not be optimal under every circumstance. Lastly, limitations of this study will be listed.

5.1 Key findings

In this section, the results will be briefly summarized and discussed. This section will highlight and discuss any remarkable results that were found. This section is divided into four sections. Each section discusses another topic that has a profound impact on the strength and shape accuracy of the 3DCP object.

5.1.1 Particle size distribution

In section 4.1, different particle size distributions were tested and displayed in the figures. Changing the PSD was found to significantly influence the strength and shape accuracy of the printed specimens. Both the linear and the MAA distributions showed an increase in strength over the 'standard'. For the MAA distribution, the strength and shape accuracy increase might however (partly) be attributed to the increased cement content, which will be discussed in the next section.

The increased strength of the linear distribution over the benchmark was unexpected. The hypothesis was that it would perform worse than the benchmark tests since this PSD was not optimized using the Modified Andreasen and Andersen method, or any other method. For this reason, the PSD of the linear mix design is likely worse, and consequently, the mechanical properties suffer. Interestingly, the opposite is true. It was predicted that the shape accuracy would also suffer from this lack of optimization since the water would more easily disperse through the more porous packing, but its performance is similar to that of the standard.

Perhaps this higher porosity is the reason why the strength is higher. The water easily penetrates outside the area where it was deposited due to this porosity, improving hydration of the entire layer. The linear distribution exhibits particularly high strength at elevated w/c ratios, further supporting the explanation that higher porosity can lead to increased strength. A higher w/c ratio causes higher pore saturation and therefore promotes more water transport to the area outside of the initially printed area. A counterargument to this theory is that due to this higher water transport, less detail would be visible and more partially hydrated cement would be visible on the sides of the specimen, resulting in a poor shape accuracy. While the shape accuracy of the linear distribution indeed was graded lower, the substantial increase in strength more than compensated for this limitation. Perhaps it is true that the test specimens of the linear distribution were a bit bigger (this was not noticed) and thus seemed to be stronger, and at the same time were still easily cleanable since the strength of the hydrated part outside the printed area was low enough.

While this explanation definitely is possible, it is unlikely since it would be noticeable that the test specimens with a higher w/c ratio would be bigger than the ones with a lower w/c ratio. Additionally, the material surrounding the printed area is something that was thoroughly investigated when cleaning and would be a big reason to deduct shape accuracy points.

Another, more likely explanation is that for these w/c ratios, up to 0.4, the deterioration in shape accuracy is simply not as pronounced as it might be for higher w/c ratios, and therefore the scoring for both the linear distribution and standard distribution is equal. The strength however might be higher due to better water transport in the cube. It is easier for the water to migrate to all the pores when the pore size is bigger. Or, the porosity of the linear PSD is not as bad as expected. The porosity of the specimens printed with different PSD's was not measured in this study, and so it is unclear whether the linear PSD is more porous.

5.1.2 Alternative binders and B/A ratio

Both alternative binders and the B/A ratio were found to have a profound effect on the strength, and to a lesser extent, the shape accuracy. Additionally, the choice of binder and the B/A ratio are the main factors affecting the sustainability of the mix design.

In the Results section it becomes evident that test specimens with increased C/A ratios have higher strength than the control test for the same w/c ratio. It needs to be noted however, that the w/c ratio can stay equal, but the total volume of water used in the specimens with elevated C/A ratios is substantially higher. If the C/A ratio is increased to for instance 40%, the total volume of water is doubled to reach the same w/c ratio when comparing it to the 'standard' C/A ratio of 20%. This is important to note, since more water generally means higher strength for one given mix design. For mix designs with higher w/c ratios, the specimens with higher C/A ratios will have more free water in the pores. The additional water increases the saturation level within these pores, thereby providing more available water for cement hydration, which in turn results in higher strength. Another advantage of a higher cement/ aggregate ratio closely ties into this: the PSD is likely also improved (see section 2.1.2.1). This results in less pore space for this excess water, leading to an even higher pore saturation level. Furthermore, this possibly improved PSD also results in a less porous material, preventing the water from migrating out of the pore space it is intended for.

Calcium aluminate cement was tested in different quantities and combinations with both OPC and CS. While the strength of some combinations resulted in a slight improvement over using OPC, the most notable benefit of CAC blends over regular OPC was their improved shape accuracy. Before testing, it was hypothesized that adding CAC would decrease the setting time and therefore would decrease the water penetration depth. Looking at the increased shape accuracy, this indeed seems to be the case.

Notable is that after cleaning, the specimens containing CAC often seemed to be underhydrated at the lower w/c ratios that were tested (for reference, see figure 26). A possible explanation for this is that since the products containing CAC have a faster setting time (see section 2.1.2.3), there is less time for capillary forces to migrate the water through the pores before hydration products form, restricting pore space. In combination with an already low capillary pressure due to the pores not being completely filled in a scenario with a lower w/c ratio, this results in the water not having time to migrate from the centre of the structure, the most saturated part, to the edges of the structure, which are perhaps less saturated. Another, simpler explanation is that the water requirement of this binary or ternary blend is higher for proper hydration to occur.

5.1.3 Additives and Fibres

In regular concrete, fibres are added for their tensile strength, increasing the bending strength of the concrete, or for reducing the crack width (Senapathi & Peiris, 2025). In this study, glass fibres were used that were designed to decrease the crack width, and cellulose fibres were incorporated for their ability to enhance the microstructure and increase both compression and bending strength (Li et al., 2025). Cellulose microfibers also retain a small amount of water, reducing the amount of excess water.

An additive named cellulose ether was studied for the same reason; to reduce the water penetration depth by retaining water and by increasing the viscosity of the water. Findings on both additives and fibres are discussed in this section.

Glass fibres were tested and as expected showed no increase in bending strength but did seem to make the test specimens behave more ductile. However, this effect was only noticeable when using a high amount of fibres. This in turn came with some problems: the fibres protruded from the layers, making it very difficult to properly print them without clogging the machine, and were therefore also very hard to clean. The surfaces were also quite rough and there was a very high loss of detail in the test specimens.

While the results of using these glass fibres were disappointing, it does not necessarily mean that fibres do not have a place in 3DCP. There is a large variety in types of fibres and dimensions available on the market. For instance, steel fibres have been shown to increase the bending strength of 3D printed concrete (de la Fuente et al., 2022). Unfortunately, steel fibres were out of the scope of this research since this study investigated a seawater application, where steel will corrode.

The microfibres that were studied were all cellulose based. These cellulose fibres were chosen since cellulose is a sustainable material that can be harvested from different plants or trees. The hypothesis was that these fibres would increase the bending strength and the shape accuracy, whilst slightly decreasing the carbon footprint by decreasing the amount of cement and aggregate of the product. However, as was found in section 4.4, there was no significant increase in shape accuracy or bending strength. Moreover, incorporating too many microfibres resulted in a decrease in compressive strength (see Figure 38). However, a dosage of one percent microfibres proved to be an improvement over the standard mix design, while only slightly. It showed improved strengths in bending and compression, as well as better shape accuracy. A dosage of half a percent decreased bending strength and had similar compressive strength and shape accuracy to the standard mix. This could indicate that the dosage of fibres is too low to show any significant effect. In contrast, the results of the specimens with two percent fibres showed indications that the dosage might be too high, resulting in a worse PSD, and lower strength as a consequence. Both the bending strength and shape accuracy showed no improvement over the benchmark test, and the compressive strength was around 35% lower than that of the standard mix design. Especially this decrease in compressive strength is a strong indicator that the dosage is too high, as increasing the amount of fibres in the mix results in a reduction of the amount of cement and aggregate. Since fibres hardly participate in transferring compressive loads (Li et al., 2025), adding fibres are analogous to increasing the void space in the case of compression. Also, the cellulose microfibres have a far lower density than the cement or the aggregate. This means that these two percent of fibres occupy a lot more than two percent of the volume of the material. This example, where too many fibres were added shows the importance of printing with a dense material with good compaction and a good particle size distribution.

So, the results on microfibres are not completely convincing. On the one hand, a correct dosage of microfibres could help with water retention and increase shape accuracy and might even increase bending strength slightly. Perhaps, the correct type of microfibre with the right properties could act similar to a cellulose powder with the added effect of decreasing cracking. But on the other hand, the results of one percent fibres were only slightly better than the standard mix and might not be worth the added extra work and cost of mixing in these microfibres. Furthermore, only the specimens containing one percent fibres show any promising results, while the other dosages do not.

It is possible that this better performance is due to external factors like slightly higher temperatures while curing or statistical deviation (see section 5.3). In addition, two other types of microfibres of the same supplier were also tested, one longer and one shorter than the one featured in this study. Both these fibres showed worse results than medium- length B00 fibre. Therefore, it is unlikely that there is a type of microfibre that when added to the mix would yield very good results, meaning a big increase in both bending strength and shape accuracy, while not decreasing the compressive strength too much.

In Figures 33 and 34 in section 4.3, horizontal lines can be observed in the cross- section when using cellulose ether. It was observed that the dark lines are flat on the top side, suggesting that the top part of the dark lines are where the scraper blade of the printer flattens the powder. This would mean that the top of the dark line is also the place where the water is sprayed on the layer. Cellulose ether is normally used in construction as a thickener or rheology modifier. When mixed with water, it increases the viscosity, creating a more gel-like fluid. When the water comes into contact with the CE in the layer, the viscosity of the water is increased, making it harder for the water to enter the empty pores surrounding it. The further the water penetrates the powder mix, the more CE will be absorbed into the water, until at some point the viscosity is too great for the water to penetrate any further. The water retention of CE thus occurs because water migration between pores is blocked (Chen et al., 2020).

This likely is an explanation of what can be seen in Figure 32 and 33. The CE prevents further water migration from the dark lines into the surrounding dry powder, confining all the water in the dark line. If this is indeed the case, it would mean that the dark line is dark simply due to the pores in that part still being saturated. This would also explain why the dark lines become more apparent when increasing the w/c ratio. Adding more water would mean that more water is confined in the same pore space, making the lines appear darker due to this increased saturation. The problem however is that if all the water is confined to just the dark parts, the water cannot penetrate through the entire layer. This results in the beams not consisting of one piece of concrete but is instead 12 thin concrete layers on top of each other separated by a layer of dry powder. And indeed, during testing the material seems to behave as separate layers instead of one block of concrete. The bending strength was close to zero, which is unsurprising for 12 separate very thin layers of concrete. And when testing the cubes for compression, the blocks seemed to behave quite ductile, possibly due to the layers of dry powder being compressed between the layers. The trend where the strength increases when the w/c ratio increases can also hardly be found when looking at Figure 31, especially for the mixes containing higher amounts of HEMC. This is likely due to the strength of all of them being close to zero, because of the poor bonding between the layers. As discussed, these blocks now act more like stacked layers instead of one block with sand in between. As a result, these ‘cubes’ now behave unexpectedly when compressed, resulting in some large deviations and outliers.

5.1.4 Curing

Four different methods of curing were tested and compared in this research. Two of the four involved wetting the specimens for seven days, one experiment was performed on dry curing, the final curing approach consisted of de-powdering the specimens after a 72-hour period, in contrast to the 24-hour de-powdering protocol applied in this research. Most results found in section 4.9 are as expected, wetting the specimens performing better than dry curing, and delaying the de-powdering process yielding an increase in strength. However, two results were surprising.

Firstly, from the results it seems that underwater curing yields better compressive strength, while misting the specimens resulted in higher bending strength. This result is surprising, as it was expected that underwater curing would yield better results in both compression and bending. Underwater curing guarantees the availability of water for hydration (unless the cement is not accessible through the pore space. Mai et al. (2022b) found that only 62 percent of the pores were transport relevant) everywhere in the specimen, whereas periodically spraying the water onto the beams and cubes does not. Furthermore, the 'misting' approach involved manually spraying the water onto the specimens, making it likely that not all parts of the beams and cubes receive the same amount of fluids. Spraying the water also means that the bottom of the beams and cubes come into contact more with the water than the rest of the object, since the water will drip down and form puddles on the bottom of the container. The containers were however sealed in plastic, likely resulting in a high humidity, transporting the water into the pores of the specimens, similar to the gunny bag approach from Pawar and Kate (2020). Furthermore, the specimens were only sprayed every 24 hours, meaning that it might be possible some surfaces dry up in between watering sessions. It is therefore unlikely that the 'misting' approach is more effective in increasing the bending strength, and the large differences between both methods is likely a statistical outlier, or due to another external factor (see section 5.3). However, since the beams and cubes of the misting approach were all printed and cured at once, and all specimens were cured in the same container, it is interesting that the cubes made with the 'misting' method do not also result in higher mechanical test results. More research is needed to find a satisfactory explanation for this matter.

The second surprising result is found when comparing the strength results of the specimens de-powdered after 72 hours, and the specimens that were dry- cured over 7 days (see Figure 52 and Figure 53). Despite the large difference in curing time, both perform similarly, with the specimens that were tested after 3 days even yielding slightly higher strength test results. The difference between the two experiments, is that one set of specimens was de-powdered and left exposed to the dry air, while the other set was still surrounded by the powder mix. The air exposure resulted in the specimens losing moisture and drying out, while the powder mix in the other setup prevented this loss of moisture. When delaying the de-powdering, moisture will still freely transport through the pore space governed by capillary pressure differences, even after the onset of hydration (Zuo et al., 2020). This transport will result in the moisture migrating away from the volume it was initially deposited, slowly moving to the surrounding dry pores (see section 2.1.1). However, this is a slow process, so the loss of water is smaller.

5.2 Comparison of Mix Designs

At the end of the Results section, promising materials were combined, tested and compared to the 'standard' design. Some of these combinations certainly seem to yield stronger results while also having higher shape accuracy compared to the 'standard'. And some other additives can certainly be very useful in some design situations. This all poses the questions: what is the best mix design?

When looking at the graphs in the results section, it might be tempting to look for the highest strength and declare that as the 'best' mixture. However, the strength graphs do not include important information on the workability or shape accuracy of the material. This key information can however be found in the other main type of graph used in this study, where the shape accuracy is plotted against the strength. Comparing the materials this way however has one major disadvantage: The shape accuracy is subjective. While efforts were made to eliminate this subjectiveness by looking for other ways to measure or quantify the shape accuracy, as discussed in section 3.2, at the end it was deemed that this grading method was most convenient.

By clearly stating how the material was graded, this subjectiveness can be decreased slightly, however it is of course hard to determine whether a test piece scores a 6 or a 7.

When analysing the findings on the different PSD's, it became apparent that the MAA performed significantly better than both the linear distribution and the 'standard'. However, the MAA was comparable to the mix design with a C/A ratio of 0.4, indicating that the increased strength could be attributed to the increased cement content, and that the MAA distribution was not much better than the 'standard' distribution. But the opposite could also be true: The reason a C/A ratio of 0.4 results in better strength than the other C/A ratios can be a result of the increased PSD. In any case, the cement to aggregate ratio had the best strength results, and will therefore be incorporated into the final mix design. CAC blends were found to slightly increase both the strength and the shape accuracy. Of the tested combinations, a ternary system containing 90% OPC, 5% CAC and 5% CS performed best. Where OPC was graded a 6 or a 5 depending on w/c ratio, this 90-5-5% ratio was graded an eight. Since incorporating CAC is strictly beneficial to the mix design criteria, it was added to the final mix design. The only thing to consider when incorporating this ternary system is that the w/c ratio needs increasing to prevent underhydration.

From the results section, it can be concluded that CEM I outperformed CEM III. This difference in strength however was attributed to the different strength classes of the two types of cement, as well as the differences in hydration speed. The CEM I used has class 52.5 R and CEM III had class 42.5 N, and therefore it was expected that CEM I would yield better mechanical test results. EN 197-1 states that the obtained strength when using 52.5 R should be over 30 MPa, and when using 42.5 N, the strength is required to be 42.5 N. However, figure 38 does not show a threefold difference in strength between CEM I and CEM III. The reason for this is that the strength rating of a cement only has limited influence on the strength of the concrete or mortar. Other factors, like porosity and degree of hydration also influence the strength of the mortar or concrete. These two factors are likely also the biggest reasons as to why the 3DCP specimens show relatively low strength when compared to cast concrete. High performance concrete (HPC) can get a 24-hour strength of over 25 MPa (Dushimimana et al., 2021), while the best performing specimens in this study reached strengths of slightly over 1 MPa. CEM III is significantly more sustainable than CEM I however, so when the strength classes would be equal, the choice should be made in favour of CEM III. Other CEM III types were unavailable in this study, so CEM I is used instead in the final mix design. Additionally, the effects of combining CEM III with CAC and CS are not investigated in this study.

Cellulose ether significantly improves the shape accuracy with minimal downsides if the correct dosage is applied. The CE shows a sudden decrease in strength when increasing the dosage from 0.25 to 0.5%. The low performance of the higher CE dosages can be attributed to the reduction in water penetration depth due to the CE (see section 2.1.2.4). This drastic strength reduction indicates that there likely is an optimum dosage where the penetration depth is equal or slightly over the layer height, resulting in the best achievable shape accuracy whilst still retaining strength (Mai et al., 2022b). This optimum is likely close to the 0.25%, which therefore is the chosen ratio for incorporation in the final design. There is a risk of decreasing the water penetration depth too much with the use of cellulose ether. Cellulose fibres were expected to have a similar effect; retaining water and increasing the shape accuracy. However, this effect was not present in the results and the cellulose fibres are therefore omitted from the final design.

Since the optimum dosage of CE is unknown, especially when combined with alternative binders and an increased C/A ratio, the decision was made to make two final mix designs. One would contain the CE, the other would not.

This approach allowed for studying whether this dosage would not be too high. The expected result was that the first version would be slightly stronger than the second version, due to the assumption that adding HEMC would decrease the 24-hour strength. However, this was only found to be the case for the cube strength (Figure 47) but not for the bending strength (Figure 48). This could be due to environmental factors or slight deviations in material quality, or other testing limitations (see section 2.1.2.4). Another explanation can be that such a small quantity of HEMC has (almost) no effect on the strength. Figure 32 also shows that when only adding very small quantities of HEMC, the strength is still comparable to that of cubes without HEMC. Lowke et al. (2022a) reported that a small dosage of CE could result in a slight increase in strength due to the water retention and subsequent release, resulting in more water available for hydration at a later stage. This could serve as an explanation for this finding. Both mix designs show excellent results, with its strength being comparable to other mixes containing 40% binder, but with a significant increase in shape accuracy.

5.3 Practical implications

The final mix designs are the optimal result found in this study for the requirements and limitations posed in the introduction. Both final mix designs exhibit better shape accuracy and strength than any of the other designs. The differences in both final mix designs are slight, so the added practical risks associated with the addition of cellulose ether, being the risk of overdosing and obtaining unusable products, need to be considered. This risk of adding cellulose ether is an example of some of the practical implications associated with these changes in binders and additives. There are still numerous other reasons to differ from the suggested final mix designs, such as:

Availability. Some materials used in this study might be harder to come by in certain parts of the world.

Cost. Some materials might not be worth the price for the added performance. For example, the results section shows how adding CAC to the mix increases the strength and shape accuracy grade. However, CAC is more expensive than OPC. So in order to reach similar performance, we might instead opt for increasing the OPC content.

Sustainability. Some test specimens are more environmentally friendly than others. For example, to decrease the CO2 footprint of the product, a lower cement to aggregate ratio can be used than what would be optimal for performance.

Printing time. Some mixes take significantly more time to print than others. The printing time is mainly determined by the speed at which the nozzle moves, which is in turn determined by the w/c ratio that is required.

Recyclability. Some materials require very precise dosages in order to deliver proper results, while others are a bit more ‘robust’. After printing, the particles around the product will be removed and recycled. However, some of this material might contain partially hydrated cement. When recycling the material, it is hard to know how much of it has come into contact with moisture during the printing process. This means that the exact content of remaining ‘usable’ activator is now unknown. Another example, mixes containing HEMC are very hard to recycle, since the dosage of HEMC needs to be determined quite accurately in order to achieve the optimal penetration depth.

Ease of use. Some materials, like fibres, can be troublesome to work with as they can clog up your machinery. Others, like HEMC are hard to properly mix into your powder bed.

Durability. Some printed concrete materials might have a shorter lifespan than others, especially when the concrete is expected to be subject to harsh conditions. Examples of harsh conditions are freeze- thaw cycles and exposure to chlorides or other chemicals. Taking durability into account is especially relevant when incorporating rebar into a design. Durability issues depend on the application environment. For the use case examined here, structures located at the seabed, freeze-thaw cycles are not a governing factor, but chloride ingress can be.

While the decision was made to not use fibres in the final mix design, it does not mean they are never to be recommended. Fibres can offer crack resistance. During some large-scale tests for another study, problems were encountered with handling some bigger structures, due to them being very brittle. Some of these structures suddenly cracked and completely failed during removal from the supportive powder bed and could not be repaired. For these types of failure modes, glass fibres or other types of fibres might offer a solution. They could decrease the brittleness of the concrete and stop the crack from propagating all the way through the structure, limiting the damage. This added ductility was however not found when testing the cellulose microfibres. Other situations where glass fibres can be helpful is for example when there is a lot of drying shrinkage. For example, as discussed earlier, the usage of accelerators or faster setting types of cement can decrease the water penetration depth whilst also increase the early age strength of the concrete. But some, if not most, of these accelerators and cement types are prone to shrinkage problems (see section 2.1.2.3). Adding fibres can help mitigate these added problems of fast- setting concrete.

To conclude, there likely is not one best mixture for all circumstances. Moreover, the best mixture for one given situation might even contain additives and materials that are not even in this study, given the sheer amount of options available on the market. It is therefore important to keep innovating and studying alternatives to come closer to the best design.

5.4 Limitations

In this study it was found that conditions like temperature, humidity, and material quality and age also have a big impact on the performance of the print. To address this issue, the product requires quality monitoring and may necessitate minor adjustments to the mixture design or curing procedure to compensate for the varying conditions. These conditions that affect the product are further discussed below.

5.3.1 Low test volume

In the strength versus water to cement ratio figures, some plotted lines can be seen to behave less linear than the others. This is because of two reasons: The first reason being that most powders were only tested 2 or 3 times, giving a quite poor estimate on what the mean strength of that specific mix should be. The result is that all three mixes could either end up on the high end of the actual mean strength value or on the low end, resulting in a value that does not fall in line with the expectation of a somewhat linear relationship between the strength and the w/c ratio.

5.3.2 Environmental factors and material quality

Another explanation for these deviations is that unforeseen external factors have played a role in the strength development of the concrete. An example is where the specimens of HEMC 0.5% with low w/c ratios exhibited higher strength than the specimens of the same mix with a higher w/c ratio Initially, the researchers were uncertain as to the underlying cause of this phenomenon. All test specimens were made with the same material mixed in one go and using the same printer, procedure, and curing method. Later it was found that this was not due to some unknown effect of the concrete, but because the test specimens with higher w/c ratios were tested 3 weeks later than the first test specimens.

In the meantime, the mix was stored in thick plastic bags and were wrapped airtight. However, after searching for an explanation, it was discovered that the bags were of quite poor quality and this particular bag had some small holes in it. Air could then enter the bag and the moisture in the air could then interact with the mix, and this was likely the reason the concrete test specimens performed poorly. After this discovery all the tests made with mixes in those particular bags had to be redone and only double bagged the mixes or stored them in sealed containers onwards (interestingly, even after redoing the tests with freshly mixed cement, the test specimens of HEMC with low w/c ratios still show unexpectedly high strengths compared to higher w/c ratios). But still, some material deterioration could have occurred during some of the tests without it being discovered.

5.3.3 Testing equipment limitations

What also stands out from the strength graphs is that the strength of MAA with 0.6 w/c ratio is omitted from the graph. The strength of these samples were so high that the testing equipment was not strong enough to reach the ultimate strength of the cubes. Therefore, it is unknown how strong the cubes actually were. This posed to be a significant limitation, as this not only happened with MAA, but also with the final mix designs, and the curing experiments.

5.3.4 Direction of testing

All specimens were only tested in the z- direction, perpendicular to the layers. Since the specimens are printed layer by layer, the material properties are not homogeneous in every direction; some loading directions are stronger than others. This is mainly because of the possibility of delamination between the layers. Similar to composite materials like a concrete deck connected to steel beams or plywood panels, the strength of 3D printed concrete in part depends on the bond between the different parts. In concrete deck to steel beams connections, this is achieved using shear connectors. In plywood this can be achieved using glue. But in 3D printed concrete, the only bonding between the layers are the cement hydration products and some particle interlocking from the aggregates, fibres can also increase the interlayer bonding (de la Fuente et al., 2022).

5.3.5 Shape accuracy

Determining the shape accuracy is of itself a very subjective task. Using such a method heavily relies on the objectiveness of the researcher. The researcher could have graded a certain mix better or worse because of consciously or unconsciously having a preference on what the outcome needs to be. While the researchers tried to prevent this by adhering to a certain methodology to assess the small structures, it is difficult to prevent such a bias from being reflected in the results. Another issue with this grading system is that in order to accurately grade all the test specimens, the researcher first need to develop a frame of reference. In practice, this means that the researcher could only assess the structures based off the structures previously examined. Consequently, the grades assigned to earlier test specimens had to be revised multiple times, as the frame of reference evolved with each new assessment. To support this re-evaluation process, the cleaning procedure after each test was carefully documented and written down.

A more objective method of evaluating the shape accuracy would have been by using a standardized method of cleaning and then measuring the shape after going through this standardized process. The caveats of using a standardized cleaning method however is that it will need to be chosen very carefully in order to be able to accurately find out which shape is easier to clean. For example, before deciding on cleaning by hand, other methods of cleaning the structures have been explored, like sandblasting or power- washing. However, for these methods it needs to be decided what pressure to exert on the structures to clean them.

The problem is that this pressure will have to be different for different mix designs, due to the different mixes having vastly different strengths, and therefore the strength of the partially hydrated concrete surrounding the structure is also very different. Using a high force for removing this partially hydrated concrete is perfect for high strength test specimens but might damage or destroy the weaker structures. Due to these issues, and the time it takes to create such a setup, it was deemed too difficult and time consuming for this research.

5.3.6 Size inconsistency

The size of the specimens was observed to increase with increasing w/c ratio, as discussed in the methods section. In this research, the influence of deviations in specimen size was not accounted for, as the observed size differences were relatively small. Moreover, it was assumed that the increase in size could largely be mitigated through rigorous cleaning of the larger specimens. It was further hypothesized that the observed size increase was primarily caused by partially hydrated cement adhering to the specimen surface. This material is expected to exhibit relatively low mechanical strength compared to the more fully hydrated cement within the specimen and is therefore unlikely to contribute significantly to the measured strength. Nevertheless, specimen size is an important parameter in strength determination. In compression testing, both the length and width of the specimen directly influence the strength (see Equation (*11*)). Deviations in size are even more significant in the case of bending, as the length and width, as well as the square of the specimen height, are incorporated into the calculation of the flexural bending moment (see Equation (*16*)). Consequently, even small increases in specimen dimensions may still affect the measured strength values. This effect is particularly relevant for specimens with lower shape accuracy grades, as these specimens are more likely to be oversaturated and therefore larger. As a result, the potential influence of specimen size cannot be excluded and should be considered a limitation of this study when interpreting the strength test results.

6. Conclusion

At the end of the Introduction section of this paper the following research question was posed:

How to design a strong and sustainable concrete mix for use in 3D concrete printing artificial reefs?

This thesis has tried to answer this question by reading literature, to find possible solutions that would fall within the scope of this research. Next, methods were established to determine whether the solutions from the literature are suitable for the application outlined at the start of this report. Several materials were identified that could potentially improve the strength, sustainability, or shape accuracy of the printed product. Next, over 20 different mix designs divided into six different material categories or properties were tested in the Results section.

From the Discussion and the Results, it can be concluded that some mix designs certainly improved 24-hour strength, sustainability, and/ or shape accuracy. The most effective ways of increasing the strength, while still having an acceptable shape accuracy, are increasing the cement content or by using calcium aluminate cement in combination with calcium sulphate. To be more specific, a cement content of 40% yielded the best result, and a combination of 5% CAC, 5% CS and 90% OPC was the most effective proportion.

The shape accuracy, the measure of how closely the printed product matched the design and how well it could be cleaned or post- processed, was another important metric that was set out to improve. The water penetration depth was found to be the governing factor of the shape accuracy. The penetration depth is the measure of how far the water will propagate downwards in a certain timeframe. Too much penetration depth, and the water would propagate too far, resulting in a big loss in detail as the water will now hydrate the cement outside of the intended area. Too little penetration depth, and the water will not be able to reach the layer below it, resulting in delamination, and a huge loss in strength. The most potent way of improving the shape accuracy found in this study is by adding a cellulose ether powder. When this powder comes into contact with water, it increases the viscosity of the water, limiting the propagation of the water through the pores and thus decreasing the penetration depth. However, there is a fine line between too much and too little penetration depth, and the highly potent cellulose powder was proven to be difficult correctly dose. Adding cellulose powder drastically improves shape accuracy, but also reduces the strength, especially when the dosage is slightly too high. Another option of improving the shape accuracy is by using a combination of CAC, CS and OPC. This mixture drastically decreases the setting time, thereby decreasing the time the water has to propagate before hydration occurs. While not as strong as cellulose powder, it still significantly improved the shape accuracy. Lastly, it was found that increased C/A ratios also improved the shape accuracy, but only slightly.

It can be concluded that adding an accelerator like CAC improves the mix design with almost no downsides. This however cannot be said for most other things that were tested. Increasing the cement content does increase the strength tremendously but is costly and not a sustainable solution. Incorporating fibres can improve ductility and reduce cracking, but longer fibres are prone to clogging up the machinery. Cellulose ethers have the potential to tremendously increase shape accuracy, but a slight change in dosage can render the printed object useless.

So, is there an ideal mix design? That entirely depends on the applications, limitations and possibilities within a given project. Even for the specific application that has been discussed in this report, the ideal mix design very likely has not been found, but it certainly has improved. There are still so many different additives, binders, and activators to research and test. But looking back at the main research question, there now definitely is a strong, and accurate concrete mix.

7. Recommendations

In the previous chapter it has been concluded that some researched additives and binders can help improve mix design, but there are still a lot more aspects of this printing technique to be researched. Not only binders, additives, activators or aggregates affect the product outcome. Software and hardware also influence the strength and shape accuracy of the printed item, perhaps even more so than the material itself. During this thesis, some possible software and hardware adaptations were found to play a big role in the quality of the print. These adaptations, amongst others, will be discussed in this chapter and might be interesting topics for future research. Furthermore, recommendations on how to choose the right additives or binders will also be discussed in this chapter.

7.1 Recommendations on mix design

The discussion has identified some additives or alternative binders with positive qualities, of which only CAC in combination with CS seem to be without (or limited) downsides. Besides CAC, when the goal is to improve strength, increasing the cement content is an effective way. However, increasing the cement content is not a sustainable solution to increasing the strength. Generally, a w/c ratio of at least 0.3 is advised when using CAC or when increasing the C/A ratio for the product to not be undersaturated. But a w/c ratio up to 0.4, or even slightly higher can still yield strong products with good shape accuracy. When increasing the C/A ratio, the recommended ratio is 40%, which can be lowered to reduce climate impact. Even higher ratios might yield even better results, but at that point the particle size distribution will be negatively impacted, possibly leading to a loss in shape accuracy. If both strength and shape accuracy need to be improved, CAC is again a good recommendation. But when using CAC, it is important to know that the setting time is very fast, so this might not yield the same results when the layer height is increased or when there is a long pause between the printing of two vertically adjacent layers.

When only the shape accuracy needs to be improved, cellulose powders can be used. Only small amounts of cellulose powder (<0.5wt%) already yield great improvements, but it does negatively impact the strength of the product. Therefore, it is recommended to start off with a dosage of only 0.5%. After cleaning, a test piece can be broken in half to easily see whether the layers have bonded correctly, like in Figure 33. If so, adjust dosage accordingly. When using cellulose powder, keep in mind that small deviations from the correct dosage can be detrimental. Therefore, constant quality monitoring is useful, especially when recycling the printed material. In that case, the amount of unreacted cellulose powder is unknown since some of it might have already been partially hydrated and will have lost its effectiveness.

Changing binder from CEM I to CEM III is recommended for creating a more sustainable product, and possibly improved durability for use in salt water. The class of the binder however is recommended to be 52.5 R to obtain good early age strength of the product. This study has however not researched the use of CEM III in combination with other binders like CAC, CS or geopolymers. Further research on these combinations is therefore recommended.

A recommended approach for finding the right mix design for a given project is to start with the shape accuracy, rather than with the strength. If a high shape accuracy is required, consider using ternary binder blends and adding CE, in combination with a lower w/c ratio. Once the shape accuracy requirement has been set, consider the preferred amount of strength.

Increasing the strength however, is usually at the cost of sustainability and/ or shape accuracy. Cost is another consideration affecting the amount of additives and C/A ratio.

7.2 Recommendations on procedural processes

The printing process is not finished after the printer deposits the last layer. Cleaning and curing are two essential steps that follow. Efficient and safe cleaning is important in speeding up production, and implementing a good curing regime is essential for proper hydration.

7.2.1 Cleaning

In this study, roughly 170 cubes and 170 beams have been cleaned. So while not strictly in the scope of this study, some recommendations can be made on the cleaning procedure based on this gained experience. First, there is a multitude of tools to choose from when cleaning. But simple protective gloves proved to be the most effective. When using spoons or brushes, it is hard to gauge how much pressure is put on the item. Gloves solve this problem and make it easy to clean more complex shapes. The only other recommended item is an industrial vacuum cleaner to quickly remove all the loose powder. The added benefit of such a vacuum cleaner is that mostly only the sand is removed that is not or is barely hydrated. Therefore, the powder that is sucked out can safely be reused.

Semi or fully automated cleaning is a topic for future studies, but some considerations on this topic are given: Sand blasting or cleaning with pressurised air both have the potential to completely automate this process, but can be more destructive and might damage the structures when done incorrectly. Consider using the known strength of the material to adjust the cleaning process accordingly in order to remove as much partially hydrated cement without damaging the structure itself. Another cleaning solution that can take advantage of the known material strength is by using brushes or sponges that can assert a similar pressure.

7.2.2 Curing

The section 2.1.2.3 has shown that curing is an important step in increasing the strength of the 3DCP object. Different methods of curing resulted in large differences in bending and compression strengths.

Section 4.9 also revealed some unexpected results: The ‘misting’ method bending test results surprisingly outperformed the results of the specimens that were submerged. Section 5.1.4 attributed this to chance, but further research is required to confirm this. The differences were large, and therefore it might be worth to investigate the cause. Nevertheless, these results show the importance of implementing a proper curing regime.

Section 5.1.4 further mentioned the increased strength obtained by delaying the de-powdering by 2 more days. The increased strength could for example be beneficial when de-powdering a delicate object, to decrease the risk of breaking. However, since the object will have lost more moisture than when de-powdering after 24 hours, the risk of cracking due to drying shrinkage is increased. The exact mechanics of this drying process is however unknown as it is dependent on the migration of fluid through the porous medium. Further research on this topic is required to more accurately estimate the potential risks and rewards from this curing method.

7.3 Recommendations on future research

During this study, we have come across some information on 3D printing that was out of the scope of this study, but that are nonetheless very much relevant to this topic and are worth studying to improve strength and shape accuracy.

7.3.1 Hardware and software

Not only the powder bed or the binder influences the quality of the product, but the printer itself too. Regarding software, the most promising topic worth researching might be where the water can be sprayed to maximise strength and minimise water transport outside of the intended volume. The printer used in this study controls the w/c ratio by adjusting the speed at which the nozzle moves, while keeping the rate of flow constant. This makes it possible to accurately adjust the w/c ratio. This allows for hydrating parts of the design more than other parts, strengthening the design where needed. One principle that uses this technique is called the shell- core principle (see Figure 54) where the design is split into two: the shell and the core. The core has a higher w/c ratio, acting like the reinforcement of the design. The core region in turn has a lower w/c ratio to prevent oversaturation. Examples of previous studies using this principle are: (Xia et al., 2018) and (Xia et al., 2019a). The illustration in Figure 54 is of course a simple design, but with more complex designs it might be worth using finite element methods (FEM) or similar software tools to locate the parts of the design where structural reinforcement is most necessary.

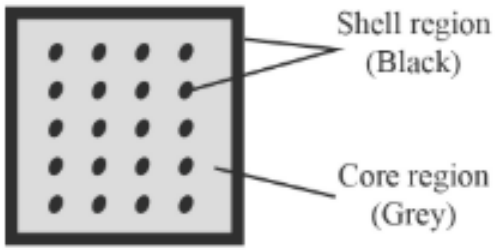

Figure 54: The core and shell principle (Xia et al., 2018)

The part of the printer that has the most effect on the outcome is the compacting roller or scraper blade. This part of the machine creates pressure onto the layer after depositing, compacting the layer and reducing pore space. Different studies have shown that testing with different types and degrees of compaction might come with a big increase in strength (de la Fuente et al., 2022; Lowke et al., 2022a; Talke et al., 2023). When done correctly, the degree of compaction is as high as possible without pressuring the lower layers too much that they crack. Ensuring a good degree of compaction is likely one of the most important things that can be done to improve the strength of the product, and is therefore worth studying.

7.3.2 Curing

This research has shown that the method of curing can have a big impact on the final strength. However, since it was not a main part of this study, this topic has only lightly been touched upon. More research on curing might include:

1. Researching the strength development over time during curing, to find the optimal time to cure a product in order to reach a certain strength
2. Researching the effects of some additives on the curing process. This is especially interesting when using alternative binders, water absorbing additives or rheology modifiers like cellulose powder.
3. Testing different ways of curing, like curing in a misting chamber, steam curing, or curing at elevated temperatures.
4. Researching the effect of delayed de-powdering on crack formation due to dry shrinkage or autogenous shrinkage.

7.3.3 Durability

Testing the durability of a product is generally time consuming and might require specialised equipment. But since the product is very likely relatively porous, it would be interesting to see or predict the long- term effects of exposure to the elements on the product. Porosity has shown to significantly decrease the durability performance of 3DCP (Ler et al., 2024). Studying the long- term strength development of different mix designs would be an interesting and useful follow- up research. Such a study should contain a literature review on the durability to make it less time consuming and might include methods like x-ray computed tomography (XCT) and mercury intrusion porosimetry (MIP) to quantify the porosity.

7.3.4 Sustainability

Climate change is one of the biggest problems the world is facing right now. As discussed in the introduction of this study, about 4 to 8% of global emissions is caused by concrete and this can be reduced by up to 70% when using 3DCP (de Brito & Kurda, 2021; Lowke et al., 2020). Therefore, it is imperative that cement usage is reduced. But still, this study does recommend a higher cement content when a higher strength is required, taking away from this benefit that additive manufacturing techniques have over traditional casting. For this reason, it is highly recommended to also experiment with different, more sustainable types of binder. Examples of this are alkali activated binders, also known as geopolymers, of which fly ash, metakaolin and blast furnace slag are the most well-known. The added benefit of these types of binders is that they usually exhibit very good early age strength (Santhanam et al., 2025). However, the downside, and the reason that they are not included in this study, is that they require an alkaline activator. This means that personal protective equipment is needed to work with these chemicals, and that the printer itself needs to be able to handle these chemicals. Nevertheless, alkali activated binders might be worth the trouble and are recommended to do further research on.

Especially for applications like the one discussed in this study, where marine life will come into close contact with the printed structures, it is important to know whether the structures do not leech out dangerous metals or chemicals into the water. Therefore, it is recommended that when a new mix design is made, it should undergo a leeching test. A simple version of this test is done by placing the cured structure into a water filled container, and after some time test what dangerous substances and how much of it has entered the water.

7.4 Recommendations on future experimental procedures

This research has tested multiple additives and alternative binders, but there are still numerous others to be tested. Here are some recommendations to properly and efficiently do this.

The first thing that could be improved is the testing equipment. This research used a compression machine with a maximum force of only 1000 N. This is one of the reasons why the testing cubes in this research are so small, any larger and the strength of the cube would always exceed the maximum force. Better equipment with a higher force allowance will allow future researchers to print regular sized compression test cubes or cylinders to properly compare them to regular concrete.

Another improvement would be to cure the cubes in a climate-controlled environment. While this research used a curing chamber, it could only warm the cubes but did not have the option to cool the curing space. So, cubes that were tested on the warmer days could have been slightly stronger than others due to the accelerated curing accompanied by elevated temperatures (Al-gburi et al., 2025). Furthermore, to really eliminate the variable of temperature, the aggregate and water could also be heated up or cooled to the right temperature before testing.

This temperature variable can also be eliminated by always doing two prints in succession. One of those prints would be the mix design of interest, while the other would be a standardized mix. Then after testing, the results of the standardized mix can then be compared to other standardized tests done on different days. The results of the mix design of interest can then be scaled up or down based on how much better or worse the standardized mix performed that day. Not only would this eliminate the effect of temperature, but also other variables like incorrect water pressure, a layer height that is slightly off, a nozzle that is set too low or too high, amongst others. The disadvantage of course is that there now need to be twice as many prints and tests.

Another issue that was encountered, is that of deviations in powder bed quality. Sometimes, testing on one type of additive would happen over the course of a week or more. But to save some time, the materials for these tests would all be prepared on the same day and would then be stored in plastic bags. However, we noticed that sometimes the material would inexplicably perform a lot worse than the (similar) materials that were tested some days prior. It was discovered that this was due to the plastic bags having small holes in them. The water in the air would partially hydrate the cement in the bags, resulting in a big loss in strength. The same issue arose when experimenting with reusing the powder from a prior mix. A part of the cement would have come into contact with water during the first round of testing. The most logical way to prevent this is to use proper storage containers and to not reuse any material, which is what the researchers ended up doing. But this can become quite costly on large scale tests using expensive additives. If reusing materials is desired, a heat of hydration test can be a good option to check the quality of the powder. In short, the heat of hydration test involves taking a certain amount of the powder of interest and placing it in an insulated box. Then, water is added to the powder, and a thermometer will measure the temperature inside the box. When plotting this temperature development over time and comparing it to the known temperature of fresh powder, an estimate can be made on the quality of the cement.

References

Al-gburi, M., Almssad, A., & Al-Zuhairi, O. (2025). Evaluating Concrete Strength Under Various Curing Conditions Using Artificial Neural Networks. *Nordic Concrete Research*, *71*, 1-23. https://doi.org/10.2478/ncr-2024-0007

Berthomier, M., Lors, C., Damidot, D., De Larrard, T., Guerandel, C., & Bertron, A. (2021). Leaching of CEM III paste by demineralised or mineralised water at pH 7 in relation with aluminium release in drinking water network. *Cement and Concrete Research*, *143*, Article 106399. https://doi.org/10.1016/j.cemconres.2021.106399

Chen, N., Wang, P., Zhao, L., & Zhang, G. (2020). Water Retention Mechanism of HPMC in Cement Mortar. *Materials (Basel)*, *13*(13). https://doi.org/10.3390/ma13132918

Chen, Y., Chang, Z., He, S., Çopuroğlu, O., Šavija, B., & Schlangen, E. (2022). Effect of curing methods during a long time gap between two printing sessions on the interlayer bonding of 3D printed cementitious materials. *Construction and Building Materials*, *332*, 127394. https://doi.org/https://doi.org/10.1016/j.conbuildmat.2022.127394

Chen, Y., Veer, F., & Çopuroğlu, O. (2017). A critical review of 3D concrete printing as a low CO 2 concrete approach. *Heron*, *62*, 167-194.

Coastruction. (2023). *Coastruction*. coastruction.com

Das, A., Reiter, L., Mantellato, S., & Flatt, R. J. (2022). Early-age rheology and hydration control of ternary binders for 3D printing applications. *Cement and Concrete Research*, *162*, Article 107004. https://doi.org/10.1016/j.cemconres.2022.107004

de Brito, J., & Kurda, R. (2021). The past and future of sustainable concrete: A critical review and new strategies on cement-based materials. *Journal of Cleaner Production*, *281*, 123558. https://doi.org/https://doi.org/10.1016/j.jclepro.2020.123558

de la Fuente, A., Blanco, A., Galeote, E., & Cavalaro, S. (2022). Structural fibre-reinforced cement-based composite designed for particle bed 3D printing systems. Case study Parque de Castilla Footbridge in Madrid. *Cement and Concrete Research*, *157*, 106801. https://doi.org/https://doi.org/10.1016/j.cemconres.2022.106801

Dorn, T., Blask, O., & Stephan, D. (2022). Acceleration of cement hydration – A review of the working mechanisms, effects on setting time, and compressive strength development of accelerating admixtures. *Construction and Building Materials*, *323*, 126554. https://doi.org/https://doi.org/10.1016/j.conbuildmat.2022.126554

Dushimimana, A., Niyonsenga, A. A., & Nzamurambaho, F. (2021). A review on strength development of high performance concrete. *Construction and Building Materials*, *307*, 124865. https://doi.org/https://doi.org/10.1016/j.conbuildmat.2021.124865

Gao, H., Zhang, X., & Zhang, Y. (2015). Effect of the entrained air void on strength and interfacial transition zone of air-entrained mortar. *Journal of Wuhan University of Technology-Mater. Sci. Ed.*, *30*(5), 1020-1028. https://doi.org/10.1007/s11595-015-1267-6

Indhumathi, S., Praveen Kumar, S., & Pichumani, M. (2022). Reconnoitring principles and practice of Modified Andreasen and Andersen particle packing theory to augment Engineered cementitious composite. *Construction and Building Materials*, *353*, 129106. https://doi.org/https://doi.org/10.1016/j.conbuildmat.2022.129106

Jau, W. C., & Tsay, D. S. (1998). A study of the basic engineering properties of slag cement concrete and its resistance to seawater corrosion [Article]. *Cement and Concrete Research*, *28*(10), 1363-1371. https://doi.org/10.1016/S0008-8846(98)00117-3

Keramost. (2008). *Product safety data sheet Metakaolin KM 60* https://www.keramost.cz/dokumenty/sds-metakaolin-en.pdf

Ler, K.-H., Ma, C.-K., Chin, C.-L., Ibrahim, I. S., Padil, K. H., Ab Ghafar, M. A. I., & Lenya, A. A. (2024). Porosity and durability tests on 3D printing concrete: A review. *Construction and Building Materials*, *446*, 137973. https://doi.org/https://doi.org/10.1016/j.conbuildmat.2024.137973

Li, S., Corelli, J., Tran, P., & Fan, L. (2025). 3D printable cellulose concrete: a review and pathway to future research. *Journal of Building Engineering*, *113*, 114187. https://doi.org/https://doi.org/10.1016/j.jobe.2025.114187

Lowke, D., Dini, E., Perrot, A., Weger, D., Gehlen, C., & Dillenburger, B. (2018). Particle-bed 3D printing in concrete construction – Possibilities and challenges. *Cement and Concrete Research*, *112*, 50-65. https://doi.org/https://doi.org/10.1016/j.cemconres.2018.05.018

Lowke, D., Mai, I., Keita, E., Perrot, A., Weger, D., Gehlen, C., Herding, F., Zuo, W., & Roussel, N. (2022a). Material-process interactions in particle bed 3D printing and the underlying physics. *Cement and Concrete Research*, *156*, 106748. https://doi.org/https://doi.org/10.1016/j.cemconres.2022.106748

Lowke, D., Mai, I., Keita, E., Perrot, A., Weger, D., Gehlen, C., Herding, F., Zuo, W., & Roussel, N. (2022b). Material-process interactions in particle bed 3D printing and the underlying physics. *Cement and Concrete Research*, *156*, Article 106748. https://doi.org/10.1016/j.cemconres.2022.106748

Lowke, D., Talke, D., Dressler, I., Weger, D., Gehlen, C., Ostertag, C., & Rael, R. (2020). Particle bed 3D printing by selective cement activation – Applications, material and process technology. *Cement and Concrete Research*, *134*, 106077. https://doi.org/https://doi.org/10.1016/j.cemconres.2020.106077

Mai, I., Lowke, D., & Perrot, A. (2022a). Fluid intrusion in powder beds for selective cement activation - An experimental and analytical study. *Cement and Concrete Research*, *156*, Article 106771. https://doi.org/10.1016/j.cemconres.2022.106771

Mai, I., Lowke, D., & Perrot, A. (2022b). Fluid intrusion in powder beds for selective cement activation – An experimental and analytical study. *Cement and Concrete Research*, *156*, 106771. https://doi.org/https://doi.org/10.1016/j.cemconres.2022.106771

Mohan, M. K., Rahul, A. V., De Schutter, G., & Van Tittelboom, K. (2021). Extrusion-based concrete 3D printing from a material perspective: A state-of-the-art review. *Cement and Concrete Composites*, *115*, 103855. https://doi.org/https://doi.org/10.1016/j.cemconcomp.2020.103855

Narayan, S., Beck, M. W., Reguero, B. G., Losada, I. J., Van Wesenbeeck, B., Pontee, N., Sanchirico, J. N., Ingram, J. C., Lange, G.-M., & Burks-Copes, K. A. (2016). The Effectiveness, Costs and Coastal Protection Benefits of Natural and Nature-Based Defences. *PLOS ONE*, *11*(5), e0154735. https://doi.org/10.1371/journal.pone.0154735

Pacheco-Torgal, F., & Jalali, S. (2011). Cementitious building materials reinforced with vegetable fibres: A review. *Construction and Building Materials*, *25*(2), 575-581. https://doi.org/https://doi.org/10.1016/j.conbuildmat.2010.07.024

Pawar, Y., & Kate, S. (2020). *Curing of Concrete: A Review*. https://doi.org/10.13140/RG.2.2.32095.07848

Project Milestone. Retrieved 31-8 from https://www.3dprintedhouse.nl/en/

Qu, F., Li, W., Dong, W., Tam, V. W. Y., & Yu, T. (2021). Durability deterioration of concrete under marine environment from material to structure: A critical review. *Journal of Building Engineering*, *35*, 102074. https://doi.org/10.1016/j.jobe.2020.102074

Razzaghian Ghadikolaee, M., Cerro-Prada, E., Pan, Z., & Habibnejad Korayem, A. (2023). Nanomaterials as Promising Additives for High-Performance 3D-Printed Concrete: A Critical Review. *Nanomaterials*, *13*(9), 1440. https://www.mdpi.com/2079-4991/13/9/1440

Santhanam, K., Reshma, E. K., K, T., & George, C. (2025). Exploring the potential of alkali-activated cassava peel ash for early-age geopolymer concrete strength development. *Construction and Building Materials*, *498*, 144062. https://doi.org/https://doi.org/10.1016/j.conbuildmat.2025.144062

Santos, R. F., Ribeiro, J. C. L., Franco de Carvalho, J. M., Magalhães, W. L. E., Pedroti, L. G., Nalon, G. H., & Lima, G. E. S. d. (2021). Nanofibrillated cellulose and its applications in cement-based composites: A review. *Construction and Building Materials*, *288*, 123122. https://doi.org/https://doi.org/10.1016/j.conbuildmat.2021.123122

Scrivener, K. (2003). 2 - Calcium aluminate cements. In J. Newman & B. S. Choo (Eds.), *Advanced Concrete Technology* (pp. 1-31). Butterworth-Heinemann. https://doi.org/https://doi.org/10.1016/B978-075065686-3/50278-0

Scrivener, K. L., John, V. M., & Gartner, E. M. (2018). Eco-efficient cements: Potential economically viable solutions for a low-CO2 cement-based materials industry. *Cement and Concrete Research*, *114*, 2-26. https://doi.org/https://doi.org/10.1016/j.cemconres.2018.03.015

Senapathi, A., & Peiris, A. (2025). A comprehensive study of steel fiber alternatives on mechanical properties, long-term performance, and durability of ultra-high-performance concrete: A review. *Journal of Building Engineering*, *108*, 112900. https://doi.org/https://doi.org/10.1016/j.jobe.2025.112900

Talke, D., Saile, B., Meier, N., Herding, F., Mai, I., Zetzener, H., Kwade, A., & Lowke, D. (2023). Particle-bed 3D printing by selective cement activation – Influence of process parameters on particle-bed density. *Cement and Concrete Research*, *168*, 107140. https://doi.org/https://doi.org/10.1016/j.cemconres.2023.107140

Tracz, T., Zdeb, T., Witkowski, K., & Szkotak, D. (2025). Influence of Hydration and Natural Carbonation Evolution on the Gas Permeability and Microstructure of Blended Cement Pastes. *Materials*, *18*, 4416. https://doi.org/10.3390/ma18184416

TU/e. (2021). *Nijmegen has the longest 3D printed concrete bycicle bridge in the world*. Retrieved 31-8 from https://www.tue.nl/en/news-and-events/news-overview/01-01-1970-nijmegen-has-the-longest-3d-printed-concrete-bicycle-bridge-in-the-world/

UNEP, U. N. E. P. (2022). *Sand and Sustainability: 10 strategic recommendations to avert a crisis*.

Verma, M., Dev, N., Rahman, I., Nigam, M., Ahmed, M., & Mallick, J. (2022). Geopolymer Concrete: A Material for Sustainable Development in Indian Construction Industries. *Crystals*, *12*(4), 514. https://www.mdpi.com/2073-4352/12/4/514

Wang, L., Yu, A., Li, E., Shen, H., & Zhou, Z. (2021). Effects of spreader geometry on powder spreading process in powder bed additive manufacturing. *Powder Technology*, *384*, 211-222. https://doi.org/https://doi.org/10.1016/j.powtec.2021.02.022

Xia, M., Nematollahi, B., & Sanjayan, J. (2018). Influence of Binder Saturation Level on Compressive Strength and Dimensional Accuracy of Powder-Based 3D Printed Geopolymer. *Materials Science Forum*, *939*, 177-183. https://doi.org/10.4028/www.scientific.net/MSF.939.177

Xia, M., Nematollahi, B., & Sanjayan, J. (2019a). Compressive Strength and Dimensional Accuracy of Portland Cement Mortar Made Using Powder-Based 3D Printing for Construction Applications. In (pp. 245-254). Springer International Publishing. https://doi.org/10.1007/978-3-319-99519-9_23

Xia, M., Nematollahi, B., & Sanjayan, J. (2019b). Printability, accuracy and strength of geopolymer made using powder-based 3D printing for construction applications. *Automation in Construction*, *101*, 179-189. https://doi.org/https://doi.org/10.1016/j.autcon.2019.01.013

Xiao, J., Qiang, C., Nanni, A., & Zhang, K. (2017). Use of sea-sand and seawater in concrete construction: Current status and future opportunities. *Construction and Building Materials*, *155*, 1101-1111. https://doi.org/https://doi.org/10.1016/j.conbuildmat.2017.08.130

Yu, R., Spiesz, P., & Brouwers, H. J. H. (2015). Development of an eco-friendly Ultra-High Performance Concrete (UHPC) with efficient cement and mineral admixtures uses. *Cement and Concrete Composites*, *55*, 383-394. https://doi.org/10.1016/j.cemconcomp.2014.09.024

Zuo, W., Dong, C., Belin, P., Roussel, N., & Keita, E. (2022). Capillary imbibition depth in particle-bed 3D printing – Physical frame and one-dimensional experiments. *Cement and Concrete Research*, *156*, 106740. https://doi.org/https://doi.org/10.1016/j.cemconres.2022.106740

Zuo, W., Dong, C., Keita, E., & Roussel, N. (2020). Penetration Study of Liquid in Powder Bed for 3D Powder-Bed Printing. In *RILEM Bookseries* (pp. 379-386). Springer International Publishing. https://doi.org/10.1007/978-3-030-49916-7_39

Appendices

Appendix A: Alternative figures

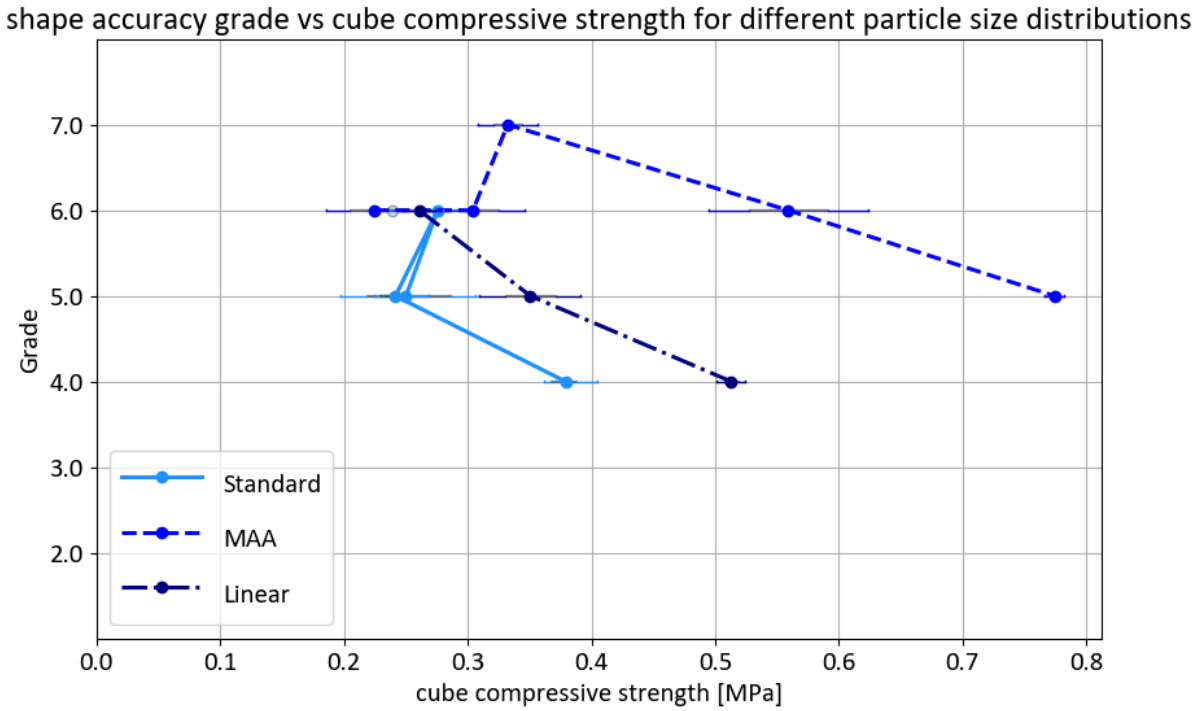

Figure 55: Shape accuracy grade vs cube compressive strength for different particle size distributions

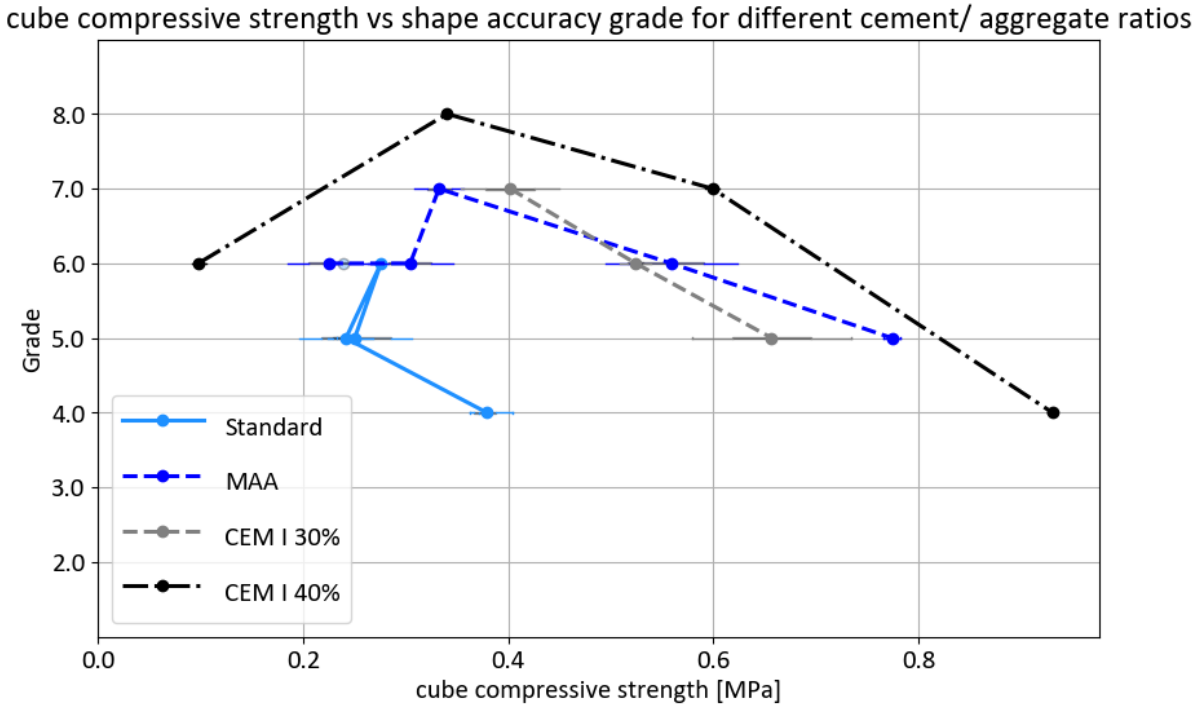

Figure 56: Cube compressive strength vs shape accuracy grade for different cement/ aggregate ratios

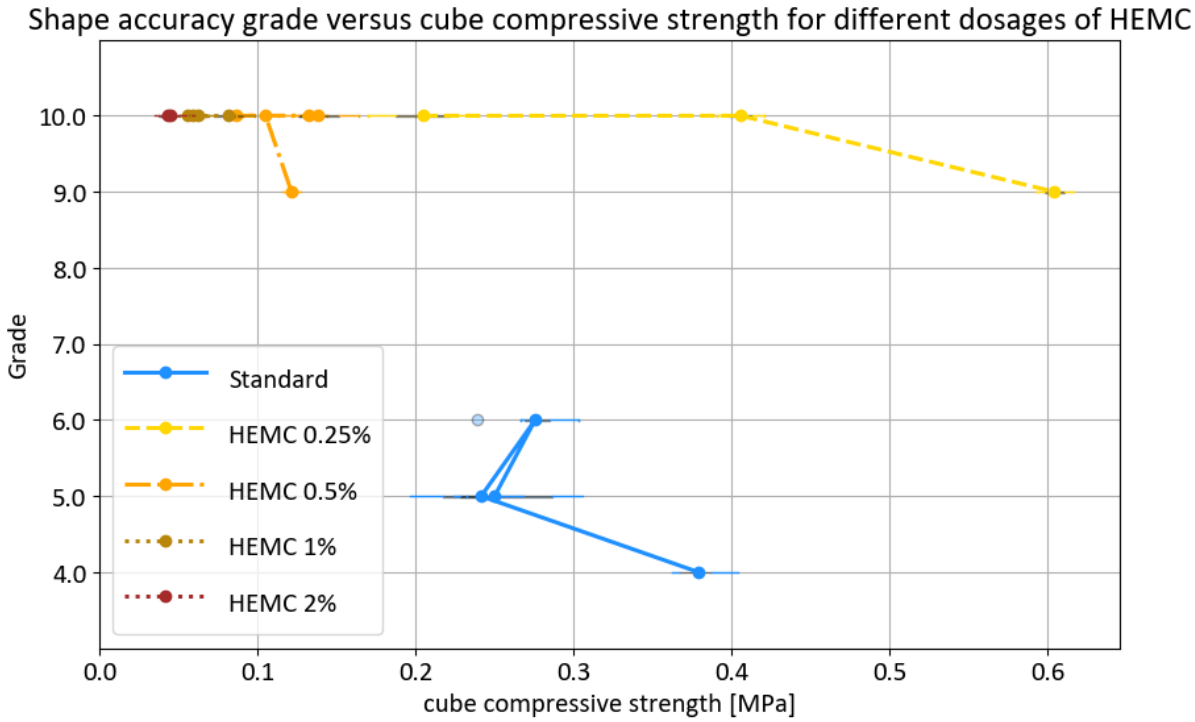

Figure 57: Shape accuracy grade versus cube compressive strength for different dosages of HEMC

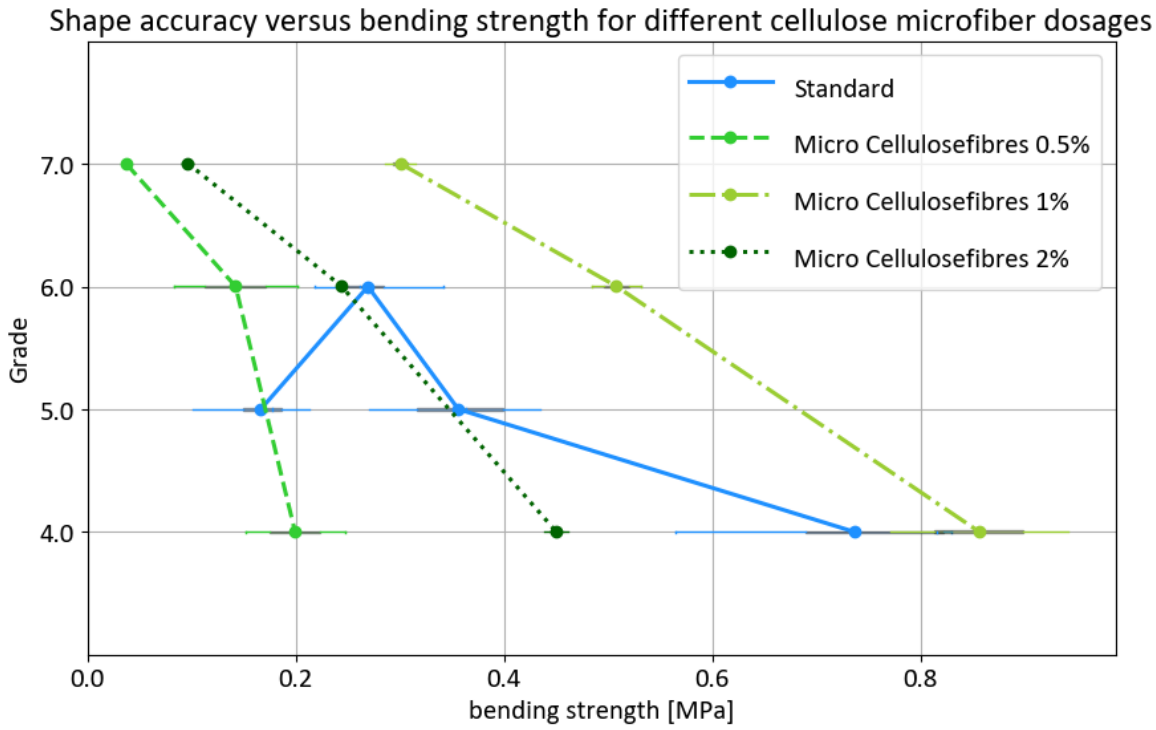

Figure 58: Shape accuracy versus bending strength for different cellulose microfibre dosages

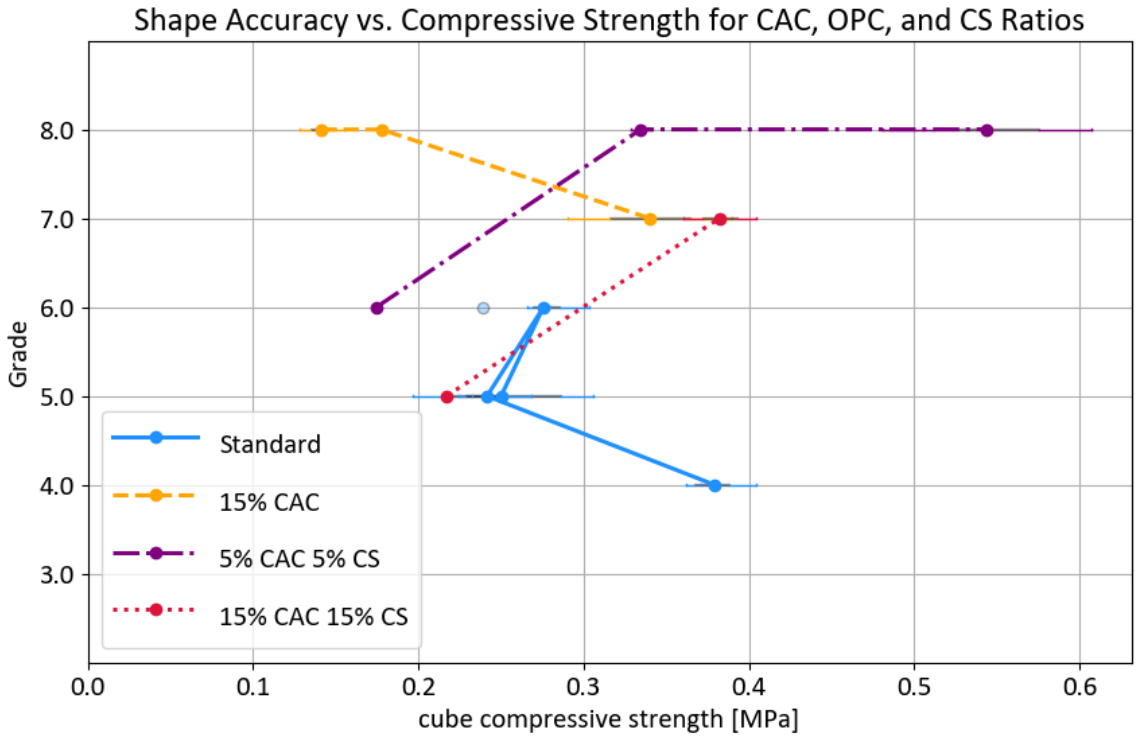

Figure 59:Shape accuracy grade versus cube compressive strength of different ratios of CAC,OPC and CS

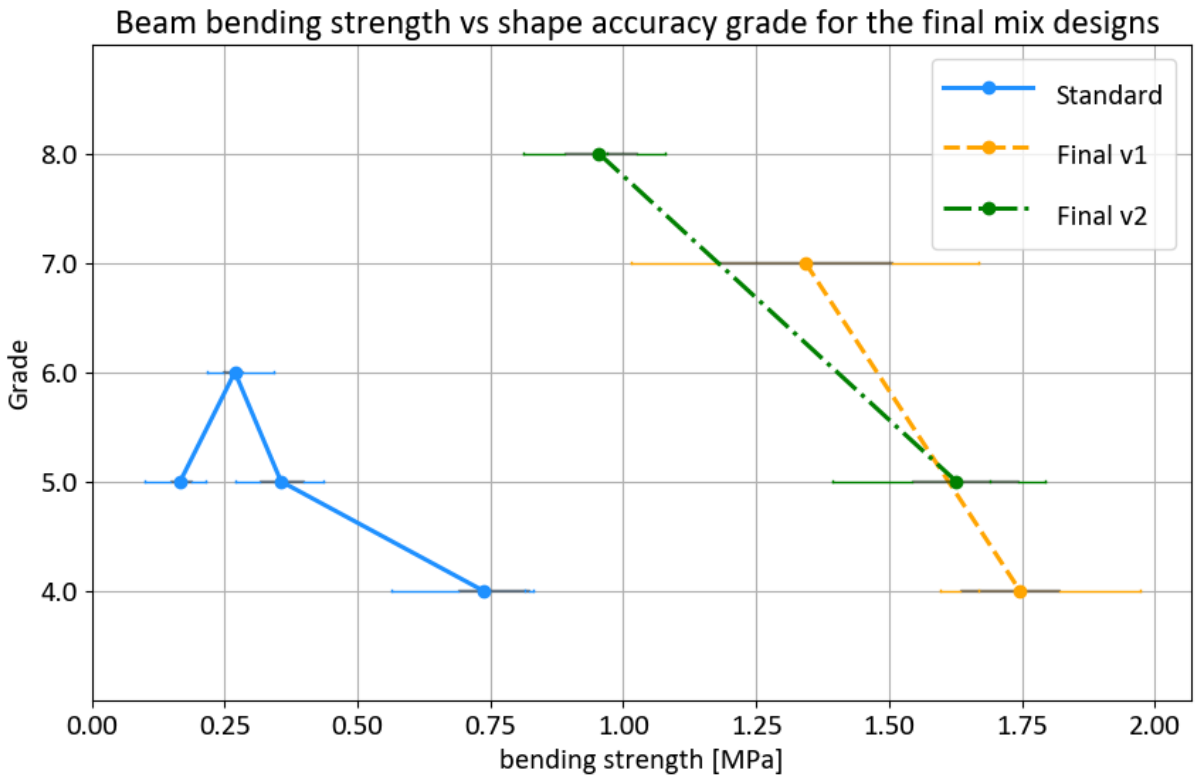

Figure 60: Beam bending stregnth vs shape accuracy grade for the final mix designs

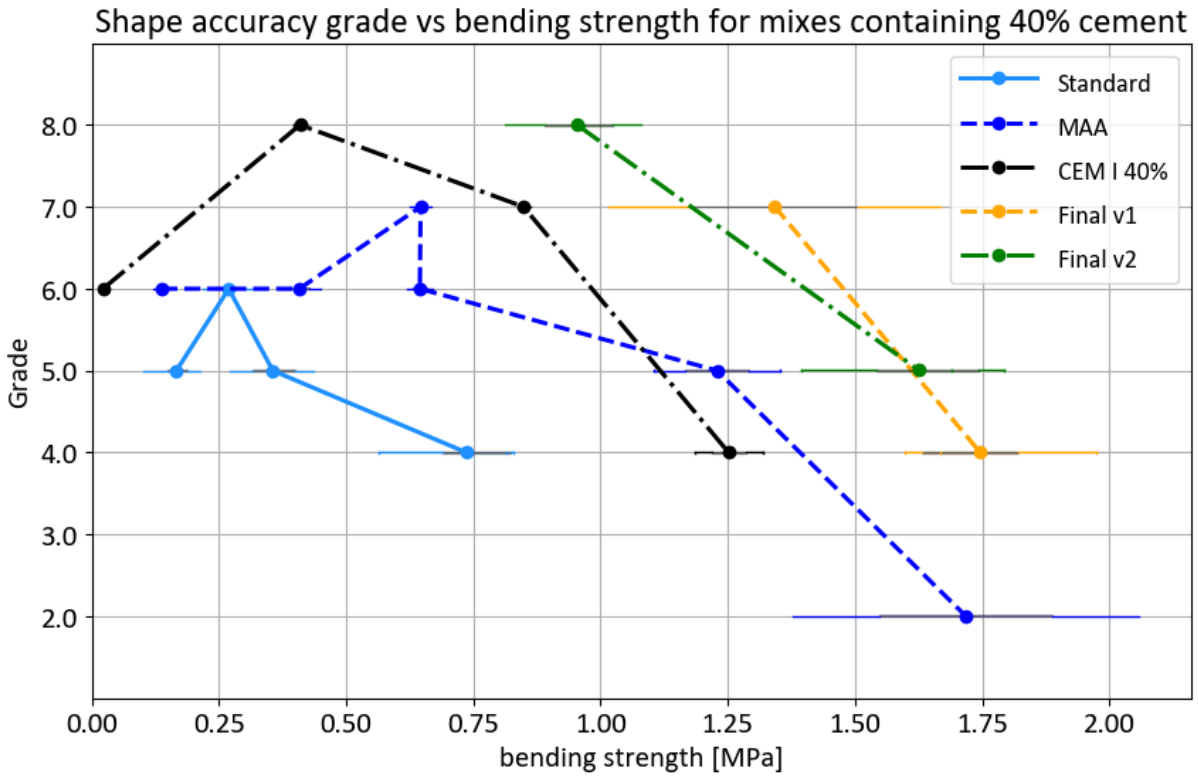

Figure 61: Shape accuracy grade vs bending strength mixes containing 40% cement

Appendix B: Extra figures

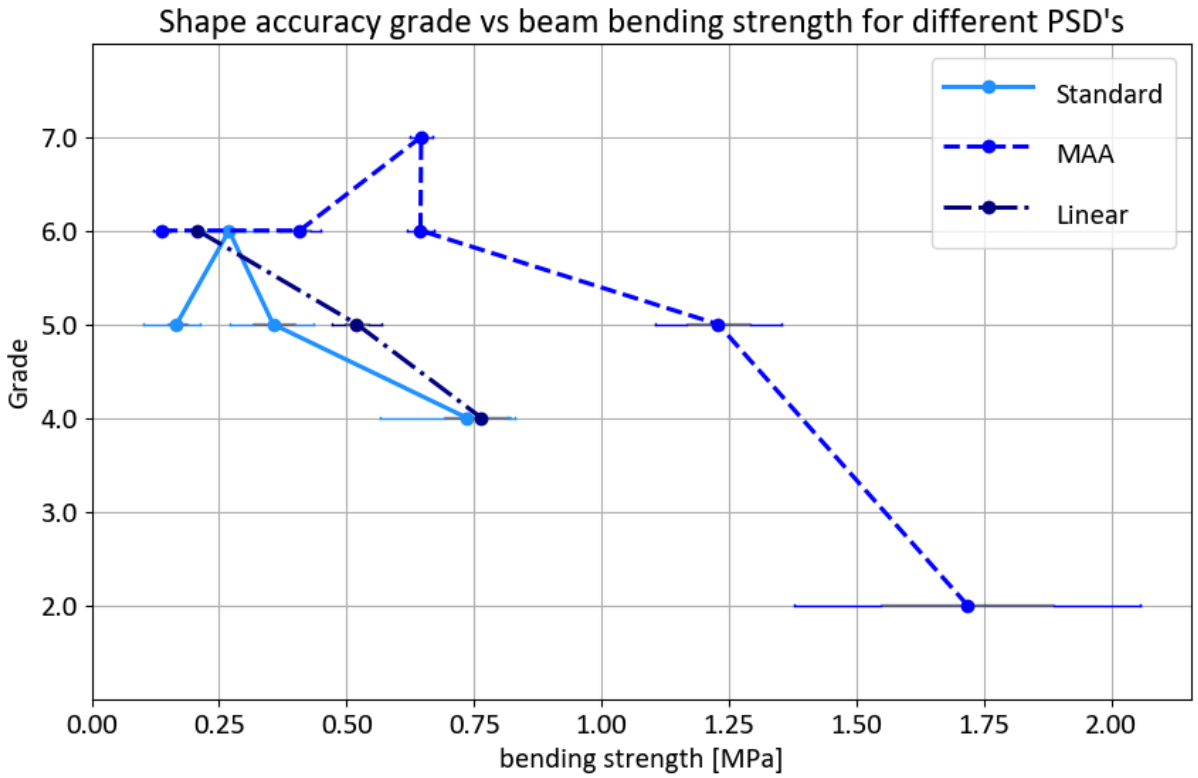

Figure 62: Shape accuracy grade vs beam bending strength for different particle size distributions

Appendix C: Test volume

Test name	Amount of cubes (compressive)	Amount of beams (bending)
Standard	6	6
HEMC 0.25%	2	2
HEMC 0.5%	3	3
HEMC 1%	3	3
HEMC 2%	3	3
MAA	2	2
Linear	2	2
Micro cellulose fibres 0.5%	2	2
Micro cellulose fibres 1.0%	2	2
Micro cellulose fibres 2.0%	2	2
CEM I 30%	2	2
CEM I 40%	2	2
CEM I 100%	2	2
CEM III 20%	6	6
15% CAC	2	2
5% CAC 5% CS	2	2
15% CAC 15% CS	2	2
Glass fibre 900g/m3	2	2
Glass fibre 1%	2	2
7- day submerged	2	2
7- day dry	2	2
3-day delayed	2	2
7-day misting	2	2
Final v1	3	3
Final v2	3	3

Table 5: Test volume

Appendix D: Shape accuracy grades

Test name	w/c ratios	Grades
Standard	0.2-0.3-0.4-0.6	5-6-5-4
HEMC 0.25%	0.4-0.6-0.8	10-10-9
HEMC 0.5%	0.2-0.3-0.4-0.6-0.8	10-10-10-10-9
HEMC 1%	0.2-0.3-0.4-0.6	10-10-10-10
HEMC 2%	0.4-0.6	10-10
MAA	0.1-0.15-0.2-0.3-0.4-0.6	6-7-6-5-2
Linear	0.2-0.3-0.4	6-5-4
Micro cellulose fibres 0.5%	0.3-0.4-0.6	7-6-4
Micro cellulose fibres 1.0%	0.3-0.4-0.6	7-6-4
Micro cellulose fibres 2.0%	0.3-0.4-0.6	7-6-4
CEM I 30%	0.2-0.3-0.4	7-6-5
CEM I 40%	0.1-0.2-0.3-0.4	6-8-7-4
CEM I 100%	0.3-0.4	5-3
CEM III 20%	0.3-0.4-0.6	6-5-3
15% CAC	0.3-0.4-0.6	8-8-7
5% CAC 5% CS	0.3-0.4-0.6	6-8-8
15% CAC 15% CS	0.3-0.4-0.6	3-5-7
Glass fibre 900g/m3	0.3-0.4-0.6	6-5-4
Glass fibre 1%	0.3-0.4-0.6	2-4-4
7- day submerged	0.3-0.4-0.6	6-5-4
7- day dry	0.3-0.4-0.6	6-5-4
3-day delayed	0.3-0.4-0.6	6-5-4
7-day misting	0.3-0.4-0.6	6-5-4
Final v1	0.4-0.6	7-4
Final v2	0.4-0.6	8-5

Table 6: Shape accuracy grades and w/c ratios for all mix designs